CHALMERS

Next-Generation Optimized Joystick for Construction Equipment

Master's thesis in Mobility engineering and Applied mechanics

Erik Lydig
Gillian Makrof-Johansson

Department of Industrial and Materials Science IMSX30
CHALMERS UNIVERSITY OF TECHNOLOGY
Gothenburg, Sweden 2025
www.chalmers.se

Masters thesis 2025

Next-Generation Optimized Joystick for Construction Equipment

Erik Lydig
Gillian Makrof-Johansson

CHALMERS

Department of Industrial and Materials Science IMSX30
Chalmers university of technology
Gothenburg, Sweden 2025

Next-Generation Optimized Joystick for Construction Equipment
Erik Lydig
Gillian Makrof-Johansson

Supervisor: Mikael Gårdfeldt, R&D Manager at CPAC systems AB
Supervisor: Adam Lindkvist, Chalmers University of Chalmers Postdoc, Product Development, Industrial and Materials Science
Examiner: Gauti Asbjörnsson, Chalmers University of Technology Associate Professor, Product Development, Industrial and Materials Science

Master's thesis 2025
Department of Industrial and Materials Science IMSX30
Chalmers University of Technology
SE-412 96 Gothenburg
Sweden
Telephone +46 (0)31-772 1000

Cover: CAD model of Joystick

Chalmers Reproservice
Gothenburg, Sweden 2025

Next-Generation Optimized Joystick for Construction Equipment
Master's thesis in Mobility engineering and Applied mechanics
Erik Lydig
Gillian Makrof-Johansson
Department of Industrial and Materials Science IMSX30
Chalmers University of Technology

Abstract

This thesis presents the development of a next-generation single-lever joystick for wheel loaders, focusing on improved ergonomics, functionality, and manufacturability. The lack of significant updates since the introduction of Volvo's original single-lever system in 2012 has created a need for a modernized joystick solution that addresses current demands for improved ergonomics, functionality, and compatibility with operator requirements. The project aimed to develop a new concept for a joystick in collaboration with CPAC Systems and targets improved user experience and suited for the operator needs.

The outcome of this thesis is a fully developed joystick concept, accompanied by technical documentation. This includes detailed CAD models, manufacturing considerations, and button selection, among other elements—all of which provide a solid foundation for continued development and industrial implementation. Both FEA and DOE were conducted, ensuring that an optimized design was achieved. Joystick prototypes and a test rig were manufactured for further testing and evaluation.

Keywords: Product development, DOE, Joystick, Injection molding, FEA, Wheel loader, Single lever.

Acknowledgments

> "994an, den kör man med joystick o de e najs"
> — Mikael Nilsson, Automotive enthusiast [1]

We would like to express our gratitude to our examiner, Gauti Asbjörnsson and supervisors, Adam Lindkvist and Mikael Gårdfeldt, for their guidance and support throughout this project. We also thank our colleagues Leonardo Kremer, Peder Arvidsson, Stefan Högberg, Julius Jernlås, Jörgen Schröder, Adrian Stanikowski, Anton Alm and Niklas Sjöstedt for their helpful discussions and assistance.

Erik Lydig & Gillian Makrof-Johansson, Gothenburg, June 2025

Acronyms

Below is the list of acronyms that have been used throughout this thesis listed in alphabetical order:

AM	Additive Manufacturing
APS	Automatic Power Shift
BC	Boundary Condition
BVP	Boundary Value Problem
CAD	Computer Aided Design
CAN	Controller Area Network
CDC	Comfort Drive Control
CNC	Computer Numerical Control
CPAC	CPAC systems
DE	Differential Equation
DFA	Design for Assembly
DFM	Design for Manufacturing
DFMA	Design for Manufacturing and Assembly
Diff-lock	Differential-lock
DLP	Digital Light Processing
DOE	Design of Experiments
DSD	Definitive Screening Designs
EBF3	Electron Beam Freeform Fabrication
EBM	Electron Beam Melting
ECU	Electronic Control Unit
EDM	Electro Discharge Machine
FDM	Fused Deposition Modeling
FEA	Finite Element Analysis
FEM	Finite Element Method
FFF	Fused Filament Fabrication
FNR	Front, Neutral & Revers Switch
F/R	Front/Reverse
FR	Front & Revers
HST	Hydrostatic Transmission
IM	Injection Molding
IP	Ingress Protection
ISO	International Organization for Standardization
LC	Load Case

LMD	Laser Melt Deposition
LOM	Laminated Object Manufacturing
MJF	Multijet Fusion
MJP	MultiJet Printing
PCB	Printed Circuit Board
PDE	Partial Differential Equation
PPE	Personal Protective Equipment
RA	Roughness Average
SAF	Selective Absorption Fusing
SF	Strong Form
SLA	Stereolithography
SLM	Selective laser Melting
SLS	Selective Laser Sintering
STL	Standard Template Library
TC Factor	Time Correction Factor
TPE	Thermoplastic Elastomer
VCE	Volvo Construction Equipment
VDI	Verein Deutscher Ingenieure
VSL	Volvo Single Lever
WF	Weak form
WLO	Wheel Loader

Contents

List of Figures

List of Tables

1
Introduction

Joysticks are essential for operating construction machinery, acting as the main interface for operators. Since CPAC Systems (CPAC) and Volvo developed a single-lever joystick for wheel loaders (WLO) in 2012, little progress has been made in joystick design. To stay competitive and meet demands for better ergonomics and functionality, CPAC is exploring developing a new generation of joysticks that enhance usability, comfort, and adaptability to various operators.

1.1 Background

In 2012, CPAC developed a single-lever joystick system for wheel loaders in collaboration with Volvo Construction Equipment (VCE). VCE is one of the largest manufacturers of construction equipment, producing a diverse range of machines across various sectors. Since the introduction of the Volvo Single Lever (VSL), there have been no significant updates, while the market has grown with numerous manufacturers competing to introduce their own joystick designs. To remain competitive, CPAC must develop a new joystick that meets market demands and enhances user experience and ergonomic comfort.

1.2 Purpose

The purpose of this project is to develop a new generation of (single-lever) joysticks specially designed for wheel loaders and their applications. Next generations joystick should incorporate more features on the joystick to minimize the movement of the hand for ergonomic reasons. The new design is expected to surpass its predecessor in both functionality and user-friendliness, while also offering customization options to accommodate various applications and operator preferences.

1.3 Objective

At the end of this project, CPAC should have a complete joystick prototype with technical drawings and Computer Aided Design (CAD) files, along with a report with all the design choices and necessary documentation. The joystick should meet the requirements set by CPAC and follow the necessary Volvo and International Organization for Standardization (ISO) standards. The new joystick concept should outperform the previous VSL in terms of user ergonomics and also facilitate the daily

work of the operator. It should also be simple enough for the novel user but also meet the user demand from the experienced user, this would be achieved through modularity and intuitive design choices.

1.4 Scope & Limitations

The project time span is equivalent to 60 credits split between two individuals, which adds to 1600 hours combined. The time frame is therefore from the end of January until the middle of June, 2025. Since the project does not have unlimited time, it needs to be limited to what the time frame allows and therefore has certain limitations.

- Electrical integration is not a primary priority; however, it remains an important consideration.
- The prototype will not include electrical components except buttons and switches.
- Plastic parts in the final prototype will be manufactured using additive manufacturing.
- Final material choice will not be presented, but a recommendation will be provided.
- Manufacturing technique will be considered during the design process, but final injection molding orientation will not be set, and only simpler molding simulations will be done in Creo PTC.
- The parts that will be considered for redesigning are the joystick and hand/wrist rest. But no further integration changes will be investigated to ensure that the part within the scope gets enough time to mature in the design.

1.5 Research questions

This thesis project will aim to answer the following questions:

- What kind of functions are required for a joystick assembly in WLO, and what buttons/switches are required to perform these functions?
- In what areas can modern optimization tools be used in the design of a WLO joystick, and how can it improve the design?

2
Theoretical Background

This chapter serves as an introduction to key terminology used throughout the report. A clear understanding of the function of each button and switch, along with the operations they control, is essential for determining their frequency of use and informing optimal placement. Additionally, because the joystick will be manufactured from plastic, a knowledge of plastic manufacturing processes is necessary to recognize production limitations. To ensure the most ergonomic hand and wrist positioning, the biomechanics of ergonomics are examined. Finally, methods for optimization, including Design of Experiments (DOE) and Finite Element Analysis (FEA), are presented.

2.1 How does a Joystick in a WLO work?

A joystick is the operators' way of controlling the hydraulic functions of the WLO. A WLO has two main functions, tilting the bucket in/out and lowering/lift the boom, see the joystick movement by the red and blue arrows in Figure 2.1 and corresponding movement of the bucket and WLO in Figure 2.2. These functions make up the basis of the daily usage and are essential for many tasks the WLO will perform. There are also other attachments than a bucket that use additional hydraulic functions, see Figure 2.10 and Figure 2.11.

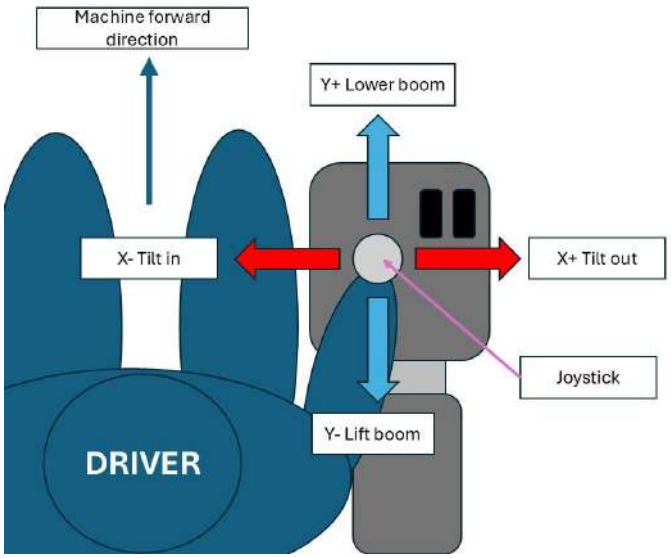

Figure 2.1: Joystick movement seen from above

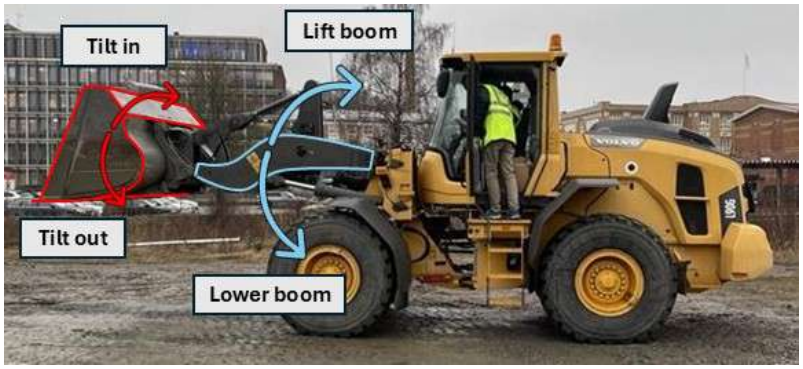

Figure 2.2: Main functions of a WLO

The joystick is coupled to a hydraulic system to control valves, pumps, and hydraulic cylinders. When the joystick is operated, it either sends an electrical signal to a set of actuators or directly actuates the hydraulics see Figure 2.3. Modern WLOs usually have an electrically controlled mechanism because of its smaller size and easier packaging, freeing up space in the operator's cab, see Figure 2.3.

Figure 2.3: Electrical mechanisms for joystick

2.2 Basic Driveline mechanics

This section is meant to familiarize the reader with basic driveline terminology which are used in the context of WLO. It will also serve as an incite into what happens in the vehicle driveline when a button is activated on the joystick.

- **APS - Automatic Power Shift**

  VOLVOs APS are fitted in Larger Wheel Loaders such as L60H, L70H, L90H, L110H, L120H, L150H, L180H, L200H High Lift, L220H, L260H, L350H. It features a torque converter connected to a 4-speed (Forward and Reverse) automatic transmission. By using hydraulics clutch packs that are engaged/disengaged in specific combinations, gears can be changed without the loss of drive power. Different shifting programs can be chosen, which control in which gear span the operator allows the automatic transmission to switch between. As with any WLO, using the Kick-Down button will force the transmission to shift to the lowest gear to achieve the highest wheel torque.

- **HST - Hydrostatic Transmission**

  Hydrostatic transmission controls the direction, speed and torque of the WLO. It is constructed from a variable displacement pump connected to the combustion engine and a hydraulic motor (can also be variable displacement) which is connected to the rest of the driveline ending at the wheels. Generally, a hydrostatic pump and motor are continuously variable, meaning they can achieve any gear ratio in between the highest and lowest possible gear ratios. For VOLVOs Compact Wheel Loaders (L30, L35, L45H, L50H), which use a hy-

drostatic transmission, the transmission is usually designed to operate in three fixed speeds, neutral, 1st gear and 2nd gear. What should be taken away from this is that even if the transmission is hydrostatic, it still has a certain number of fixed gear ratios, which are switched between when driving.

- **Differential-lock**

  The differential is the connection between the transmission output and the drive axles. In an open differential, the transmission output torque will be the sum of the left and right wheel torques divided by the final drive gear reduction, see Figure 2.4. The left and right wheel torques will always be the same, but wheel speeds will be different. The pros of a differential are to reduce scrubbing when turning, since the wheel speeds will adapt to the specific turning radius for each wheel. The downside would be that if one wheel loses traction and can not transmit any torque, the other side with more traction will receive the same torque as the side with lower traction. In other words, the overall propulsion force will be low and the vehicle can have a hard time moving. For this reason, a differential-lock (diff-lock) is used to lock the left and right wheels together, meaning they will turn with the same speed but different torques. This can be useful when operating on loose gravel or slippery surfaces. By pressing the Diff-Lock pushbutton, the differential would switch from open to locked. Depending on the model of WLO, diff-lock might be available on just one or on both axles.

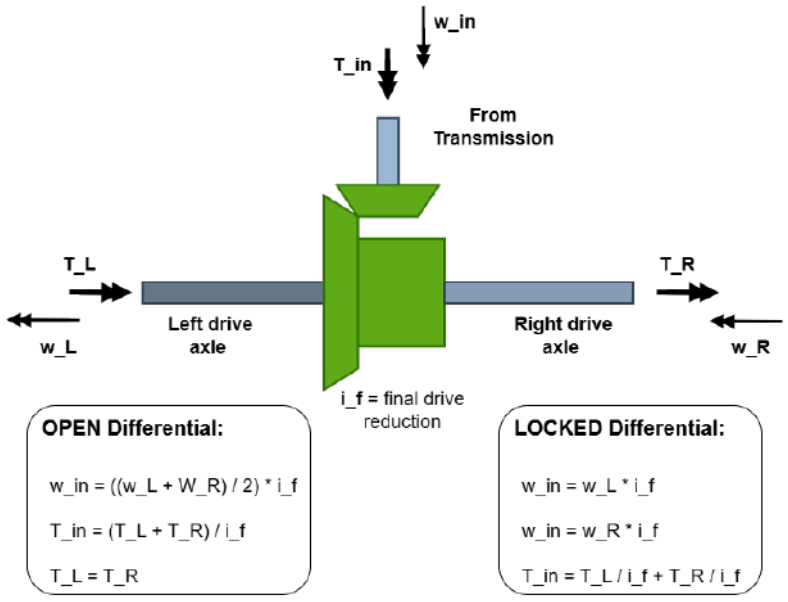

Figure 2.4: Equations for an open and locked differential

2.3 Product definition

The first step in improving a product is to understand the current product, its strengths and shortcomings. A literature study on joysticks used in WLO is performed to understand what functions are required and how they are used. Furthermore, investigating external joysticks from competitors or vehicles within the VCE to gain a wider perspective on potential improvements. For the rest of the report, buttons, switches (FNR) and thumb wheels will be referred to as just buttons or the specific button type, depending on whether several buttons are referred to or just one.

The interior cockpit of a VCE WLO and key features are noted in Figure 2.5. The first thing to note is the Comfort Drive Control (CDC) which is mounted on the left armrest and features a one-axis (left/right) joystick that is used to steer the WLO and helps reduce fatigue versus using the steering wheel. For driving on public roads CDC can be deactivated and a regular steering wheel is used, to make sure the vehicle complies with road safety regulations. On the A-pillar, several switches are mounted, everything from ON/OFF to different gear switching modes.

Figure 2.5: Interior of a VCE WLO L150H [2], Reproduced with permission

There are many different models of the VCE WLO vehicles, and they are divided into two categories: Large Wheel Loaders and Compact Wheel Loaders. Models for the Large Wheel Loaders include, but are not limited to: L60H, L70H, L90H, L110H, L120H, L150H, L180H, L200H High Lift, L220H, L260H, and L350H. Models for the Compact Wheel Loaders include, but are not limited to: L30, L35, L45H, and L50H.

For all the Large Wheel Loaders, Co-Pilot (12″ touch screen) is available with Load Assist, which provides features like On-Board Weighing or different task modes like

Trip Meter, Truck Loading, Stockpiling, or Process Loading. Figure 2.6 illustrates how the Co-Pilot is integrated in the cab of the WLO.

Figure 2.6: VOLVO Co-Pilot using Load Assist in WLO [3], reproduced with permission

VCE Larger Wheel Loaders come standard with multiple levers (one per hydraulic function) as seen in Figure 2.7. An option is available to change the lever system to a VSL, or referred to as a Joystick, see Figure 2.8. Both systems offer the same functions however, with a different layout. A difference between the two examples is that an additional programmable button is added for the Joystick. The fundamental variation is that the Bucket tilt and Boom lift are controlled by moving the Joystick forward/backwards and right/left. Furthermore, the 3rd and 4th functions are replaced with two Thumbwheels. Preferences between the two systems differ greatly, and individual operators usually prefer one exclusively.

Figure 2.7: 4 lever system in Larger Wheel Loaders [3], reproduced with permission

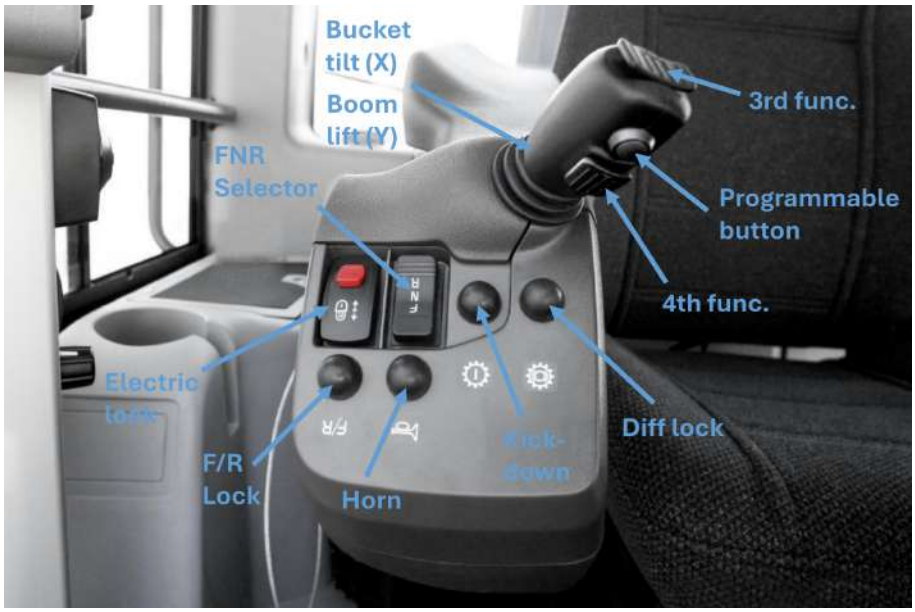

Figure 2.8: VSL system in Larger Wheel Loaders [3], reproduced with permission

List of all functions and explanation on what they do:

- **FNR (FR) Selector:**
  The FNR switch selects between Forward, Neutral & Reverse. For larger WLO with APS and 4 gears, the FNR only switches between the forward and reverse gear. A separate switch can be used to manually switch between the 4 gears, or this can be done automatically in different gear ranges. There are joystick configurations with only Front & Reverse (FR) switch, where the Neutral is a separate button.

- **F/R Lock:**
  Front/Reverse lock is the activation button for the FNR switch. If active, FNR can only be selected using the lever under the steering wheel. On the left armrest were the CDC is located, there is another F/R Lock that activates/deactivates the CDC. When operating the WLO on the road, the CDC is turned off, and steering is controlled via the steering wheel.

- **Main function (1st, 2nd)**:
  The main hydraulic functions control the Bucket tilt (X) and the Boom lift (Y). Also referred to as the 1st and 2nd hydraulic functions.

- **3rd function:**
  The 3rd function is used to control an additional hydraulic cylinder. This can be used for attachments, replacing the bucket with a snowplow, brush or similar.

- **4th function:**
  Similar to the 3rd function, the 4th function can be used to control a second

additional hydraulic cylinder. An example where both 3rd and 4th functions are used simultaneously is when controlling the speed of a brush with the 3rd function and the angle of the brush with the 4th function.

- **Horn:**
  Used to alert the surrounding people of other vehicles.

- **Diff-lock:**
  Locks up the differential on the front axle to increase grip. The front axle differential lock is standard on VCE WLO, and the rear differential lock is an optional feature.

- **Kick-down:**
  Since the transmission is automatic, there are situations where it is required to force the transmission to shift down to 1st to increase torque, this is the function of the kick-down. It is useful when approaching a dig pile and the operator wants to downshift earlier than the automatic logic.

- **Electronic Lock:**
  The electronic lock is used to stop any unwanted movements from the joystick. This can be used during service to be sure the hydraulics will not actuate.

Looking at the control system for the Compact Wheel Loaders the control system is more similar to what would be found in an excavator, except only using one Joystick, see Figure 2.9. The VSL for Larger WLO is similar to this Joystick, however the form factor of the handle is much more ergonomic and more functions are moved from the base to the handle to reduce the finger movement.

Figure 2.9: Joystick in Compact Wheel Loaders [3], reproduced with permission

2.4 Attachments

There are many different attachments for a WLO, a wide range of buckets for general purpose, high tip, side dump buckets and rock buckets. For example attachments for crane jibs, folding grass forks, fork attachments with manual actuation of the forks or hydraulic actuation, snow plows in V-configuration, diagonal snow plow, with and without side skirts, and also sand spreading buckets to complement the snow plowing. For cleaning the streets, sweepers are brushing the dirt to the side or pick-up sweepers, and there are many more attachments and configurations for all purposes.

The buckets usually only use the main functions when loading trucks and moving dirt. For other attachments, there are often more hydraulic actuated functions that are called the 3rd and 4th functions. These extra functions are used to actuate two hydraulic valves by operating two thumbwheels on the joystick. If there's no need for the 3rd and 4th functions in the WLO, the most basic VSL comes without the thumbwheels, but there are options to have one or two thumbwheels depending on the application of the WLO and if there is a need for the 3rd and 4th functions.

In Figure 2.11 and Figure 2.10, there are four different types of attachments with different applications but they have in common that they use the 3rd function and in some cases the 4th function. The lifting forks in Figure 2.11b use the 3rd function to shift the forks in relation to each other, and the 4th function shifts the forks together. The lifting fork is used to lift pallets in warehouses, among other places. The grapple in Figure 2.10a uses the 3rd function to grip stacked logs in forests. The V snow plow in Figure 2.11a uses the 3rd and 4th functions to angle the scoops, there are often possibilities to open and close valves on the snow plow to actuate it in different ways. The sweeper works in a similar way, see Figure 2.10b, it has a 3rd function, but the operator can lock the function with a button and retain the hydraulic pressure and thereby keep the brush spinning.

(a) Grapple **(b)** Sweeper

Figure 2.10: Attachments for a wheel loader using the 3rd function [4], CC-BY-SA

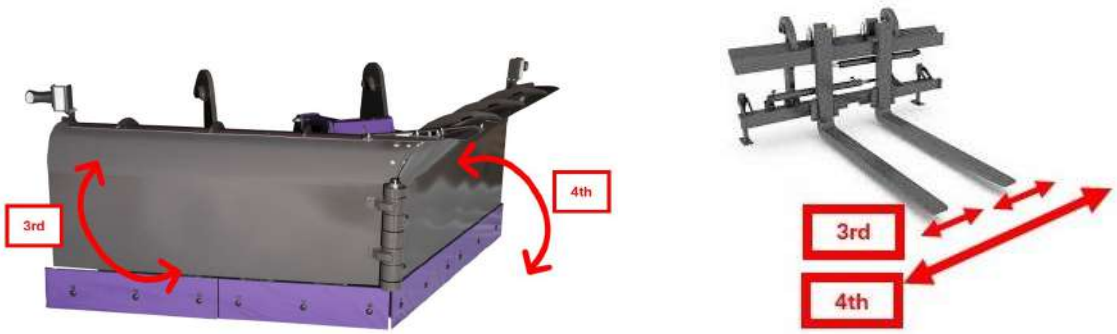

(a) Snow plow **(b)** Lifting forks

Figure 2.11: Attachments for a wheel loader using the 3rd and/or 4th function[4], CC-BY-SA

2.5 Co-Pilot

CPAC and VOLVO CE has introduced a Co-Pilot to support and aid the operators in their daily work and is visualized through a display in the cab. There are many ways of using the Co-Pilot, for example, keeping track of load capacity in trucks, organizing jobs, selecting trucks for loading, weighing the load in the bucket and many more applications are available. Four ways of using the display are shown in Figure 2.13.

The most common application is the loading option, in this case the job covers loading 2000 tons of kryptonite material in several truckloads, see Figure 2.12b. 224 tons have already been loaded and the operator now has to select what type of truck is coming next to be able to know the capacity. There is a built-in logic in the Co-Pilot to present the three trucks most likely to come next based on GPS position and elapsed time from last loading among other parameters. If the next truck is not presented among the three, the operator has to select the target manually and the target list would open, see Figure 2.12b. The operator can now select the truck from a list of trucks in the system. If a new truck arrives at the site that is not in the system, the operator has to create a new truck and define the capacity and type. The feature of selecting trucks supports the driver in the sense that each job is easier to keep track of and the possibility to see how much to load the truck simplifies the loading operation.

When the operator has selected the incoming truck, the load capacity will be shown on the display, see Figure 2.13a. The total capacity is 25 tons and after two buckets, the truck is filled with 16 tons of kryptonite. While the operator is loading the truck, the display shows the pitch and roll angle of the WLO in case it is close to tipping in any direction. On top of the display, the load of the bucket is presented for an easier and quicker loading operation. Previously, the truck would be resting on a scale and the WLO would fill up the truck based on the scale, but with the Co-Pilot, the WLO can solve the scale itself and through that open the possibility

of a more accurate loading when no scale is available.

In certain cases, the truck could have one or multiple trailers to fill up, the operator chooses the truck or trailer and the capacity will be shown on the screen along with the quantity already filled up, see Figure 2.13b. When the job is done, the operator has the option to print the receipt for the job and could use it for an invoicing basis.

If the operator would like to change the content on the display, there is a wide range of different parameters and data options to choose from.

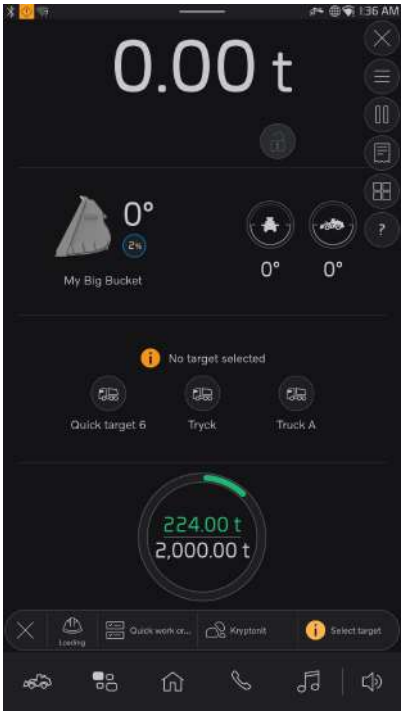

(a) Truck selection while loading

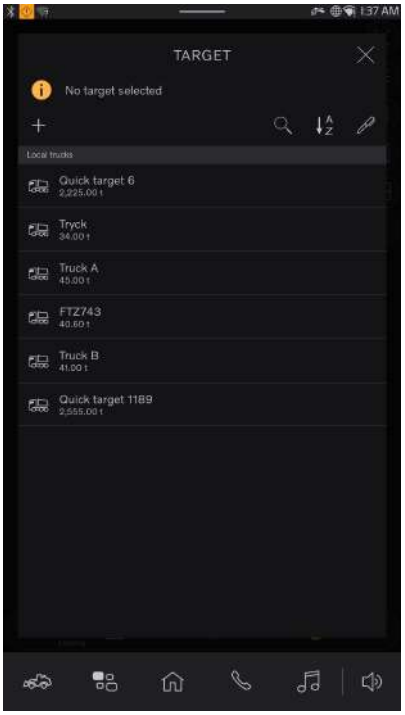

(b) Truck selection

Figure 2.12: Truck selection options in the Co-Pilot

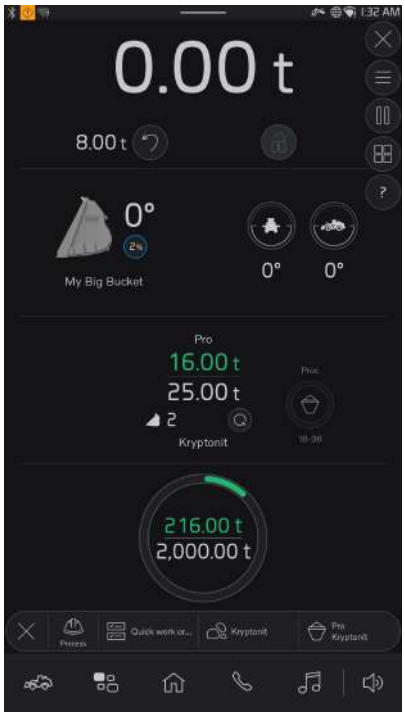

(a) Truck and trailer loading

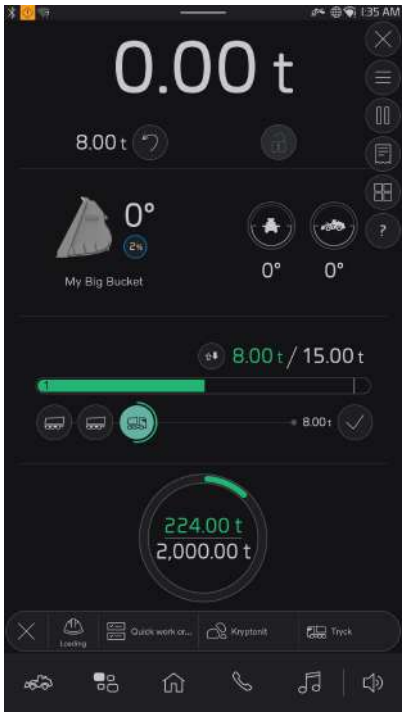

(b) Truck loading

Figure 2.13: Different applications for the Co-Pilot

2.6 Plastics

The polymeric structure of plastics can be split up into two main groups: thermoplastics and thermosets, see Figure 2.14. Thermoplastics have a reversible chemical bond with no cross-link between the polymer chains, meaning they soften when heated, making them suitable for injection molding. On the other hand, the strong covalent bond between the polymer chains of a thermoset creates an irreversible chemical bond, therefore making it more heat resistant and cannot be remelted. [5] There are plastic groups that share properties with the main groups. Thermoplastic Elastomer (TPE) is rubber-like elastic after cooling and, as the name suggests, can be re-shaped. Thermoset elastomers are cross-linked when vulcanized (cured), meaning they can not be re-shaped. Examples of elastomers include natural rubber and silicone rubber.

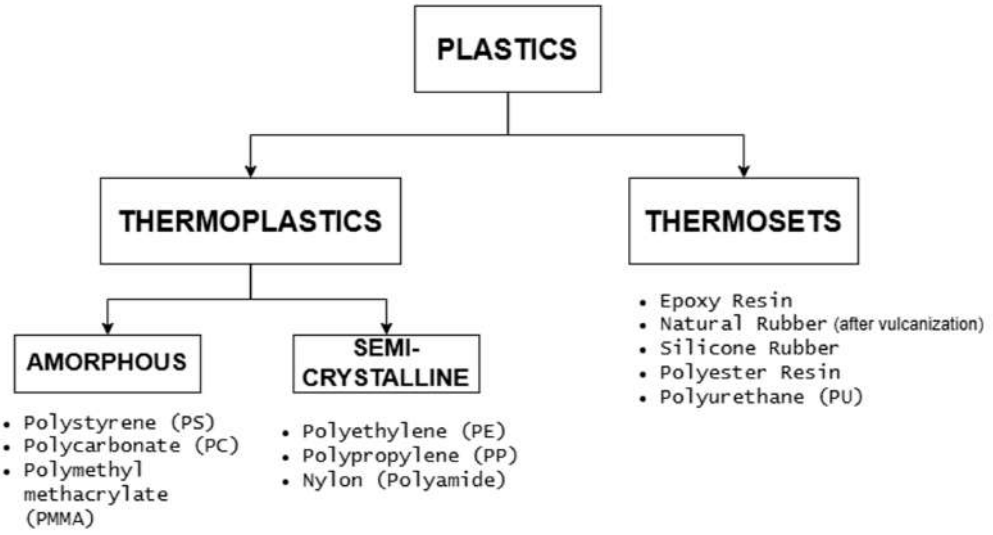

Figure 2.14: Plastic polymer structure

2.6.1 Connection methods in plastics

There are many different ways of joining plastic components together and creating a rigid assembly. The classification of connection methods is not very precise according to [6] they can be roughly divided into detachable, semi-detachable and non-detachable connections. For the application in this project, it is known that the two halves of the joystick need to be joined together. They are split into two pieces (front and back joystick handles) for manufacturing and assembly purposes. After buttons and switches are mounted from the inside of each handle half, they are joined together either using a permanent or non-permanent method. For brevity, not all connection types will be discussed, only the ones practical for the application of joining the two joystick halves.

Detachable Connections:
Detachable connections are required in case of serviceability.

- **Screws**
  Screws for plastic assemblies are designed for direct assembly into plastic materials. The pilot holes are molded into the part with the correct dimensions so that the screw form the threads itself. The exact type of screw depends on the material choice and will affect for example the flank angle to reduce the risk of cracking. The assembly process is simple and both tools and materials are inexpensive, making this process a candidate for the joystick. The con with screws are that they increase the number of parts, require space and increases assembly time and therefore cost. Furthermore, visible holes can be negative for aesthetics but can be plugged if necessary, which also requires additional components. The orientation of the holes needs to be parallel with the movement direction of the molds to avoid undercuts and provide acceptable release angles. This manufacturing constraint is critical and needs to be taken into

account when the parting line is decided.

- **Snap fit**
  Snap-fit tabs are molded into the parts with a hook-like feature on one half and a matching groove on the other half, see Figure 2.15. The connection is quick and easy to install, meaning the assembly time would be minimal. A downside would be increased mold complexity due to undercuts. There are different types of snap fit geometries, but the principles are all the same: hook with latch. Depending on the latch geometry, they can either be detachable or semi-detachable, meaning there is no obvious way to release the latch. For aesthetic reasons, you want to minimize visible connections, but this can make disassembly nearly impossible without damage to the plastic components.

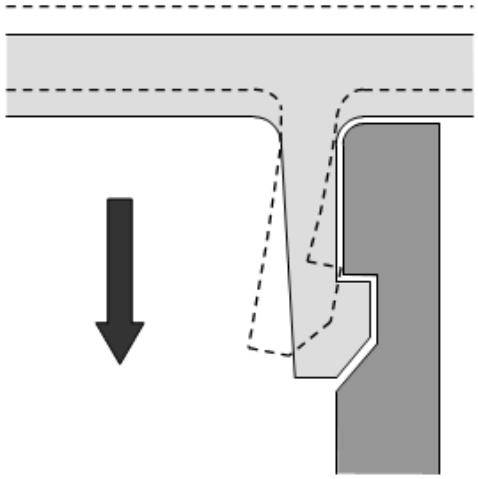

Figure 2.15: Cantilever Snap-fit [7], CC-BY-SA 3.0

Non-detachable Connections:
Non-detachable connections can offer better IP protection and a nicer finish, with the downside of being permanently attached, meaning no repairs can be performed without completely changing the joystick's handles for new ones. The assembly process is usually more complex or time-consuming compared to the detachable connections, requiring tailor-made machines.

- **Welding**
  Welding in plastics can be done in several different ways, the following methods will be discussed: ultrasonic, vibration and hot plate welding. Ultrasonic welding converts high-frequency electrical energy into mechanical motion that generates heat locally on the mating surfaces. The parts vibrate vertically (20-40 kHz) within microns. The difference from friction welding is that the parts move horizontally under higher pressure and lower frequencies. Vibration welding is, however, limited to 2D weld planes, which would make it unfeasible unless the parting line is a perfect plane. Hot plate welding uses a heated

surface to melt the joining surfaces on the two halves, which are then moved together to create a strong bond. Welding is usually done around the circumference of the part which is good in terms of saving space. The geometry of the welded surfaces is rather simple, featuring a lip for alignment which has a small influence on the maneuverability. Welding can provide a nice finish, with the downside of the need for expensive equipment and a permanent connection.

It should be noted that the materials for the welding methods must be two thermoplastics that are chemically compatible to create the molecular bond. It is possible to weld two different thermoplastics with similar molecular structure however, the melting temperature needs to be within 6 degrees Celsius [8]. Furthermore, it is explained that "only similar amorphous polymers have an excellent likelihood of being weldable to each other. The chemical properties of any semi-crystalline material make each one only compatible with itself." [8]. For the joystick, a thermoplastic will most likely be used (since injection molding) and the same material for both handle halves, so these problems are not relevant, but good to consider.

- **Adhesive**
  Similar to welding, adhesives will create a clean look, with the downside of being impossible to perform any repairs without the need for replacing the plastic handles. The glue can be tricky to apply in the correct areas and PPE (Personal Protective Equipment) is required for the safety of the operator. Gluing by hand can be time-consuming and using a machine is both complicated and expensive.

2.6.2 Surface finish

One commonly used mold texture standard is VDI 3400 and SPI finish. VDI 3400 is a standard set by the Society of German Engineers, Verein Deutscher Ingenieure (VDI) and covers 45 grades of textures with the naming convention VDI 3400 #0 to #45 [9]. The Roughness Average (RA) which describes the surface roughness of a material ranges from 0.10 to 18.00 μm. There are several methods to achieve the textured surface finish, ranging from chemical etching, laser texturing, abrasive polishing, to Electro Discharge Machining (EDM). What method used depends on the mold-making company, the type of surface texture and mold geometry.

2.7 Injection molding principles

Injection molding (IM) is a common manufacturing technique for medium and large production volumes of identical plastic parts (1000-100.000+ units) at a relatively low cost, but could occasionally be used in lower volumes as low as 500 units [10]. The process of IM consists of a few steps: melt plastic pellets and build pressure, clamp mold together, fill mold cavity with melted plastic, cool the plastic until so-

lidified, mold opening and eject the part. The process is then repeated, producing plastic components that match the shape of the mold cavity [11].

An injection molding machine comprises the injector and the clamping machine, see Figure 2.16. The injector is fed with plastic granulate pellets in a hopper, which guides them into the barrel. The barrel is wrapped with heater bands which melt the plastic granulate and is mixed using the reciprocating screw. Once the desired amount of plastic is mixed and melted, the screw plunges forward and the plastic is injected in the mold cavity thru the nozzle. The cavity half of the mold is stationary, while the core half of the mold is part of the movable plate. Once the plastic has been injected and the part is ready for ejection, the part is designed to stick to the core half of the mold since this is where the ejector pins are mounted. The motion of the mold opening will push the ejector pins, which are later retracted automatically due to them being spring-loaded.

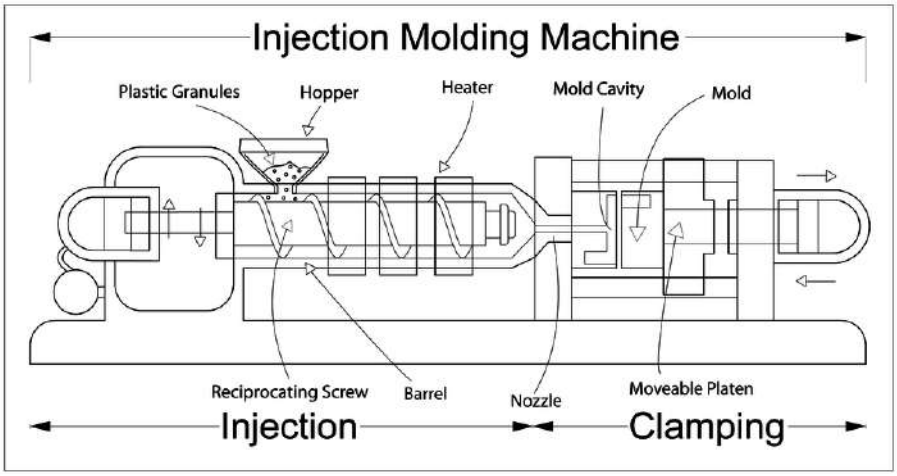

Figure 2.16: Injection molding machine [12], CC-BY-SA

Since the plastic flows in the mold cavity and then solidifies there are significant design restrictions to the manufacturing method. The mold usually consists of two mold halves made of either plastic, aluminum or steel depending on the production volume, but there are other factors contributing to the mold material selection. One of the mold halves is stationary while the other side moves away, therefore the part should be designed in a way such that there are no undercuts, smooth transitions, rounded edges, and draft angles ensuring that the mold can be split without harming the part, [10]. The flow of the plastic melt is another important aspect to achieve a part without imperfections. Since the plastic goes from melt to solid, large gradients in material thickness could lead to:

- **Warping**:
  When sections cool and shrink unevenly, the part could bend due to the stresses created in the material. When the plastic shrinks and warps, it may press excessively against the mold walls, potentially causing drag marks as the mold

is opened.

- **Sink marks**:
  Sink marks are created when the part has large sections where the core solidifies before the outer surface. This could lead to the surface sinking into the part and thereby leaving the walls uneven and not flat.

- **Knit lines**:
  If the geometry causes multiple flows to converge as the melt temperature decreases, a knit line may form at the meeting point where the temperature is too low for it to blend properly. The knit line appears as a thin, hair-like discoloration, and could also weaken the part according to [10].

- **Short shots**:
  Short shots are trapped air in a cavity, hindering the melted plastic from fully protruding and thereby leaving bubbles and holes in the part. Thin ribs are especially prone to short shots. Vents are therefore required to relieve the pressure buildup during the injection process. Vents are approximately 0.005-0.04 mm deep, which ensures plastic can not flow through and avoids noticeable parting lines.

IM is a cost-effective manufacturing method for larger volumes of plastic details with a wide range of materials. By following certain design guidelines, creating complex parts is possible. The drawback is that molds are expensive and tweaking the design when the mold is manufactured is costly. A mold can cost $3000, but could increase up to $100.000+ for more complex parts with multiple sliders.

The purpose of a slider is to enable the molding of undercuts and ensure the part can be ejected without becoming stuck. This makes it possible to produce more complex geometries that could not be achieved with a simple two-part mold. The slider is used to turn the movement of the mold opening/closing into either vertical, horizontal or any other direction. Figure 2.17 illustrates how the slider moves when the mold cavity opens. In the cavity, an angled guide pin is mounted which interacts with the slider to create a perpendicular motion. Sliders are complicated and increase the mold price compared to a simple cavity and core. According to [10], the estimated price increase is around 15-30 %. According to mold manufacturing experts, incorporating a single slider for the type of joystick geometry discussed in this thesis can increase the overall cost by approximately 30–50 % [13].

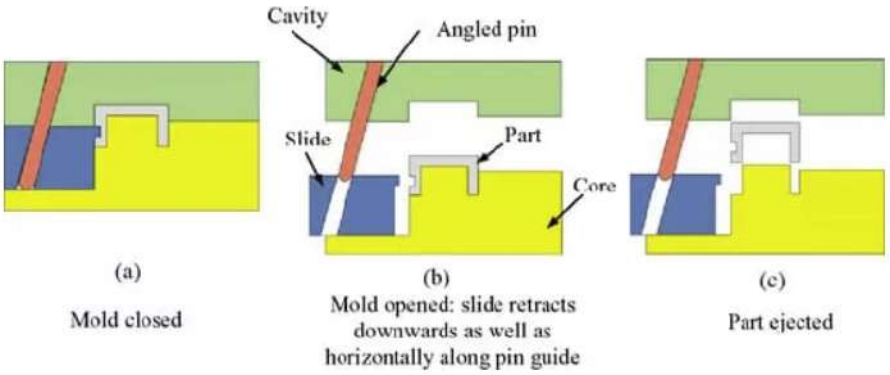

Figure 2.17: Illustration of slider mechanism in IM [14], CC-BY-SA

2.8 Additive manufacturing

Additive manufacturing (AM) is a relatively new sector with a lot of research in recent years. With a diverse application field and various materials from plastic to metals, its growth has transformed the manufacturing sector in the sense of fast and effective, highly customized components with complicated geometries, [15]. Additive manufacturing or often referred as 3D-printing, is a process of joining material in layers, creating an object from a 3D model. The additive manufacturing process can be divided into three steps, according to [15]:

- **Machine setup**:
  Create a mesh by exporting the 3D model as an STL file. In dedicated software, set build parameters and slice the 3D model into layers and export it as a gcode or other machine code.

- **Printing**:
  Insert the machine code into the machine and produce the part. The machine now builds the part layer by layer.

- **Post-processing**:
  Remove the part from the build chamber and clean the finished part from the build material and support structures. If the part is in need of polishing, surface finish or any other after treatments, it is done in this step.

There are several different additive manufacturing methods which can be divided up into seven different methods, see Figure 2.18. The most common types of printing processes are explained for each method.

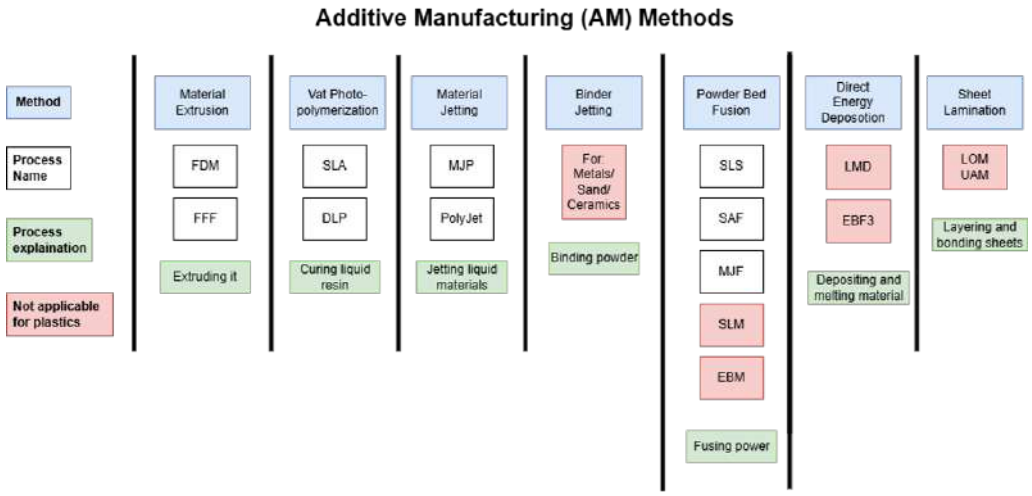

Figure 2.18: Additive manufacturing process methods

Material Extrusion works by extruding thermoplastic filament through a heated nozzle, building the object layer by layer. Fused Deposition Modeling (FDM) and Fused Filament Fabrication (FFF) describe the same method of material extrusion, but under two different names due to FDM being trademarked.

Vat Photopolymerization creates the object by curing layers of liquid resin exposed to an ultraviolet light source [16]. After a layer is cured, the part is moved into the liquid resin and a new layer is ready to be cured. This is repeated until all the layers are cured. Stereolithography (SLA) uses a laser to cure the cross-section of the part through a transparent resin tank. Digital light processing (DLP) rather uses a light projector to cure the resin. [17]

Material Jetting works by applying tiny droplets of liquid jetted onto the build surface and then cured using UV light to build up the model, similar to an ink jet printer. MultiJet Printing (MJP, by 3D Systems) and Poly Jet by Stratasys are both similar processes with slight differences in support material and print head configuration. The process allows for multi-material printing, high resolution; however, not ideal for structural parts as the material tends to degrade under UV exposure.

Binder Jetting jets a binding liquid onto a powder bed to glue the powder together. The powder plus glue together form the model. The powder material can vary from metals to technical ceramics or sand used for creating casting molds. Therefore these manufacturing methods are not applicable for this thesis.

Powder Bed Fusion works by melting and solidifying powder to create the model. Applicable for both plastics like nylon and metals like aluminum or titanium. Selective layer sintering (SLS) is a type of printing where a thin powder bed is exposed to a high-power laser, heating up specific parts of the powder bed and thereby solidifying the polymer in layers, [16]. Multi Jet Fusion (MJF, by HP) work by jet fusing liquid agent to specific areas on the powder which is later fused by thermal energy into a solid layer of part geometry. Selective Absorption Fusion (SAF, by

Stratasys) is a similar method however only uses one of the fusing liquids compared to the MJF which has fusing plus detailing agent. Selective Laser Melting (SLM) uses a fiber laser to fully melt the metal powder. Electron Beam Melting (EBM) uses an electron beam in a vacuum to melt the metal powder, similar to SLM.

Directed Energy Deposition means that the material is simultaneously deposited and melted. Laser Melt Deposition (LMD) works by feeding a wire or powder through a nozzle melted by a laser surrounded by a shielding gas. Electron Beam Freeform Fabrication (EBF3) operates in a vacuum and the material is in wire format. Applicable only for metals.

”Sheet lamination forms 3D objects by stacking material such as paper, plastic or metal foil and laminating them using welding, adhesive, heat or pressure”, [18]. After each layer is bonded the material geometry is cut och milled using a plotter. Laminated Object Manufacturing (LOM) can be used with paper or plastic films and is bonded with adhesive and heat, and cut using a blade or laser. UAM can combine dissimilar metals and is bonded using ultrasonic vibrations and pressure, later Laminated Object Manufacturing (CNC) milled after each layer.

2.9 Ergonomics

The grip can be categorized into two classes according to [19], the power grip and the precision grip. The power grip is used when a tool axis is perpendicular to the forearm and a force is exerted. There are three subclasses depending on whether the force is parallel to the forearm, a saw, for example, if the force is at an angle to the forearm as with a hammer or a pure torque when opening a jar lid. In contrast, the precision grip uses the thumb and fingers to perform precise movements. The precision grip can be split into two classes depending on the location of the tool, whether it is internal to the hand like a knife or external like a pencil. The precision grip has about 20 % of the power grip strength. The cause of this is that the precision grip uses the small muscles in the arm and forearm compared to the power grip which uses large muscle groups to generate the force needed. The power grip is favored for tools that require large forces. A precision grip joystick is of the smaller type, usually incorporating less number of buttons than the power grip joystick, see Figure 2.19.

Figure 2.19: Precision grip joystick (Left) and a power grip joystick (Right)

For the grip strength of a handle, the use of multiple fingers plays a big role. Excluding fingers while grasping an object significantly reduces the strength of the grip; excluding the little finger decreased the overall grip strength by 33 % and excluding the ring finger decreased the grip strength by an overall 21 %, according to [20]. Therefore, excluding fingers when grasping an object is not advised, but could be necessary for the operation of the joystick. The strength of each individual finger plays a big role in what kind of buttons and switches they can operate and press. A similar study in contributions of individual fingers to grip strength has concluded that the index and middle fingers have a greater contribution to grip strength than the ring and little finger in an approximate ratio of, 60:40, according to [21]. Since all fingers contribute to the overall grip strength, no finger can be excluded from grasping the joystick under the condition that they are not being used to actuate buttons. The little finger is weaker compared to the other fingers according to [21]. But it is contributing to such a big loss in grip strength when not included, that it has to help grasp the joystick even though it will not actuate any buttons/switches because of its lower strength.

The recommended wrist orientation is a straight handshake, this could reduce the risk of upper extremity injuries and prevent a loss in grip force [19]. And it is important to prevent unnecessary twisting and bending in the wrist to not overload the hand according to [22]. The hands resting position is described as ”The hand has a functional resting position, in which the wrist is straight, the muscles are relaxed, the fingers lightly curled, and the pressure in the carpal tunnel (the narrow passage in the wrist that encases the median nerve and several tendons) is at its lowest.”, [22]. The Joystick should therefore be designed with consideration of the natural position of the hand to not overwork or risk any injuries to the operator. The joystick at rest should allow the operator to rest his hand in a natural position and thereby minimize the strain in the wrist when deviating from that optimal position.

To design an ergonomic joystick, the interaction with the rest of the body is an important factor, specifically the angles of the arm. According to [23] the least

strained elbow angle is 100° - 110°, which is a key design parameter when designing the neutral lean angles for the joystick, see Figure 2.20. There are no standard lean angles for joysticks but it can be estimated that they are a function of the travel for the main function in the X and Y direction.

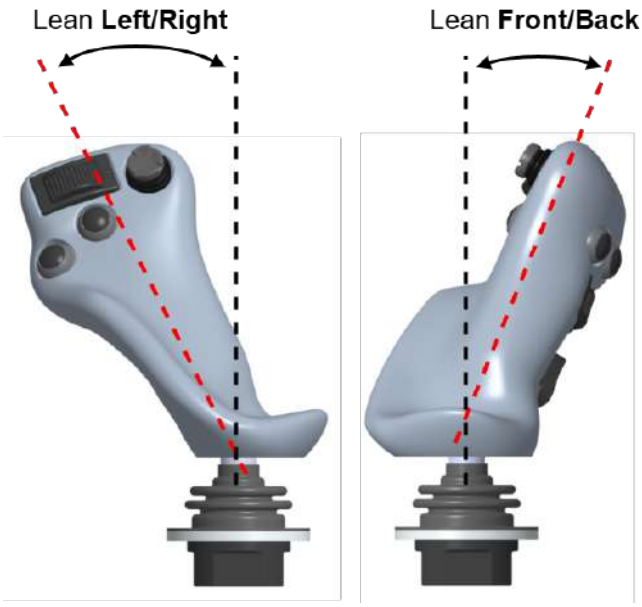

Figure 2.20: Joystick handle natural lean angles

The grip thickness is up for debate, since different studies recommend a wide range of diameters. According to [22], the men in the study had an average right-hand length of 193 mm with a standard deviation of 9 mm and a hand breadth of 87 mm with a standard deviation of 5 mm. Women had overall smaller right hands than men with an average hand length of 179 mm and a standard deviation of 9 mm, and a hand breadth of 78 mm with a standard deviation of 4 mm. Therefore, the optimal grip thickness and length should deviate between women and men but for simplicity and cost effectiveness, one joystick design will be looked at and should therefore be suited for most of operators. Males are recommended to have a grip diameter of 30-40 mm and women 10 % less [24]. There are studies where a slightly larger grip is recommended, [25] recommends a grip diameter of 55-65 mm for males and 50-60 mm for females, and [26] recommends an even larger diameter of 65 mm. Since people with smaller hands most likely will not be able to hold a grip with a larger diameter the aim should be to have a grip diameter of 55-60 mm.

The distance from the base of the wrist to the tip of the extended thumb is known to as the thumb span, see Figure 2.21. This measurement is important to consider when positioning buttons, as they should fall within easy reach of the thumb. However, the thumb span is not a commonly documented hand dimension, and reliable data on it is limited. Therefore, measurements from the 95th and 5th percentile NASA male will be used as a reference, which ranges from -165 mm. Note that these are the maximum distances to thumb tip, so in practice they are reduced in

order to activate the button at the center of the thumb.

Figure 2.21: Measuring the thumb span using a caliper

The torque required to move the joystick influences the risk of injury. Adjusting the acceleration at the end stops has a big effect on the instant of sudden palm and/or finger compression [27]. It is therefore important to have low decelerations at the end stops, which can be achieved with clever design using a secondary spring or rubber bump stops.

2.10 IP rating

Ingress Protection (IP) is a rating system that indicates how well a device or enclosure is shielded against environmental elements such as dust and water. The rating is denoted by a code beginning with "IP" followed by two digits (IPxx) and sometimes an additional letter. The joystick is located inside the cab, where it is protected against the worst environmental effects. It could still be affected by the operator, either cleaning the inside of the WLO or just spilling liquids on the joystick. The WLO may also be operated in dusty environments, such as concrete production plants, where fine chalk dust could enter the cab and potentially damage electronic components if they are not properly sealed. The IP rating is based on more or less rigorous tests depending on the required class.

In the IP code, the first "x" should be changed out by a 0-6 digit or an uppercase "X". The "X" means there is no protection rating due to insufficient data, regardless of solids or liquids. To quantify the level of protection, the "x" can be changed to a number in the range of 0-6, see table 2.1 for specific ratings.

There could also be a "K" after the number, which is defined in ISO 20653 instead of IEC 60529, it is a harsher requirement that tends to be used in the automotive

industry, where the tests are performed with vibrations or specific dust. The second "x" in the IP-rating is aimed for liquid ingress and is a digit between 0-9 and could be combined with a "K" for a harsher requirement, such as powerful jets, see table 2.2

Table 2.1: IP Rating Protection Levels for Solids

Rating	Protection Against	Effective Against
0	—	No protection against contact or entry of objects.
1	$>$ 50 mm	Shields against large surfaces such as the back of a hand but does not prevent intentional contact.
2	$>$ 12.5 mm	Prevents access to fingers or similarly sized objects.
3	$>$ 2.5 mm	Protects against tools, thick wires, and similar objects.
4	$>$ 1 mm	Blocks entry of most wires, slender screws, and small insects.
5	Dust-protected	Some dust may enter, but not in amounts that could interfere with the operation of the device.
6	Fully dust-tight	Complete protection from dust, prevents all contact.

Table 2.2: IP Rating Protection Levels for Liquid

Level	Protection Against	Effective Against
0	None	No protection
1	Dripping water	Dripping water (vertically falling drops)
2	Dripping water (tilted)	Dripping water when tilted at **15°**
3	Spraying water	Water spray up to **60° angle**
4	Splashing water	Water splashing from any direction
5	Water jets	Water projected from a **6.3 mm nozzle**
6	Powerful water jets	Water projected from a **12.5 mm nozzle**
6K	Powerful water jets (high pressure)	Strong water jets from any direction
7	Immersion (up to 1 m)	Temporary water immersion
8	Immersion (beyond 1 m)	Continuous immersion
9	High-temperature water jets	High-pressure, high-temperature jets

2.11 Electrical Hardware Considerations

Electrical components exposed to humidity over extended periods can absorb moisture, leading to corrosion, material degradation, and potentially causing short circuits or component failure [28]. Preventing humidity from accessing terminals, Printed Circuit Board (PCB), buttons and switches is essential for the function. There are two ways of preventing humidity and water from accessing the terminals,

either the enclosed area is protected from humidity entering by sealing the gap between the component and the panel with a type of gasket. If the humidity is allowed to enter the enclosed area, the exposed terminals need to be protected from the humidity by, for example, a coating of silicone gel, conformal coating or epoxy.

"The type of terminal for the button/switches (solder, connector or with pre-installed wires) is chosen depending on the sealing of the joystick. If the joystick is completely sealed any terminal can be chosen since there is no risk of the terminal shorting." -[29].

Figure 2.22 illustrates the naming convention for the components that will be used in this thesis. Components circled in blue are inside the scope of the thesis and are therefore the main focus. The following lists categorize buttons as either "on the base" or "on the handle", with the exact button types subject to further discussion.

- **Buttons on base:**
- F/R Lock
- Electronic Lock
- Main function (1st, 2nd)

- **Buttons on handle:**
- FNR Selector
- 3rd function
- 4th function
- Horn
- Diff-lock
- Kick-down
- Co-Pilot remote control
- Additional Programmable Button(s)

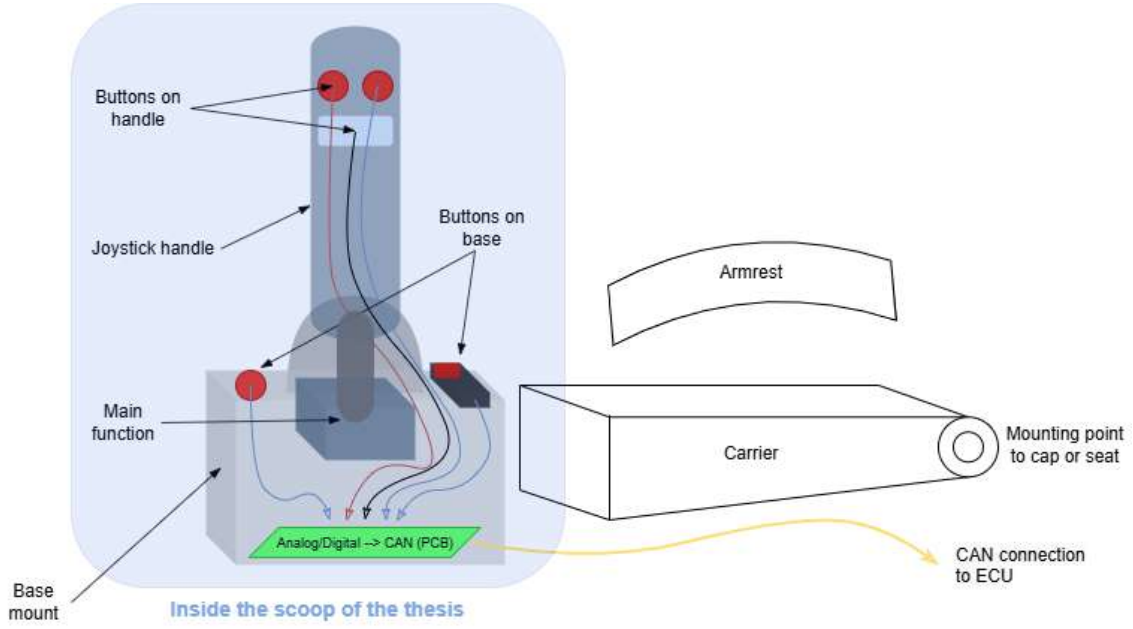

Figure 2.22: Naming convention for components

2.12 Optimization

Optimization can mean many things but in general it comes down to finding the input variables that create the best response(s) for a specific goal. For this thesis, two types of optimization methods were applied, DOE and FEA.

There are many input variables in the IM process that will affect part quality, including injection location, mold temperature, injection temperature, injection time, and melt temperature. The goal is therefore to perform a DOE to map out which variables impact different results in the IM process.

To verify the structural integrity of the joysticks under anticipated operational loads, FEA is conducted. This simulation-based approach enables the identification of stress concentrations and potential failure areas.

2.12.1 Design of Experiments (DOE)

The aim of DOE is to analyze the relationship between several input variables and output variables, to determine which input variables are responsible for the observed changes in the response, and to use this model for process improvements or other decision-making. [30] The input variables are called factors and the output variable is the response, see Figure 2.23. Each factor has at least two levels, where the levels are specific values a factor can take.

DOE is a way to systematically create a response model (also called a surrogate model) with a limited number of data points (runs). Each run (can be a simulation

or test experiment) is expensive, and you want to perform the least possible runs, but still enough to create an accurate model.

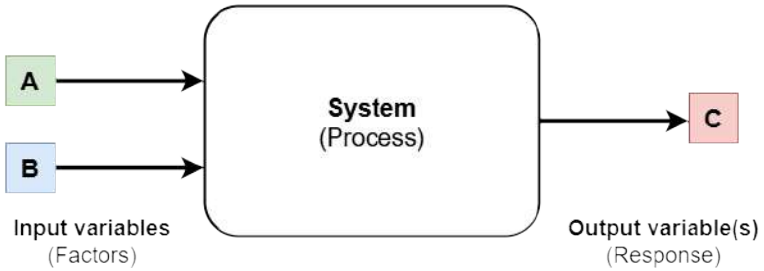

Figure 2.23: Overview of the DOE process

First step when a new system with many factors is to be analyzed, is to identify which factors have the most influence on the response(s) and which can be screened out before the optimization. This is done by performing a factor screening design. Screening designs are a type of experimental design, but specifically setup to identify main effects and interactions for linear and non-linear systems. Usually only 2 or 3 level designs with fewer runs than an optimization design. Below are some common terms that are used in the context of DOE:

- A **main effect** is the primary impact of a single factor on the response variable.
- An **interaction** occurs when the effect of one factor on the response depends on the level of another factor.
- **Confounding (Aliasing)** occurs when the effects of two or more factors or interactions cannot be distinguished from one another due to the structure of the experimental design. For example, if *Factor A*Factor B* is confounded with *Factor C*, it is not possible to tell if either *Factor A*Factor B* or *Factor C* is causing the effect on the response. This happens in designs where not every combination of factors is tested to keep the number of runs low however, it limits the ability to draw clear conclusions.
- **Orthogonality** means that factor interactions are uncorrelated and independent. If the main effects are orthogonal to two-factor interactions means that confounding is prevented. Otherwise, changes in the main effect might appear as changes in interactions. Orthogonality is therefore desired to easier to analyze the response.

Most screening designs assume minimal or no interactions, which means main effects are confounded with two-factor interactions. This is the case for standard screening designs like Plackett-Burman where interactions are partially confounded with main effects. Standard screening design focuses on estimating main effects and relies on two levels (high and low), meaning it works best for linear systems. Center points can be added to the design however, these would only detect if curvature exists, not

identify the factors responsible for the non-linear effect.

Definitive Screening Designs (DSD) can be used with a combination of 2-level categorical factors and continuous factors with 3 levels. The 3 levels allow the quadratic effects to be studied and identify the responsible factor(s). DSD avoids confounding of factors since main effects are orthogonal to interactions.

Figure 2.24 shows the absolute correlations for factors using a color map for Definitive Screening Design and Plackett-Burman (Standard Design). Blue indicates no correlation (0) and red means full correlation (1). It is evident that in the standard design, interactions are correlated with main effects for most 2-factor (and for this example, 3-factor) interactions. Compare it to the definitive screening design where all main effects are orthogonal to 2 factor interactions. The trade-off is that a few additional runs are necessary. The small correlation for *X5* is due to this factor being 2 2-level categorical however, the correlation is small.

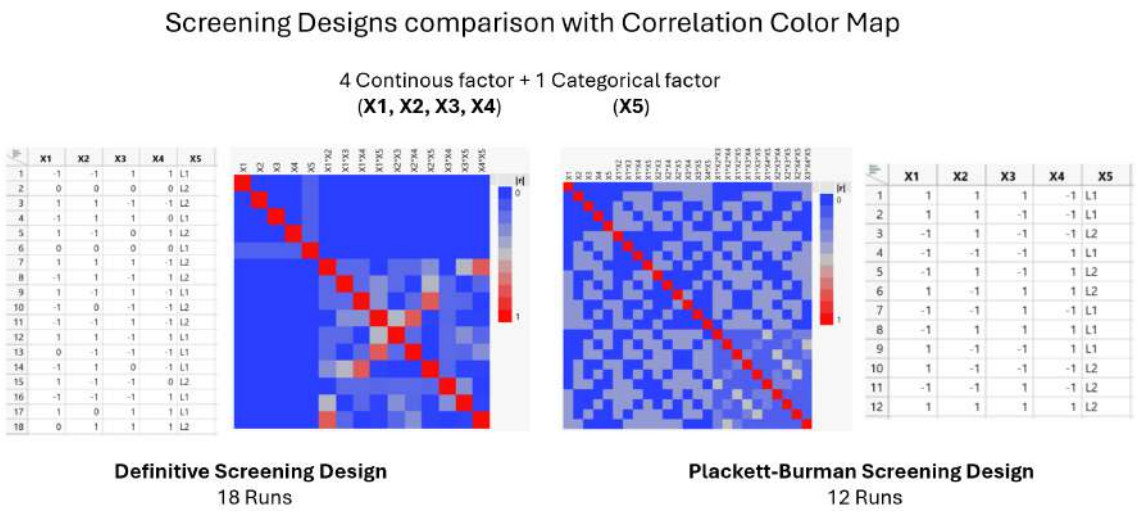

Figure 2.24: Color Map on correlations for Definitive Screening Design (left) vs Plackett-Burman (right)

Significant factors were identified using a t-test and observing the p-value. The null hypothesis (H_0) states that the effect of the arbitrary factor (i) on the response is zero. The alternative hypothesis states that the effect is non-zero (significant). Equation 2.1-2.2 provides an example for a factor i.

$$H_0 : \quad \beta_i = 0 \qquad \text{(The effect of factor } i \text{ is zero)} \tag{2.1}$$

$$H_A : \quad \beta_i \neq 0 \qquad \text{(Factor } i \text{ has significant effect)} \tag{2.2}$$

The p-value indicates the probability of observing a test statistic as extreme as the one obtained, assuming the null hypothesis (H_0) is true. It reflects the strength of evidence against H_0 and can be interpreted as the smallest significance level (typically $\alpha < 0.05$) at which H_0 would be rejected. A result is considered statistically significant if H_0 is rejected, so the p-value also shows the minimum α at which the data are significant. This allows conclusions to be drawn without predefining a specific significance level. [30]

Once the significant factors have been identified using a screening design, the next step is to perform the optimization. There are many different types of experimental designs with the same goal but different ways of using the data most efficiently. For example, Full Factorial design, Fractional Factorial design, Central Composite design or Box-Behnken design. Figure 2.25 illustrates the steps to perform a full factorial design of experiments.

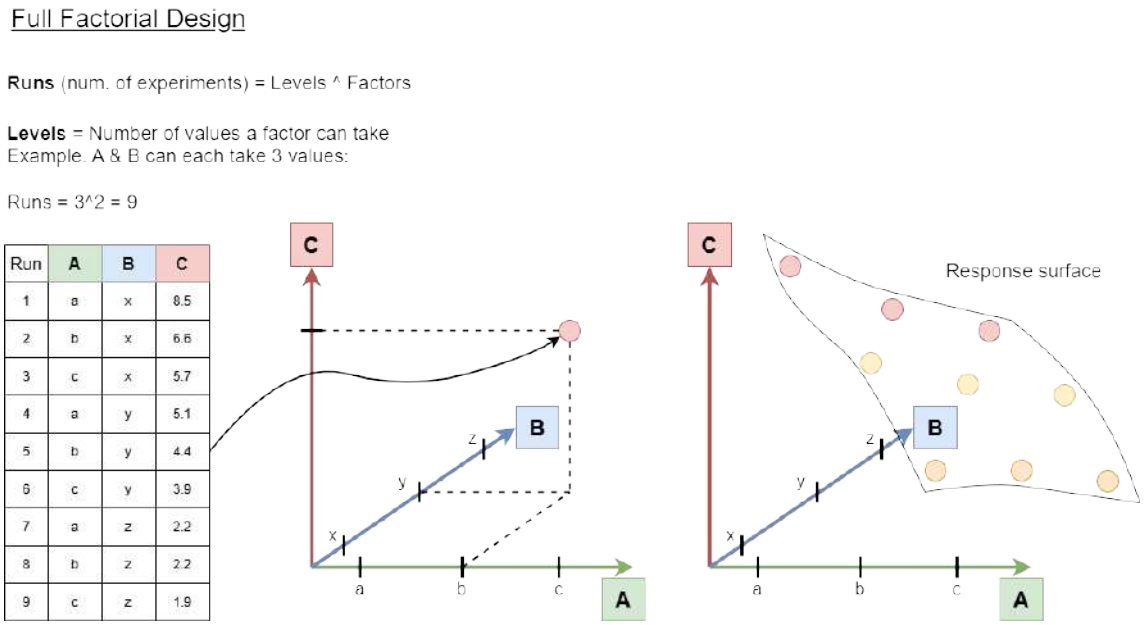

Figure 2.25: Illustration of how a Full factorial DOE is performed

Full factorial design tests all possible combinations of the levels for the factors. This will ensure both individual and interaction effects are captured. Number of runs is therefore $\text{levels}^{\text{factors}}$, meaning a lot of experiments will have to be conducted. If runs are expensive, Fractional factorial design reduces the number of experiments by strategically excluding certain combinations, while still capturing essential responses from the process.

Once the experiments are run and responses are documented, the next step is to fit a model that captures the response as accurately as possible. Depending on the physics of the experiment, the response might be for example linear, quadratic or logarithmic. An example of a linear model for two factors can be observed in Equa-

tion 2.3, as described in [31].

$$Y = \beta_0 + \beta_1 X_1 + \beta_2 X_2 + \beta_{12} X_1 X_2 + \cdots + \varepsilon \tag{2.3}$$

where:

- Y is the observed response (output).
- $X_1, X_2, \ldots$ are the input factors (independent variables), indexed by i, j.
- β_0 is the intercept parameter (overall mean).
- β_i are the main effect coefficients.
- β_{ij} are the interaction effect coefficients between factors.
- ε is the independent and normally distributed error term.

The final step is to validate the model to ensure it generalizes well and does not suffer from overfitting. A central method in this process is cross-validation, which partitions the dataset, typically using an 80/20 % training/validation split. The model is built exclusively on the training set, while the validation set provides an independent assessment of predictive accuracy. Key performance metrics such as RMSE (or RASE), R^2, and analysis of residuals are also used to evaluate model fitness. These validation steps collectively build confidence in the model's robustness. Critical indicators for assessing model validity include:

- Cross-validation using training and test datasets, split in 80/20 %.
- RMSE (Root Mean Square Error)/RASE (Root Averaged Square Error) should be close to 0.
- R^2 (Will be referred to as: "RSquare") ranges from 0 to 1. A model with an RSquare value of 1 perfectly predicts the response, while a model with 0 has no explanatory power.
- Residual is the difference between the predicted and observed value. It should be as small as possible and not show any sign of a pattern.

2.12.2 Finite Element Analysis (FEA)

This section is based on formulations described in [32].

The behavior of an object under load can be predicted using FEA. Calculations are made using the Finite Element Method (FEM) which is a mathematical interpretation of the real world and FEA is the analysis of the results provided by FEM [33]. A common application is analyzing and simulating deformation responses when a load or displacement is applied to a geometry. FEM simulations can be used to solve for stress, stiffness, fatigue life, eigen-frequencies, buckling loads, vibrations, and heat fluxes, among other physical responses. Partial Differential Equations (PDE) are numerically approximated since for the majority of geometries and problems analyzed using FEM, PDEs cannot be solved analytically. Instead, discretization methods can be used to solve the PDEs using numerical methods. A Boundary Value Problem (BVP) consists of Differential Equations (DE) and Boundary Conditions (BC) [34].

A FEM solution is building on approximating a geometry using a mesh consisting of a number of nodes combined into elements in 2D or 3D. The elements can consist of rectangular elements, see Figure 2.26a, or triangular, tetrahedral, pyramidal, and hexahedral, among other variations. The geometry is meshed and necessary boundary conditions and forces are applied, see Figure 2.26b. A mesh can include multiple types of elements and is then called a mixed mesh.

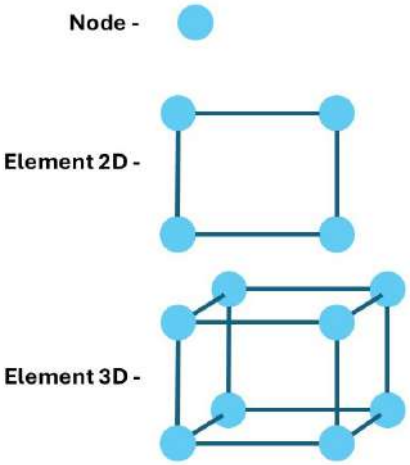

(a) Representation of nodes and 2D/3D finite elements

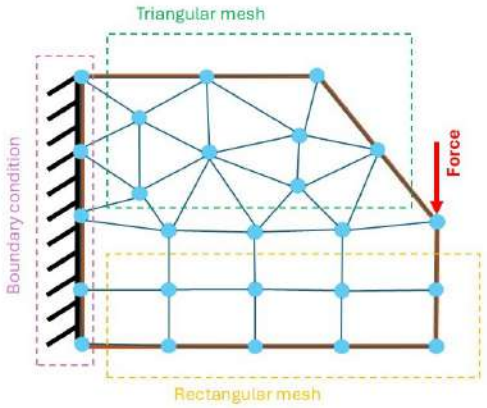

(b) A meshed structure showing a combination of triangular and rectangular elements, with fixed boundary conditions on the left and an applied force on the right

Figure 2.26: Illustration of basic FEM components and meshing strategy.

The FE equation is stated in Equation 2.4, and unknown nodal displacements are solved for in the linear system. **K** is the stiffness matrix of the system that describes how well the structure resists deformation, high values in the **K** matrix imply a stiff structure. **a** is a vector with known and unknown nodal displacements and is what the system is solved for. **Ka** forms the Left Hand Side of the equation system and should balance the Right Hand Side, where **f** is the load vector that includes body forces, traction, point loads, and reaction forces. The LHS and RHS should be in equilibrium for the internal and external forces to be in balance; the internal forces **Ka** describe how the structure resists deformation, whilst **f** describes the external forces applied to the structure [35].

FE equation

$$\mathbf{Ka} = \mathbf{f} \tag{2.4}$$

Deriving the FE equations for a linear elasticity problem involves several steps, beginning with stating the Strong Form (SF) of the problem. The stress-strain relation $\sigma = \mathbf{D}\varepsilon$ describes the stress in a material in relation to the strain. In solid mechanics, the material stiffness matrix **D** (shear and bulk modulus) relates the

stress to strain. Isotropic linear elastic materials have a bulk modulus depending on the Young's modulus and the Poisson ratio [32]. Up until the yielding point, most materials follow an isotropic linear elastic behavior. A strain tensor ε can be described as the relation between the deformation of the original shape of the structure resulting in $\varepsilon = \nabla \mathbf{u}$. If the displacement is large compared to the body dimension, the strain is high and rotation occurs without stretching, a large deformation theory could be considered. The Green-Lagrange Strain Tensor is an alternative for a large deformation simulation. In this thesis, only small deformation theory is considered, as it is sufficient for the expected load cases.

The first equation of the SF is derived from the equilibrium equation $\mathbf{F}_{int} = \mathbf{F}_{ext}$ where the equation represents that the external forces acting on the body equal the internal forces in the material. $\mathbf{F}_{int}$ can be substituted with the divergence of the stress tensor, $\nabla\sigma$. The strain tensor is substituted in the stress-strain relation which results in $\mathbf{F}_{int} = \tilde{\nabla}^T \mathbf{D} \nabla \mathbf{u}$.

$\mathbf{F}_{ext}$ represents the external forces and is replaced by bodyforces $\mathbf{f}$. The SF of the problem is defined by substituting $\mathbf{F}_{int} = \mathbf{F}_{ext}$ and include relevant displacement boundary conditions (Dirichlet) $\mathbf{u} = \mathbf{g}$ on S_g and traction boundary conditions (Neumann) $\mathbf{t} = \mathbf{h}$ on S_h. S_g and S_h are the boundary areas where the boundary condition is applied which could be a node, edge or area.

Strong Form:

$\tilde{\nabla}^T \mathbf{D} \nabla \mathbf{u} + \mathbf{f} = 0$ in Ω
$\mathbf{u} = \mathbf{g}$ on S_g
$\mathbf{t} = \mathbf{h}$ on S_h

Deriving the Weak Form (WF) includes multiplying the SF with an arbitrary test function and integrating by parts, see Equation 2.5. Shape functions $\mathbf{N}(x)$ and strain-displacement matrix $\mathbf{B}(x) = \nabla \mathbf{N}(x)$ approximates the displacement $\mathbf{u}(x) = \mathbf{N}(x)\mathbf{u}^e$ and strain is computed from displacement $\varepsilon \nabla \mathbf{u} = \mathbf{B}\mathbf{u}^e$. The FE-equation is given by assembling the stiffness matrix $\mathbf{K}^e = \int_{\Omega^e} \mathbf{B}^T \mathbf{D} \mathbf{B} \, d\Omega$ and element force vector $\mathbf{F}^e = \int_{\Omega^e} \mathbf{N}^T \mathbf{f} \, d\Omega \; + \; \int_{S_h^e} \mathbf{N}^T \mathbf{h} \, dS$ in the WF, see equation 2.6. As a result of solving the problem elementwise, the approximate solution resembles the exact solution but cannot replicate it exactly, resulting in a consistent approximation error, see Figure 2.27. While the approximated solution always contains some error, this error can be minimized through mesh convergence study, evaluating suitable element types, and ensuring accurate boundary conditions.

Weak form

$$\int_\Omega (\nabla \delta \mathbf{u})^T \mathbf{D} \nabla \mathbf{u} \, d\Omega = \int_\Omega \delta \mathbf{u}^T \mathbf{f} \, d\Omega + \int_{S_h} \delta \mathbf{u}^T \mathbf{h} \, dS \tag{2.5}$$

Full FE equation

$$\int_{\Omega^e} \mathbf{B}^T\mathbf{D}\mathbf{B}\, d\Omega \cdot \mathbf{a} \;=\; \int_{\Omega^e} \mathbf{N}^T\mathbf{f}\, d\Omega \;+\; \int_{S_h^e} \mathbf{N}^T\mathbf{h}\, dS \tag{2.6}$$

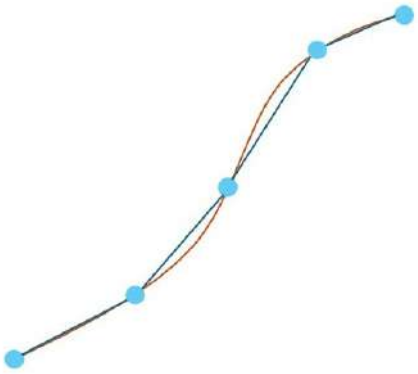

Figure 2.27: Exact solution (Brown) and approximation (black with nodes in blue)

Boundary conditions
BC are crucial in modeling a structure after its real-world application. There are two primary types of BCs: **Dirichlet** and **Neumann**. Dirichlet BCs specify a displacement of the structure at a certain point or boundary, commonly used when a part is either fixed or prescribed with a known displacement. A Neumann BC defines applied forces or tractions on the boundary, such as external forces. In most applications, both types are often used in combination with each other and thereby creating a mixed BC where the physical application of the structure depends on both prescribed displacements and applied forces.

Contacts
Contact definitions complement BCs by describing the interaction between two or more bodies within a structure that are, or may come into contact. In ANSYS there are five types of contacts: **bonded**, **no separation**, **frictionless**, **frictional** and **rough** [36]. These contacts concern how bodies intend to interact with each other and are described in the list below.

Contacts in ANSYS:

- **Bonded** - The default contact configuration, contact regions between two objects are bonded together and cannot slide or separate from each other. A linear solution will be possible since the contact area will not change during the application of a load.
- **No separation** - The affected surfaces of two objects cannot separate from each other but can slide without any frictional resistance.
- **Frictionless** - The two contact surfaces can detach from each other, resulting in zero normal pressure. In the tangential direction, the objects can slide without resistance. The solution is nonlinear since the area of contact may vary.

- **Frictional** - Similar to **Frictionless** with the difference of a frictional response force in the sliding direction. Shear stresses can occur up to a certain magnitude before the interface starts sliding.
- **Rough** - Similar to **Frictionless** with the difference of no sliding between contact bodies. The frictional response corresponds to an infinite friction coefficient between interfacing surfaces.

2.13 DFMA

Design for manufacturing and assembly (DFMA) is a strategy used in the product development process, with the goal of reducing assembly and manufacturing costs by exploring different paths early in the development cycle [37]. It provides estimated costs for manufacturing methods and assembly processes which can be used to calculate the final production cost. The methods follow the outlined process as illustrated in Figure 2.28, which begins by defining the product specifications and splitting the manufacturing and assembly into separate paths. This method can be used early in the design phase with the possibility of providing an estimated final design cost. Therefore several different designs can be compared before locking down the final design and manufacturing methods.

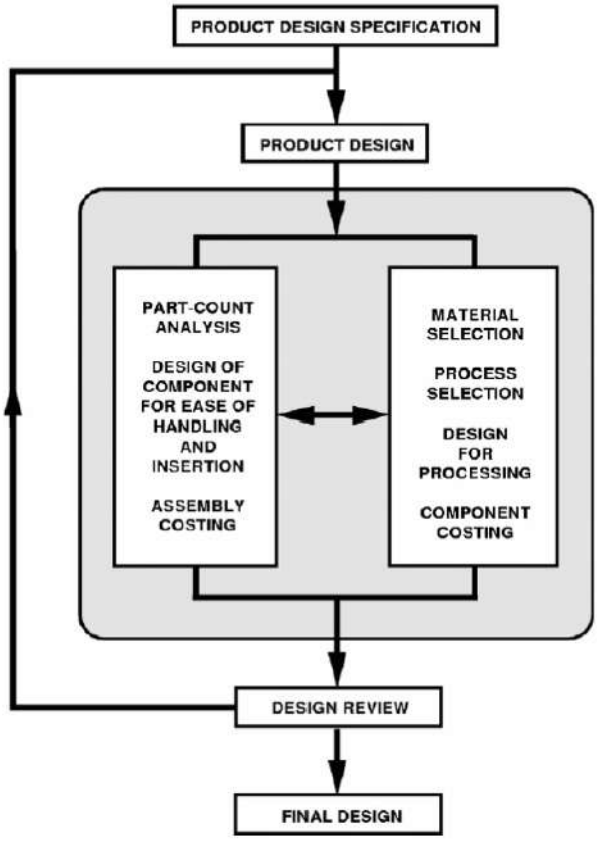

Figure 2.28: Outline process for design and manufacturing taken from [37]

Design for Assembly (DFA)

DFA is part of the DFMA process with the goal of reducing the number of parts in an assembly and thereby reducing the assembly cost. This is done by using an assembly costing model [37], which estimates the total manual assembly cost. It comprises of handling and fitting indexes which translate into handling and fitting times multiplied by the labor rate, resulting in the total assembly cost.

The total cost of manual assembly is calculated using Equation 2.7:

$$C_{ma} = C_1(F + H) \tag{2.7}$$

Component handling analysis is calculated according to Equation 2.8:

$$H = A_h + \left[\sum_{i=1}^{n} P_{o_i} + \sum_{i=1}^{n} P_{g_i}\right] \tag{2.8}$$

Component fitting analysis is according to Equation 2.9:

$$F = A_f + \left[\sum_{i=1}^{n} P_{f_i} + \sum_{i=1}^{n} P_{a_i}\right] \tag{2.9}$$

Design for manufacturing (DFM)
DFM is the practice of designing a product and having the manufacturing aspect in mind. DFM can be split up in five core concepts [38]:

- Consider manufacturing processes early
- Simplify product design
- Use standardize components if possible
- Optimize material usage
- Incorporate multiple parts in the same for a reduced number of assembly steps

The objective of the manufacturing optimization varies depending on the selected production process, product type and intended batch size. In high-volume production using IM, the focus is often aimed on minimizing cycle times to improve overall efficiency. In such cases, reducing the duration of each molding cycle can lead to time and cost savings over large batches.

If AM is chosen, the optimization may shift toward utilizing the design flexibility. This could involve increasing the complexity of the product without leading to additional printing time, therefore making full use of the manufacturing method.

For this reason, it is important that the manufacturing method be selected early in the design phase, as it influences both the form of the product and the possibility of optimization. The design must align with the strengths and limitations of the chosen manufacturing technique to ensure efficiency, functionality, and manufacturability throughout the production process.

3
Methodology

This chapter explains how the project was carried out. It begins with how requirements were gathered, based on user input, existing products, and discussions with operators. It then describes how different joystick concepts were developed and evaluated, focusing on ergonomics and usability. Prototypes were built and tested, and simulations such as FEA and DOE were applied to the design.

3.1 The product development process

The project has followed a product development methodology with influence of an optimization part [39], see Figure 3.1. A key aspect of the development process is the early consideration of both optimization and DFMA. This approach is essential to ensure product feasibility and to minimize risks such as manufacturing constraints or impractical design features. While the application of optimization and DFMA becomes more pronounced during the detailed design phase, incorporating these principles from the initial stages significantly streamlines later stages of development.

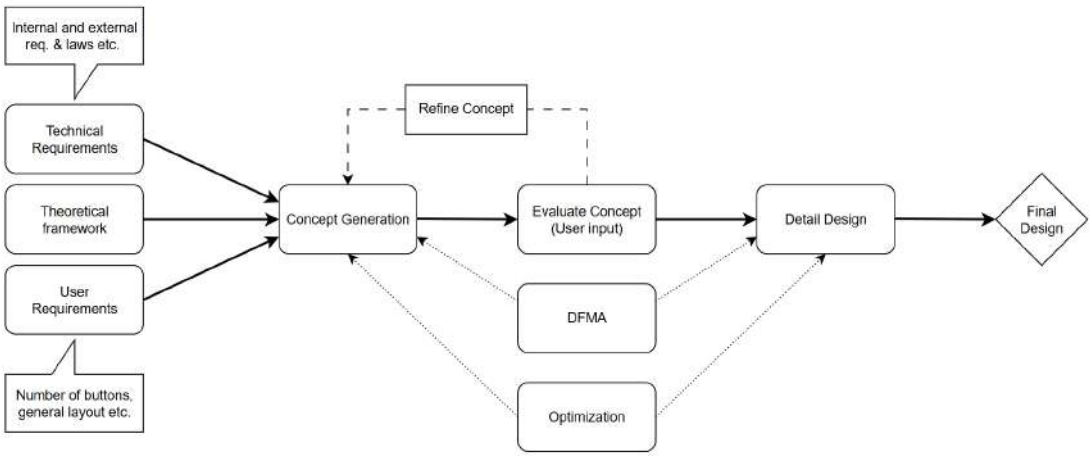

Figure 3.1: Product development process

Theoretical baseline A literature study was performed to benchmark competing solutions on the market and explore alternative solutions. A technical requirement

(TR) was defined based on requirements from users, internal and external stakeholders. The TR contains demands and wishes along with targets and verification methods when applicable.

Concept generation An iterative approach was used to the product development methodology, generating and refining concepts and leading to multiple concept generation phases. An ergonomic study was carried out to ensure the joystick design met the needs of the target user group. To accommodate a broader range of hand sizes, a CAD manikin was employed alongside input from the reference group. Throughout the project, this group provided direct feedback on design changes, contributing to a more user-centered development process.

Concept evaluation Concept evaluation was performed systematically using Pugh and Morphological matrices, enabling structured comparisons between design alternatives. In the detailed design phase, modern optimization tools were introduced to refine the design further. This was complemented by a structural validation of all critical components to ensure they met the defined requirements.

Prototyping Multiple prototypes were manufactured and evaluated in a test rig. The prototypes were made in different stages of the project and thereby the maturity of the assemblies evolved along the process. Some functional prototypes included a joystick base, buttons and a rig mount for a more realistic concept evaluation.

Detail Design and Final Design During the detailed design phase, a concept was selected from the concept generation stage, with only minor modifications made to address manufacturing constraints. Additional refinements were implemented to support further industrialization. As a project goal, a final functional prototype was made to represent a production-ready joystick.

3.2 Market analysis

To obtain an understanding of current joystick design practices and product characteristics, a market analysis was conducted, focusing on commercially available joystick solutions. Four manufacturers, designated as A, B, C, and D, were selected based on their significant global market presence and varied product portfolios. As part of the analysis, two representative joystick models were disassembled and systematically evaluated across multiple technical parameters, as detailed below.

- **Packaging**: How are buttons packaged and designed to accommodate different configurations?
- **Wiring solution**: What type of routing strategies are used?
- **Fastening method of the shell**: What type of fastening method is used for securing the shell halves?
- **Surface texture**: Are there any patterns or coatings on the joystick handles?

- **Overall impression**: Robustness of the construction, ergonomics and product quality?

3.3 Requirements

The technical requirement specification has been partially redacted to protect proprietary information, see A.4.

Technical requirements
The technical requirements cover all the requirements ensuring the joystick meets the demands of VCE, internal requirements and external requirements. VCE provides the project with a separate technical requirement, which is complemented with laws and standards from internal and external stakeholders and other goals that are set by the thesis.

Electrical requirements
The focus of this project was not on the electrical aspects of the joystick, but they were still taken into consideration to assess the feasibility of electrical integration and IP protection.

User requirements
The user requirements cover all functions that are necessary to satisfy the operator. These are in addition to the technical requirements, which are a minimum for the product to be usable and safe, according to the standards. The user requirements involve preferred button position for certain operating conditions.

3.4 Cost

An internal target price has been defined to ensure that the joystick remains competitive with existing products on the market. To estimate the overall cost of the joystick, both production and assembly costs were evaluated. A Design for Manufacturing and Assembly DFMA method was used and quotations from manufacturers enabled a cost estimation of the joystick at different production volumes. All values were normalized to preserve proprietary data.

3.5 Concept evaluation

Evaluating design concepts is essential in product development. The methods used for this evaluation are presented in this section.

3.5.1 Reference group

To support concept evaluation during the project, a reference group comprising six participants from both CPAC and external organizations was engaged. The three

external participants were active operators who use the WLO daily. Two of them were involved in benchmarking and setting performance targets for the joystick, while the remaining participant provided feedback during the later stages of product development. The remaining three participants were the reference group at CPAC, these participants had been using WLO and excavators regularly, ranging from a few years to 20+ years. The reference group, along with previously documented interviews from the two external operators, was used to evaluate the concept generation (Chapter 4.3-4.5) and final concept (Chapter 4.6). The reference group at CPAC was also involved in exchanging ideas throughout the thesis.

3.5.2 Ergonomics study

Throughout the concept generation phase, the ergonomic aspect was evaluated by the reference group and feedback on preferences and practical experience was considered. Supplementary to the feedback from the reference group, ergonomic research from Chapter 2.9 complemented the full evaluation of each concept. The test rig (Chapter 3.5.4) ensured a fair and standardized way of actuating and evaluating each concept.

3.5.3 Semi-structured interviews

Semi-structured interviews were used as a data collection method for subjective feedback from operators. Interviews are used to gather information about operators opinions and values based on a discussion of predefined or open discussion points. The semi-structured interview are a mix of predefined questions based on topics that interests the interviewer and open discussions based of topics that opened up during the interview. The following predefined questions were used in the semi-structured interviews:

- **General**
  - How comfortable is the joystick, overall impression? (Short answer)
- **Geometry**
  - How do you experience the grasp size of the joystick?
  - How do you experience the grasp length of the joystick?
- **Positioning**
  - How do you experience the placement of the 3rd and 4th function?
  - What thumb wheel would you use as the 3rd function?
  - How do you experience the button placement for kick-down, diff-lock, horn and neutral? (Programmable)
  - How do you experience the FR placement?
- **Texture**
  - What surface texture would you appreciate to have on the joystick handle?
- **Feel of function**
  - How does the movement of the joystick feel? (Spring force)

– How does the movement of the joystick feel? (Stroke length)
– How do you consider the length of the rotation axis?

3.5.4 Test rig

For evaluating joystick concepts in a manner resembling that of a VCE WLO, a metal frame construction was designed and manufactured, see Figure 3.2. The test rig has multiple degrees of freedom for easy adjustment depending on test subject and incorporates a main function (X and Y movement) for a realistic experience and a fair evaluation of prototypes. The test rig mounts on any table and has an armrest to represent what is used in a VCE WLO.

Figure 3.2: Test rig

3.6 Concept generation

The concept generation was conducted in three phases before the final concept, with each phase representing a step in refining the design to a final product.

Concept generation 1 involved the creation of a clay model, outlining the ergonomics of the joystick and developing a rough button layout based on feedback from WLO reference group.

Concept generation 2 covered the design of a prototype using additive manufacturing, incorporating real buttons to assess the overall feel of the joystick. A 3D scan was utilized to scan the clay model and surface modeling in CREO was used to

recreate the geometry. Ergonomic evaluation and relevant feedback from the reference group formed the necessary changes in concept generation 3. A proposed base mount was designed to accommodate the remaining buttons and switches that are not integrated into the joystick handle.

Concept generation 3 addressed the manufacturability aspect of the concept and further detailed design. A semi-structured interview was organized with a WLO operator from the Gothenburg area for further feedback on the design and usage of the joystick. DFMA was applied and internal feedback from CPAC was given on manufacturability and assembly of the product. Manufacturers were brought into the picture, giving their feedback on the two concepts.

Final concept addressed the issues from concept generation 3 and was fully designed for manufacturing and assembly. Final details are set and the assembly process was established.

3.7 Design of Experiments (DOE)

DOE was primarily used in the detailed design for optimizing the parameters in the IM process and establishing the impact of different factors on the response(s). JMP Student Edition 18 was used to create the table design and analyze the relationship between all the factors and the response. For simulation of the IM process, Creo Parametric 10.0.1.0 was utilized, using the Mold Analysis feature. The DOE process is comprised of four steps, which were followed in this project as described in [40]:

1. **Planning**
   Planning involves studying the IM process, identifying key factors and responses to be analyzed. Figure 3.3 illustrates all the possible inputs and outputs from the IM simulations. Not all will be relevant in the optimization process and some will therefore be eliminated in the screening process.

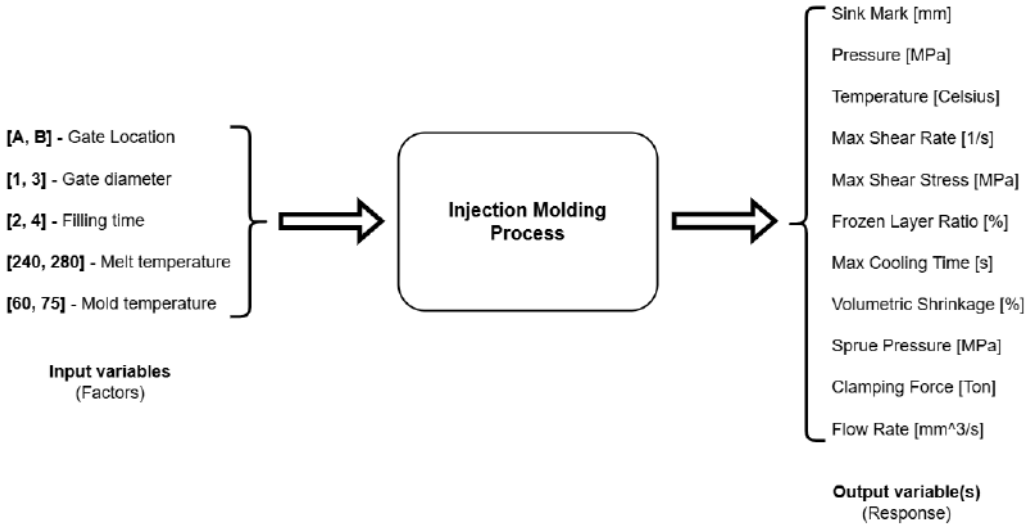

Figure 3.3: Overview of all factors (input) and responses (output) for the IM process

Factors (input variables):

- *Gate Location*
  The position of the gate where the molten plastic is injected into the cavity.

- *Gate Diameter*
  Diameter of the gate at the injection location.

- *Filling Time*
  The time given for the molten plastic to be injected into the cavity.

- *Melt Temperature*
  The temperature of the molten plastic when it is injected into the cavity.

- *Mold Temperature*
  The preheated temperature of the mold when plastic is being injected.

Responses (output variables):

- *Sink Mark*
  Depression on the part surface due to shrinking. No structural issues, however seen as bad quality.

- *Pressure*
  Pressure distribution of the plastic at the end of filling.

- *Temperature*
  Temperature distribution of the plastic at the end of filling.

- *Max Shear Rate*
  The highest recorded value of each element during the filling process. Rate of shear deformation of the material.

- *Max Shear Stress*
  The highest recorded value of each element during the filling process.

- *Frozen Layer Ratio*
  Volumetric percentage of frozen plastic with respect to part thickness.

- *Max Cooling Time*
  Cooling time in the thickness direction.

- *Volumetric Shrinkage*
  Percentage change in the part volume due to shrinkage.

- *Sprue Pressure*
  Plot of the pressure at the melt entrance during the filling process.

- *Clamping Force*
  Plot of the required mold clamping force during the filling time.

- *Flow Rate*
  Flow rate at the gate during the filling time.

Material used in simulations: PC+ABS - Polykemi AB (Producer) - POLYblend PC/ABS 45FS GF20. Physical and mechanical properties are provided from Creo, see Figure 3.4.

POLYblend PC/ABS 45FS GF20

Physical properties

Description	
Polymer type	PC+ABS
Grade name	POLYblend PC/ABS 45FS GF20
Producer	Polykemi AB
Melt flow index	MFI(240,5)= 8 g/10min
Process condition	
Melt temperature (Minimum)	240.0 °C
Melt temperature (Normal)	260.0 °C
Melt temperature (Maximum)	280.0 °C
Mold temperature (Minimum)	60.0 °C
Mold temperature (Normal)	70.0 °C
Mold temperature (Maximum)	75.0 °C
Ejection temperature	80.00 °C
Freeze temperature	100 °C

Mechanical properties

Polymer type grade producer	PC+ABS_POLYblend PC/ABS 45FS GF20_Polykemi AB
Characteristics	Fiber-reinforced polymer
Polymer Poisson's ratio	0.42 (-)
Polymer Poisson's ratio	0.45 (-)
Polymer Poisson's ratio	6.2e+10 (dyne/cm^2)
Polymer Poisson's ratio	4.2e+10 (dyne/cm^2)
Fiber shear modulus G	1.7e+10 (-)
Fiber shear modulus G	3.3e-05 (1/K)
Fiber shear modulus G	5.9e-05 (1/K)
Fiber length/diameter	20.00 (-)
Interaction coefficient	1.0e-02 (-)
Fiber weight percentage	20.00 (%)

Figure 3.4: Physical and mechanical properties for POLYblend PC/ABS 45FS GF20

2. **Screening**
   Screening is the second step in the DOE process, with the goal of identifying the most important factors that have the greatest effect on the response.

Screening is conducted if there are 4 or more factors [40]. Definitive Screening Design was used for this step since it provides a good balance between number of runs and accuracy. Figure 3.5 illustrates the table design for each experiment that was conducted, together with the color map on correlations for the Definitive Screening Design.

Table Design

	Gate Location	Gate Diameter (mm)	Filling Time (s)	Melt Temperature ...	Mold Temperature (Celsius)
1	B	2	4	280	75
2	A	2	2	240	60
3	A	3	3	280	75
4	B	1	3	240	60
5	B	3	2	260	75
6	A	1	4	260	60
7	B	3	2	240	67,5
8	A	1	4	280	67,5
9	B	3	4	240	60
10	A	1	2	280	75
11	A	3	2	280	60
12	B	1	4	240	75
13	A	3	4	240	75
14	B	1	2	280	60
15	B	3	4	280	60
16	A	1	2	240	75
17	A	2	3	260	67,5
18	B	2	3	260	67,5

Color Map on Correlations

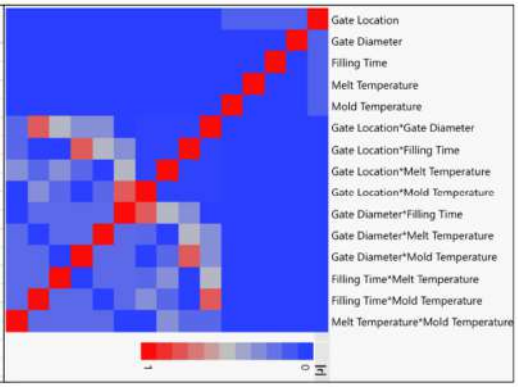

Figure 3.5: Table Design for Definitive Screening Design and Color Map on Correlations

3. **Optimization**
   After significant factors have been identified using the screening design, the optimization DOE can be conducted and a response model can be created. The model would identify which are the optimal values for each factor to achieve a specific goal. From the screening design, the problem was reduced to just one response and three factors. A Full Factorial design was used as the optimization DOE (27 runs). Figure 3.6 illustrates the Table Design used for the Full Factorial design, together with the color map for illustrations of the correlations. As per definition, the Full Factorial design tests all combinations, resulting in no confounding of any main effects or two-factor interactions. For simulation, the eliminated factors were set to the center value for their respective interval. Since these factors are insignificant, they can take any value in the interval.

Table Design

	Gate Diameter (mm)	Filling Time (s)	Melt Temperature ...	Sink Mark (mm)
1	1	2	240	0,037
2	1	2	260	0,049
3	1	2	280	0,066
4	1	3	240	0,031
5	1	3	260	0,042
6	1	3	280	0,062
7	1	4	240	0,027
8	1	4	260	0,039
9	1	4	280	0,059
10	2	2	240	0,044
11	2	2	260	0,056
12	2	2	280	0,066
13	2	3	240	0,039
14	2	3	260	0,051
15	2	3	280	0,06
16	2	4	240	0,034
17	2	4	260	0,045
18	2	4	280	0,065
19	3	2	240	0,045
20	3	2	260	0,057
21	3	2	280	0,069
22	3	3	240	0,038
23	3	3	260	0,051
24	3	3	280	0,074
25	3	4	240	0,034
26	3	4	260	0,053
27	3	4	280	0,071

Color Map on Correlations

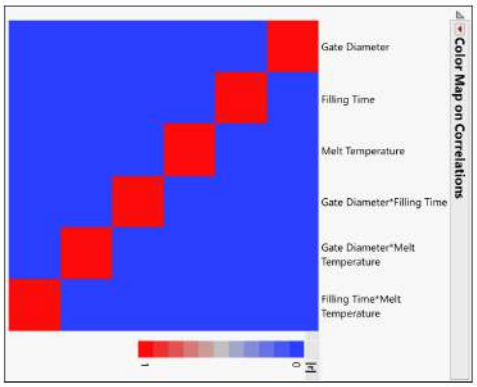

Figure 3.6: Table Design for Full Factorial Design and Color Map on Correlations

4. **Model Verification**
   To verify the model correlates with the system, cross-validation using an 80/20 % training/validation data set split was performed. By studying the RMSE, RASE, and RSquare, the residual conclusions could be drawn if the model shows any lack of fit.

3.8 Structural validation

Structural validation was done part-wise and in assemblies to simulate realistic models whilst still being simple enough to avoid excessive computational cost. Ansys Static Structural 2025 R1 was used as the simulation software, and the Load Case (LC) specified in the requirement specification was applied. The result was analyzed based on deformation, von Mises stress, contact pressure and bolt pretension. A load is applied over a surface at a distance D from the pivot point and the shaft is supported at the endstops, see Figure 3.7.

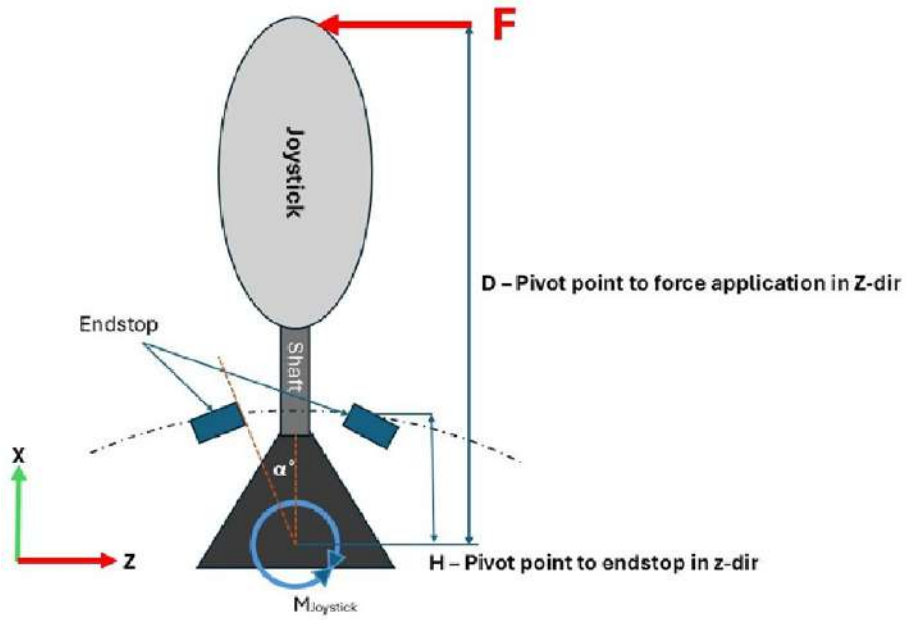

Figure 3.7: Joystick loadapplication

3.8.1 Load case evaluation

The LC was evaluated using an operator weighing 90 kg pulling in a luggage scale and the maximum load was used as the LC value, see Figure 3.8. The average force measured by the luggage scale over three tests was 30 kg. As a result, a force of 300N was selected as the LC for further analysis, see Table 3.1 for LCs LC1-LC4. The bolts securing the ball joint mechanism are tightened with a torque of 0.8 Nm which was recommended by engineers at CPAC. The tightening torque resulted in a pretension of 1 kN on each bolt.

Figure 3.8: LC evaluation

Table 3.1: Loadcas LC1-LC4

	Direction			
Loadcase	X	Y	Z	Bolt pretension
LC1	0	300 N	0	1 kN
LC2	0	-300 N	0	1 kN
LC3	0	0	300 N	1 kN
LC4	0	0	-300 N	1 kN

3.8.2 Material model

The material model used in the structural simulations for IM parts was a PC+ABS+30% GF from Ansys material library, commonly used in this type of application [41].

Table 3.2: Material parameters for PC+ABS+30 % GF

Spec.	Unit	Value
Young's modulus	GPa	6,21
Poisson ratio	-	0,3
Tensile yield strength	MPa	82,7
Tensile ultimate strength	MPa	82,7
Density	g/cm^3	1,29

A mild-steel 1018 from Ansys material library was used as a material property for the ball joint mechanism, see Table 3.3. The important parameters for the material selection was the machineability and the tensile strength of the material, as it is not a stainless steel, some sort of corrosion-resistant treatment is preferable for the durability of the components but is out of the scope for the thesis.

Table 3.3: Material parameters for a mild steel 1018 used for simulating the ball joint

Spec.	Unit	Value
Young's modulus	GPa	205
Poisson ratio	-	0,29
Tensile yield strength	MPa	400
Tensile ultimate strength	MPa	440
Density	g/cm^3	7,87

3.8.3 Mesh

The mesh applied to each component was adapted based on its geometry and complexity, see Figure 3.9. A mixed-element mesh was primarily used to accurately capture the intricate features of the joystick body, while hexahedral elements were implemented for the rotationally symmetric shaft. A mesh convergence study was performed for each component to ensure that the mesh provided accurate results for stress and deformation, without unnecessarily increasing computational cost. To

capture the bending stress accurately in cases where the stress gradient is low, there should be at least 1-3 elements in thickness. Therefore, an element size of 1 mm was chosen which ensures enough elements in thickness. Refinements in the mesh were used in particular sections, such as contact surfaces and thin-walled areas. The computational cost was reduced by not refining the mesh further and keeping the number of elements down.

Figure 3.9: Mesh of upper part of the joystick

3.8.4 Setup

The structural simulations were done in Ansys using the static structural workbench. All buttons were excluded from the simulations because of unnecessary computational power for no real gain. The high stress area was deemed in the lower regions of the shell, therefore, the interfacing part of the ball joint was included in the simulation to represent the mating conditions and result in a more realistic simulation.

Contacts
All mating surfaces were specified with a certain contact type representing the relation between surfaces, see the contact types in 2.12.2. The two shell halves have two types of contacts, bonded and frictional. The frictional support is an assumption that the two halves can slide with a specified friction and separate from each other if the deformation allows, but strictly no penetration, see Figure 3.10. The frictional support is a non-linear contact type, which will increase the computational time however, for the accuracy in the simulation, it is a necessary sacrifice. The second contact is the bonded surfaces which represent the clamping surface of the bolt holding the halves. The contact pressure in a bolted joint should always be positive, otherwise there is a gap in the contact. Therefore a bonded contact was deemed sufficient and the contact is linear, see contact surfaces in Figure 3.11. The assumed friction coefficient was 0.25 on all frictional contacts.

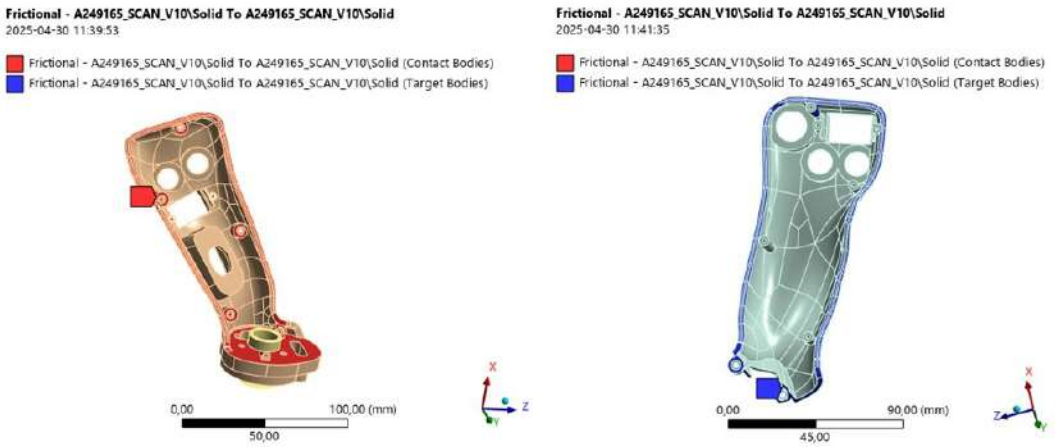

Figure 3.10: Frictional contact, shell-shell

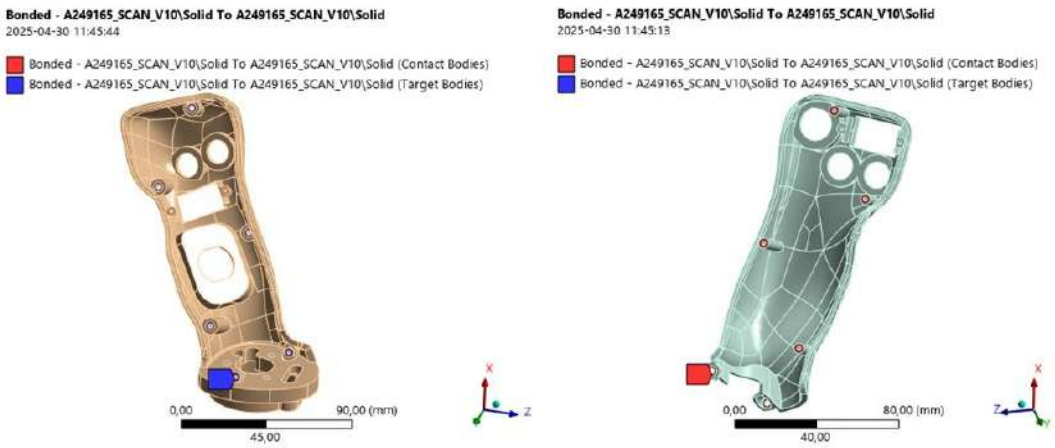

Figure 3.11: Bonded contact, shell-shell

An additional contact represents the frictional support mating the shell and the ball joint mechanism. The contact between the bodies allows sliding and separation since the bolted connection secures the bodies together. A bonded contact would over-stiffen the structure and not reflect a worst-case scenario, see Figure 3.12

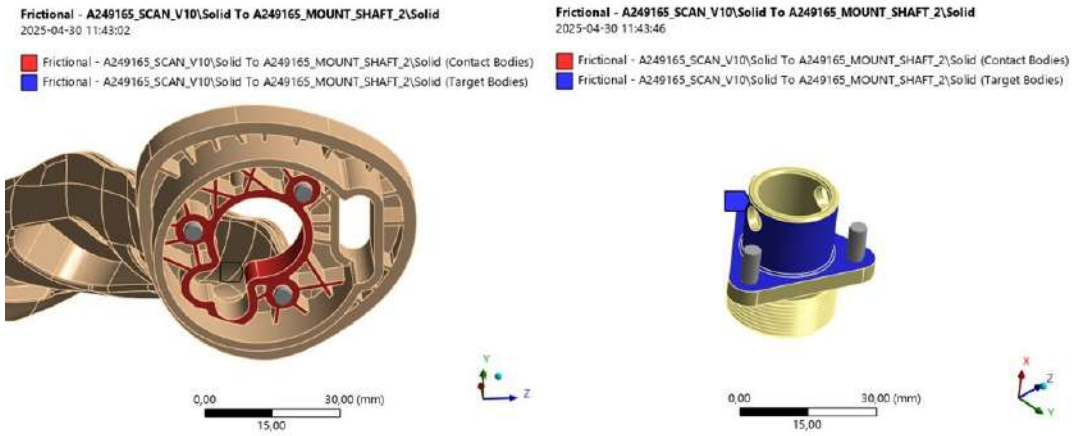

Figure 3.12: Frictional contact, shell-balljoint mechanism

Load application

The LCs specified in Table 3.1 are applied according, see Figure 3.13-3.16. A point load would lead to unrealistic stress concentrations in the shell, therefore, a remote force over a small surface was selected.

The bolts fastening the ball joint mechanism were pre-tensioned to a load of 1 kN which corresponds to a fastening torque of 0.8 Nm. The torque applied to the screws was evaluated based on the current production specifications, ensuring that the clamped material does not result in cracking after multiple years in service. For reducing the number of elements in the system, the bolts were modeled as beam elements, see the grey cylinders in Figure 3.12.

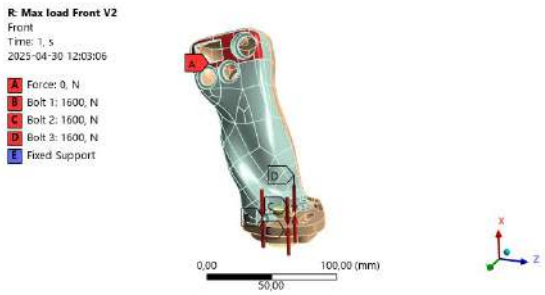

Figure 3.13: LC1: 300 N in -Y direction

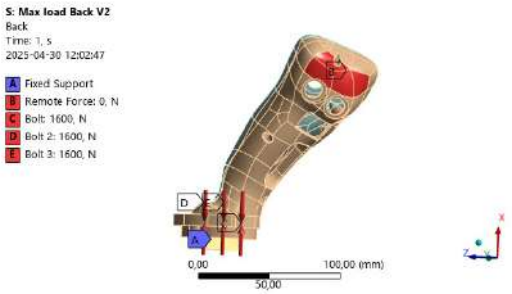

Figure 3.14: LC2: 300 N in +Y direction

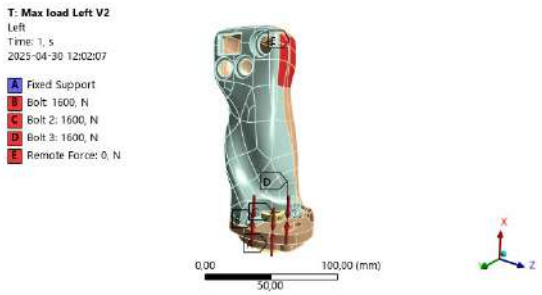

Figure 3.15: LC3: 300 N in -Z direction

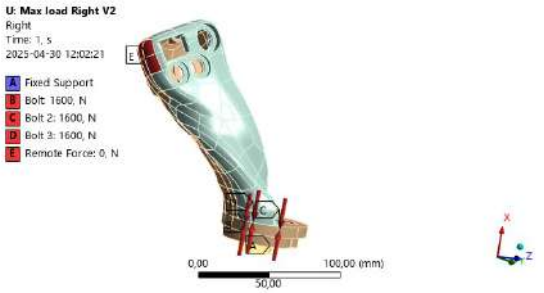

Figure 3.16: LC4: 300 N in +Z direction

3.9 Ball joint mechanism

A ball joint mechanism was evaluated for adjusting the neutral position of the joystick to improve comfort. A concept evaluation was made using morphological and Pugh matrices, four combined solutions were evaluated, A1-A4, and two Pugh matrices with different references for a systematic evaluation. The final concept was designed and dimensioned, ensuring the clamping force was large enough for the mechanism not to slide out of position.

When a force is applied to the joystick handle the ball joint mechanism should not slide or shift in position. The force clamping the ball should overcome the moment $M_{Joystick}$ created by the force applied on the joystick, see Figure 3.7. The frictional force ensures the ball remains fixed under operational loads and prevents rotational slippage.

The clamping force acting at the contact interface of the ball joint mechanism is decomposed in a normal force F_N, acting perpendicular to the contact surface, and a tangential force F_T. The tangential force can be neglected as it is symmetric around the contact area. The angle between the vertical plane and the normal component is denoted $X°$, see Figure 3.17.

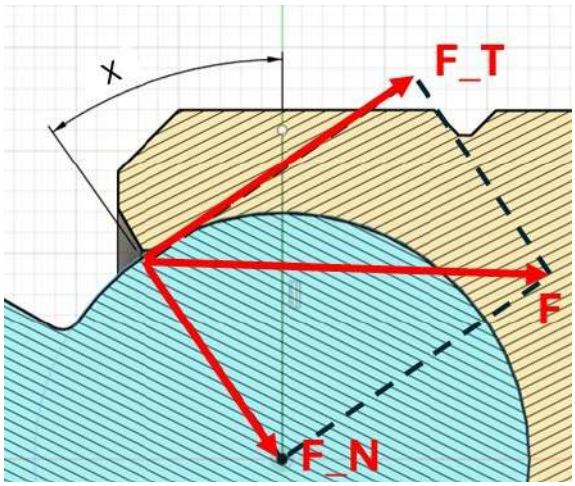

Figure 3.17: Clamping force on the ball joint

The moment induced by the ball joint is given by the friction force times the lever arm, $M_{balljoint} = F_{fric} \cdot R_{balljoint}$. If $M_{balljoint}$ is greater than or equal to $M_{Joystick}$, the ball joint remains in position and no sliding occurs. The frictional force acting on the ball due to the applied clamping force is given by Equation 3.1:

$$F_{fric} = \frac{M_{Joystick}}{R_{balljoint}} \tag{3.1}$$

From the friction force, the Normal force resisting motion is given by the Equation 3.2:

$$F_N = \frac{F_{fric}}{\mu} \tag{3.2}$$

Assuming dry friction between the threads, a friction coefficient of $\mu = 0.14$ is used. The clamping force component F is given by the Equation 3.3:

$$F = \frac{F_N}{sin(X)} \tag{3.3}$$

The clamping force generated by a threaded fastener is given by Equation 3.4. The total clamping force F_{tot} is given by the clamping force.

$$F_F = \frac{M_v}{r_m * tan(\epsilon_1 + \varphi)} \tag{3.4}$$

- M_u is the applied moment on the thread,
- r_m is the mean radius of the thread,
- ϵ_1 is the friction angle,
- φ is the lead angle of the thread.

The friction angle is calculated using Equation 3.5:

$$tan(\epsilon_1) = \frac{\mu}{cos(30°)} \tag{3.5}$$

And the thread lead angle is defined in Equation 3.6:

$$tan(\varphi) = \frac{P}{\pi * d_m} \tag{3.6}$$

From Equations 3.1–3.6, the clamping force F in Equation 3.3 was calculated and used as the LC in the FEM validation. The bending moment $M_{balljoint}$ was determined using a force of 200 N and a lever arm of $D = 130$ mm. This force corresponds to two-thirds of the load used in LCs LC1–LC4, as the design objective is for the ball joint to begin sliding before any yielding occurs in the shell. The coefficient of friction in the threads was set to 0.14, while a value of 0.25 was used for all other contact surfaces.

The FEM validation of the ball joint clamping was performed by applying a fixed constraint to the threaded section and a remote displacement load, see Figure 3.18. The resulting reaction force from the displacement was compared to the required clamping force to prevent the ball joint from sliding. Due to the rotational symmetry of the mechanism, only a quarter of the geometry was modeled to reduce computational load. A symmetry boundary condition was applied accordingly. The mesh was kept relatively coarse, with local refinements in areas of contact and high stress concentrations, see Figure 3.19.

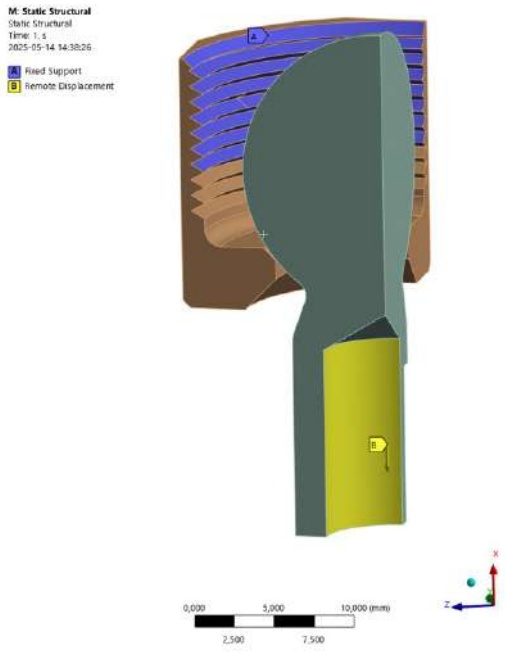

Figure 3.18: Remote displacement and fixed support ass boundary conditions

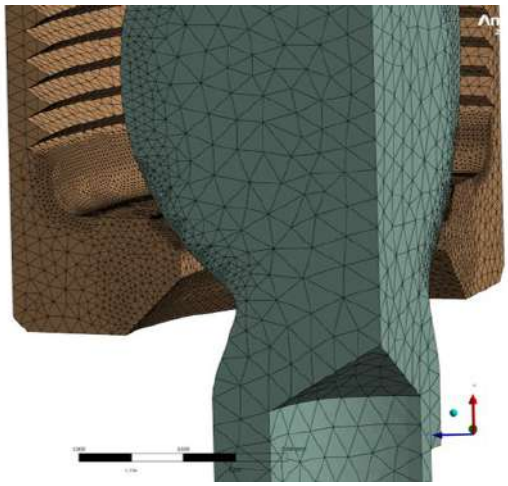

Figure 3.19: Mesh for the ball joint FEM

3.10 DFMA

The DFMA strategy described in Section 2.13 was considered early in the concept generation process, ensuring the product was feasible to manufacture. The total manual assembly cost was calculated for various configurations which helped identify what components contributed to an increase in cost and how this could be optimized in terms of minimizing assembly cost. The cost model assumes an ideal handling + fitting time of 2 s, which resulted in a lower-than-realistic assembly time. Therefore, a time correction factor $TC_{\text{factor}} = 4$ was implemented. The adjusted total cost of manual assembly was calculated according to Equation 3.7.

$$C_{ma} = C_1(F + H) * TC_{factor} \tag{3.7}$$

4
Results

This chapter presents the outcome of the work described in the previous chapter. It starts with the findings from ergonomic studies and feedback from user evaluations. Different concepts are shown and compared based on how well they met the requirements. The final concept is presented along with results from mechanical simulations and prototype testing, showing how the design holds up in terms of comfort, durability, and usability. Furthermore, the findings from the DOE are presented.

4.1 Market evaluation of joysticks for construction equipment

For operating heavy machinery, there is a wide range of solutions to get the operator's commands to the control system. The standard control option for VCEs WLO varies for the large WLO between a single lever joystick and a four-lever system. Compact WLOs are always using a single lever joystick. Many competitors are developing full-size joysticks with multiple options already on the market and with a broad range of customization options for the specific application. Depending on the button configuration, a joystick can either be fitted in excavators or WLO. In this section, a few competitor products will be discussed and evaluated.

4.1.1 Joystick A

Joystick A is from a Sweden-based company focusing on improving the machine operator's environment through innovation. The focus is on personalized joysticks for multiple applications, for example in excavators, wheel loaders and other machinery. The joysticks are made of a two or three-piece design, bolted together on the backside. It is a solution that improves the serviceability of the product, but at a cost of appearance. Some of the joysticks have the possibility of heating and also haptic feedback.

A full hand grip joystick was disassembled and analyzed based on five points, see Figure 4.1.

- **Packaging:**
  Multiple buttons and switches are packaged in the joystick. The front panel is adaptable for different button configurations by using a uniform wall thick-

ness and snap-in buttons. The button holes are later milled depending on the configuration, ensuring only one mold is required. The backside is also customizable with the option of removing the roller, the void is then replaced with an IM snap-in detail.

- **Wiring solution:**
  A wire harness with connectors on one end connects each button. The harness is presumably pre-made, and the connectors are connected at the final assembly. All cables exit the joystick in two harnesses, one for the front half and one for the rear. No IP protection appears on the connectors.
- **Fastening method of the shell:**
  The two halves are connected using 6 evenly distributed screws. A lip is used on the circumference of the joystick to localize the halves and minimize the gap between. Many cables are making the assembly difficult because of wires getting in the way.
- **Surface texture:**
  The surface is coated with a thin layer of rubber, increasing the friction. A textured pattern in the handle further improves the handling and feel of the joystick.
- **Overall impression:**
  An overall good impression of the joystick. Comfortable to use with a medium hard coating and good button placement on the back, a bit too long on the front side, making it hard to reach all the buttons. Popular choice in excavators.

Figure 4.1: Joystick A, full hand joystick

4.1.2 Joystick B

Joystick B specializes in human-machine interface. They sell either components like buttons and scroll wheels or complete products like their XD series joystick, see Figure 4.2. This joystick is constructs of a 2-piece bolted base with a customizable front plate with a clip function for easy assembly. With an all-metal construction, it can handle loads of 1780N in the horizontal direction and can be used by the operator as a handle when raising themselves [42]. Overall, a well-balanced product with many customizable options but could be a bit excessively large for a WLO.

Figure 4.2: Joystick B [42], reproduced with permission

4.1.3 Joystick C

Joystick C is from a US-based company specializing in injection molding, stamping, CNC machining, cable assembly and cable over molding. Since its founding, they have designed and manufactured control switches and have a variety of products in the field of joysticks, both for civil and military applications [43]. Their joystick features a multi button configuration and switch setup with possibilities for customization. The joysticks are made from multiple bolted-together panels, but the visible bolts and part lines make them less visually appealing.

Figure 4.3: Joystick C [43], reproduced with permission

4.1.4 Joystick D

A finger grip joystick was disassembled and analyzed based on five points, see Figure 4.4.

- **Packaging:**
  A smaller joystick with fewer buttons, but still compact and incorporates many features.
- **Wiring solution:**
  Flex PCBs instead of wires, neat way of routing ”cables” and minimizing the risk of pinching cables while assembling.
- **Fastening method of the shell:**
  Brass inserts with barbs permanently snap the halves. No visible screw holes but to the price of not being able to open the joystick up for service.
- **Surface texture:**
  No textured surface and no grip coating, resulting in a slippery shell that is hard to grasp. Since the joystick is a pinch grip, the necessity of gripping the joystick is not as significant as for a full hand grip.
- **Overall impression:**
  Overall a neat package with no visible screw holes but with the downside of no service. Flex PCB wiring enables a smaller risk of pinching cables however, more expensive compared to using only wires.

Figure 4.4: Joystick D, finger grip joystick

4.2 Evaluate button and switch type

Based on the button sub-function in the joystick, a Kesselring matrix was made of possible button types for each function, where unsuitable button selections are eliminated, see Table 4.1. For each function, the button types suitable for the application were marked green, while those deemed unsuitable were marked red.

Table 4.1: Kesselring matrix of possible button selection for sub-functions

	Switch/Button type											
Sub-function	3 position rocker	Momentray Pushbutton Switch	Linear Output Pushbutton Switch	2-Way, Finger Joystick	4-Way, Finger Joystick	2-Way, Finger Joystick with Pushbutton	4-Way, Finger Joystick with Pushbutton	Self centering Thumbwheel	Friction Actuation Thumbwheel	Joystick Base	Locking Rocker Switch	Combined Switches
												2 in 1
FNR Selector												
F/R Lock												
Main functions (1st, 2nd)												
3rd function												
4th function												
Horn												
Diff-lock												
Kick-down												
Electronic lock												
Co-Pilot remot control												
Additional Programmable Button(s)												

A morphological matrix was created for the four integrated solutions, see Table 4.2. Each solution (A, B, C and D) is a combination of possible button selections from the sub-functions. Each integrated solution represents a complete set of buttons for a joystick, all the solutions achieve these functions with different types of buttons and switches. The integrated solutions were developed by analyzing the functions

of each button and evaluating alternative button types. While numerous integrated solutions were possible, the selected solutions were considered most ”intuitive to use” according to the reference group. Critical functions need to be clear and easily understood, and therefore, it was concluded that combining several functions in the same button would not satisfy this criterion.

Table 4.2: Morphological matrix with complete button solutions

Integrated solution	Switch between FNR	F/R Lock	Main functions (X, Y)	3rd function	4th function	Horn	Difflock	Kick-down	Electronic lock	Co-Pilot remote control	Additional Programmable Button(s)
A											**N** (Neutral button)
B					2 in 1						**3rd/4th** (Switch between)
C	 Momentary 2-pos Rocker				2 in 1						**3rd/4th** (Switch between)
D	 Momentary 2-pos Rocker										**N** (Neutral button)

(A) and (B) uses a regular pushbutton as the switch between FNR with an additional neutral button, either as the additional programmable button or instead of the horn/diff-lock/kick-down. The difference between (A) and (B) is the 2-in-1 3rd and 4th function with an additional pushbutton as the switch from 3rd to 4th. (C) and (D) are similar to (A) and (B) except the FNR switch is a momentary 2-position rocker.

(B) and (C) would lose a button by having the 3rd/4th function switch and is thereby at a disadvantage from solutions (A) and (D). In addition to the switch thumb wheel, it is not possible to actuate both hydraulic functions simultaneously since the switch activates one function at a time.

(A) and (D) differ in how the FNR function is controlled, either by a button or a momentary 2-position rocker switch. Based on feedback from the reference group, the momentary rocker is considered to be more intuitive for the operator to use and is therefore preferred. The 2-position Forward/Reverse and the Neutral button have been implemented previously on Compact WLO like the electric L20, L25, L30, and

L35.

Option (D) met the defined requirement and preferences and was therefore the solution selected for further development.

Several studies have previously been conducted in collaboration with CPAC to investigate user requirements for single-lever joysticks for WLO. Based on interviews conducted by [44] and [45], see A.1 and A.2, operators were asked, among other questions, which features they considered important. Their findings can be summarized to the following key features:

- The FNR must be located on the joystick handle and not on the base mount as in previous VSL.
- Frequently used buttons easily accessible: kick-down, horn, diff-lock and communication.
- Even though the occurrence is rare, the ability to operate the 3rd and 4th functions simultaneously remains important.
- A dedicated button for controlling the Co-pilot.

Moving the FNR selector switch from the base to the handle is a key development for the next-generation joystick. Requiring the user to move the hand for every Forward/Reverse change is not efficient and increases fatigue.

The frequency of button usage varies depending on the operating scenario and the individual operator. Interviews revealed that preferences differ, where some operators frequently use the horn and want it on the joystick, while others seldom use it and are comfortable having it on the base. It became clear that assigning fixed positions to specific functions would not meet the needs of every user. Therefore, push buttons should be unmarked and programmable for different functions.

In scenarios where both the 3rd and 4th functions are used simultaneously, the design must allow for two thumb wheels. The primary thumb wheel will be positioned horizontally at the front of the joystick for improved ergonomics and thumb operation, while a second wheel will be located on the backside for index finger control, enabling simultaneous actuation.

Being able to control the Co-pilot without releasing the joystick to reach for the touchscreen is a feature designed to enhance efficiency and minimize operator fatigue. The Co-pilot has already significantly improved VCE, and integrating a joystick seamlessly with this system is expected to further boost both demand and market value for these products.

4.3 Concept generation 1 (Clay model and initial concept)

Concept generation 1 focused on creating a physical 3D geometry, fitting all necessary buttons, concluded in section 4.2 and evaluating the ergonomics of the joystick. Multiple clay models were created to come up with different button configurations and evaluate the pros and cons of each. Clay was chosen as the most suited prototyping material because of its low cost, rapid iteration, cleanliness, and moldability in reshaping the geometry.

Button placement was a key consideration during the initial concept generation phase, with significant focus on evaluating different configurations. The precision grip was deemed unsuitable for the joystick handle due to the limited surface area available for the required number of buttons. In contrast, the power grip was considered the most suitable option because of its larger mantle size and its ability to accommodate all necessary buttons. Consequently, only the power grip will be considered for the joystick handle.

3D-printed buttons and switches were placed on a clay model and based on feedback from operators handling the joystick, the buttons and switches could be moved to accommodate the operator in a more ergonomic use of the joystick. The operators reshape the overall structure of the joystick based on the grip feeling, support of the wrist and reach of the buttons. The ultimate button configuration was concluded through multiple iterations and the final version can be seen in Figure 4.5 and 4.6. The front side has a thumb wheel, a finger joystick (4-way axis + pushbutton) and two regular push buttons, which should be operated by the thumb. The backside of the joystick has two regular push buttons, a thumb wheel and an FNR switch, these should be operated by the index, middle, and ring fingers. The hand should rest in a natural handshake, hugging the joystick.

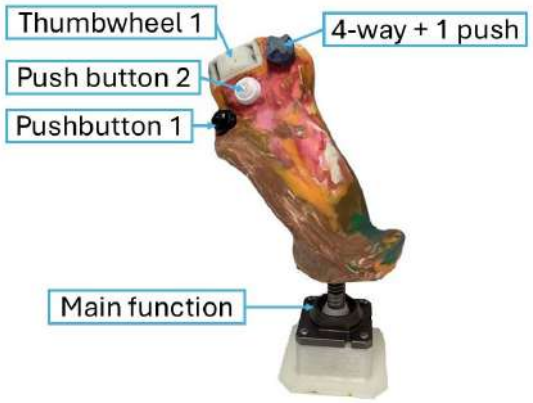

Figure 4.5: Clay model, front

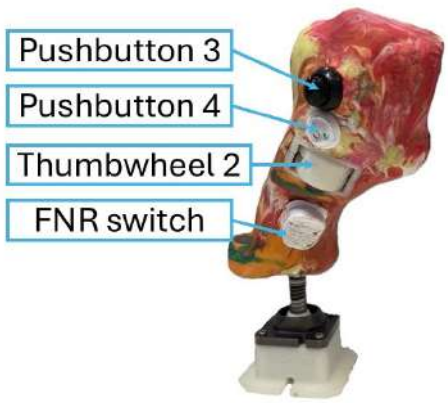

Figure 4.6: Clay model rear

Motivation for the button placement:

- **Thumb wheel 1 and 2:**
  A key requirement for the placement of the thumb wheels controlling the 3rd and 4th functions was that they needed to be operable simultaneously. The solution was to position one thumb wheel on the front side and the other on the back side, allowing them to be managed by either the thumb or the index finger.
- **Push button 1-4:**
  Due to limited space, the four buttons were split between the front and back sides, with buttons 1 and 2 placed on the front and buttons 3 and 4 on the back. Pushbutton 1 was considered the most comfortable and, therefore assigned the most frequently used function. Button 2, being less comfortable, was designated for a less frequently used function. Buttons 3 and 4 were positioned vertically above thumb wheel 2, as they are operated by the index finger, and finger reach was a major factor in their placement.
- **4 way + 1 push:**
  The finger joystick was considered the least frequently used during WLO driving and was therefore positioned away from the other buttons. However, since it is occasionally used when operating the Co-pilot and during loading, it still needs to be comfortable and easily accessible when actuating the joystick.
- **FNR switch:**
  Front and reverse are frequently used when changing the direction of the WLO and should be placed in a comfortable location that allows the operator to reach them without losing grip of the joystick. Neutral occupies one button and is seldom used; therefore, buttons 2-4 are recommended for the function.

Some of the buttons can be programmable and serve different functions depending on the application of the WLO. But certain buttons have a single set function and therefore can not be changed, the predefined buttons are the Main function that controls the 1st and 2nd function, the FNR switch that controls the forward and revers action and the finger joystick that controls the Co-pilot. The remaining buttons can be configured however the operator needs are, see table 4.3 of three example applications of the WLO.

Table 4.3: Example on programmable button configuration

Button/switch	**Loading**	**Plowing snow**	**Brooming**
Pushbutton 1	Radio	Kick-down	Horn
Pushbutton 2	Kick-down	Horn	Neutral
Pushbutton 3	Diff-lock	Neutral	Radio
Pushbutton 4	Neutral	Diff-lock	Programmable button
Thumb wheel 1	not used	3rd function	not used
Thumb wheel 2	not used	4th function	4th function

4.4 Concept generation 2 (Concept generation and CAD-translation)

Concept generation phase 2 focused on transferring the geometry of the clay model into CAD, packaging the buttons and further evaluating the geometry based on ergonomics. Additive manufacturing was frequently utilized for evaluating each iteration.

4.4.1 Ergonomics test rig

A test rig was built to be able to mimic the real operation conditions that would be found in a WLO. The rig has multiple degrees of freedom for adjustment reasons, see Figure 4.7, and enables a more standardized handling and evaluation. Each joystick iteration was evaluated on the rig, with the operator seated correctly and the arm resting in a natural position, as described in section 2.9.

Figure 4.7: Test rig with multiple degrees of freedom for ergonomic setup of the joystick and evaluating operational comfort

4.4.2 Design considerations

When the participating operators were satisfied with the overall positioning of buttons and shape of the joystick, the clay model and buttons were 3D scanned with a handheld 3D scanner, which created a Standard Template Library (STL) file. In CAD, buttons and switches were placed in approximate locations based on the STL file, see Figure 4.8. Since the buttons used in the previous concept phase did not have any depth, there were some buttons closer to each other than expected, and

therefore, some minor shifting because of packaging had to be done. The shell geometry of the joystick was created using Creo Freeform for a quick iteration process. Initial geometries had the purpose of evaluating the converted base geometry to CAD and tweaking the base to a shape that pleased the operator, see the early concepts in Figure 4.9.

Figure 4.8: Buttons packaging in raw 3D scan file

Figure 4.9: First packaging concepts and freeform creation in CAD

Based on feedback from the reference group, the design evolved into a compact and refined package, with the most significant change from the clay model being the repositioning of buttons 1–4. On the front side, the orientation of the two buttons was adjusted so they now lie on the same plane, see Figure 4.10. Aligning all front-facing buttons on a single parallel plane simplifies tooling and reduces manufacturing costs for injection molding, following principles inspired by the DFM methodology. While this change does not reduce printing costs for AM, the same button layout and shell surface were retained across both processes for simplicity. On the back side, the two buttons were reoriented from a vertical stack to a horizontal, side-by-side configuration. This adjustment reduces the travel distance required for the index finger when switching between the buttons and the roller.

Figure 4.10: Final version for concept generation 2, Front

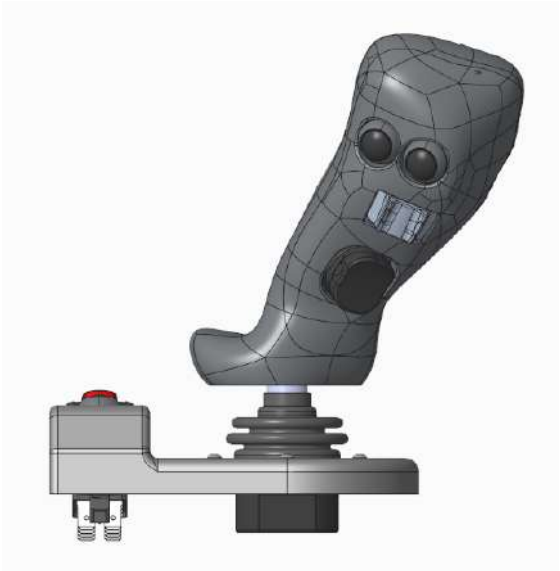

Figure 4.11: Final version for concept generation 2, Back

4.4.3 Joystick adjustment method

According to the reference group, it was important to provide the option of adjusting the joystick neutral lean angle to suit individual preferences for arm positioning while at rest. As a result, the feasibility of adjusting the joysticks angle while mounted in the WLO was evaluated. The reference group also contributed input and specific details regarding the adjustment mechanism, which led to the development of a dedicated requirement specification, see Table 4.4.

Table 4.4: Requirements for the adjustment mechanism

Nr.	Requirement
1.	Easily adjustable
2.	15-20° adjustment angle in all directions
3.	Adjustment time $<$ 2 min
4.	One person adjustable
5.	Short assembly time in manufacturing

The adjustment mechanism was divided into three functional activities: a method for fastening the joystick, a method for adjusting its angle, and a method for locking the angle in place. Based on these activities, multiple sub-solutions were developed and organized into a morphological matrix, see Figure 4.12. These sub-solutions were then cross-linked to form four complete concepts, see Figure 4.13. The initial angle locking mechanism, which relied on one or more set screws, was not considered further, as it was deemed insufficient for securely locking the angle adjustment.

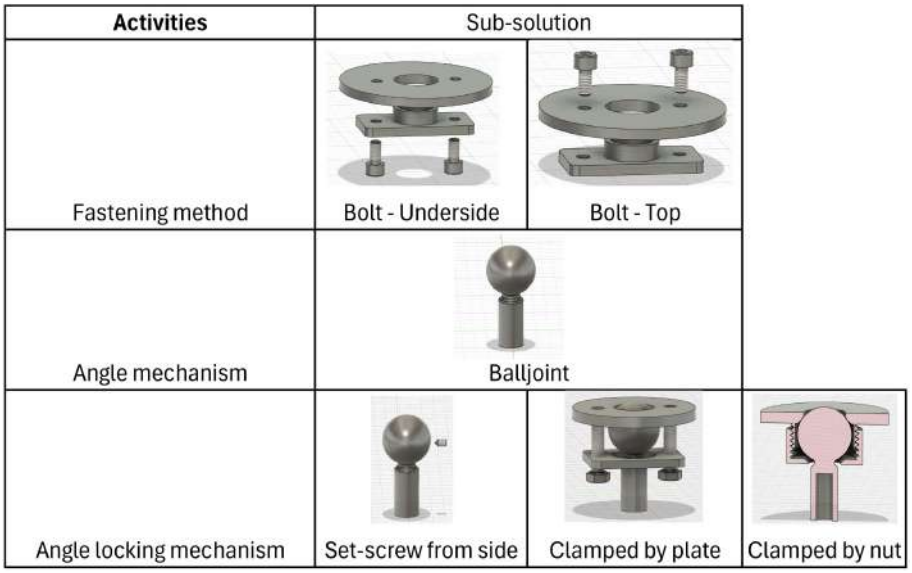

Figure 4.12: Morphological matrix with sub-solutions to each activity

Figure 4.13: Combined solutions to the morphological matrix

To evaluate the four concepts, relative decision matrices (Pugh matrix) were used. Based on seven criteria, the concepts were evaluated against a reference solution and got either a ”+”, ”-” or a ”0” depending if it performed better, worse, or equal to the reference. From the first matrix, see Figure 4.5, concept A2-A4 performed better than the reference concept A1. With A2 as reference in the second matrix, concept A4 overperformed whilst concept A1 and A3 underperformed, see Figure 4.6. Therefore, concept A4 will be developed further and integrated into the joystick design.

Table 4.5: Pughmatrix of concepts, solution A1 as reference

Chalmers	Pughmatrix 1			
			Created: 2025-03-24	
Criterias	**Alternative**			
	A1	**A2**	**A3**	**A4**
Cost	**REFERENCE**	-	+	-
Easily adjustible		+	0	+
Adjustment time		+	0	+
Assembly time		0	-	-
Number of components		+	0	+
Structural integrity		0	+	+
Durability		+	+	+
Σ+		4	3	5
Σ 0		2	3	0
Σ -		1	1	2
Nettovalue		3	2	3
Ranking	3	1	2	1
Furthur development	-/-	-/-	-/-	-/-
Conclusion				

Table 4.6: Pughmatrix of concepts, solution A2 as reference

Chalmers	Pughmatrix 2			
			Created: 2025-03-24	
Criterias	**Alternative**			
	A1	**A2**	**A3**	**A4**
Cost	-	**REFERENCE**	-	0
Easily adjustible	-		-	0
Adjustment time	-		-	0
Assembly time	-		-	-
Number of components	-		-	0
Structural integrity	0		0	+
Durability	-		-	+
Σ+	0		0	2
Σ 0	1		1	4
Σ -	6		6	1
Nettovalue	-6		-6	1
Ranking	3	2	3	1
Furthur development	No	No	No	Yes
Conclusion	A4 will be developed futhur			

4.5 Concept generation 3 (Detailed design)

Based on the second concept generation, the overall button layout and general geometry was decided. An external operator was interviewed, and the feedback was applied to the design before the final geometry was decided. The interview can be found in A.3. The following step was to create a more detailed CAD model, designing for the manufacturing method, and make changes accordingly. The structural validation of the joystick was carried out during the final stages of the detailed design phase.

4.5.1 Injection Molding vs Additive Manufacturing Costs

A cost analysis was performed comparing manufacturing methods of the joystick shell using IM and AM. Official quotes was used for tool and material costs for IM and batch pricing for AM.

The IM cost is highly dependent on the production volume as the tools cost is distributed over the parts produced and an additional material cost is added per part. The AM cost is instead calculated over the cost of a print batch and is thereby constant over the number of parts made. Four different production quantities was analyzed for the IM shell against the AM shell, the price/piece has been normalized for integrity reason, see Figure 4.14.

Given the significant cost difference, even at a low volume of 800 units per year, the advantages of AM did not justify the higher expense, especially considering the

product is expected to be sold for several years. Therefore no further development will be made for the AM version of the joystick and IM is therefore the chosen manufacturing method.

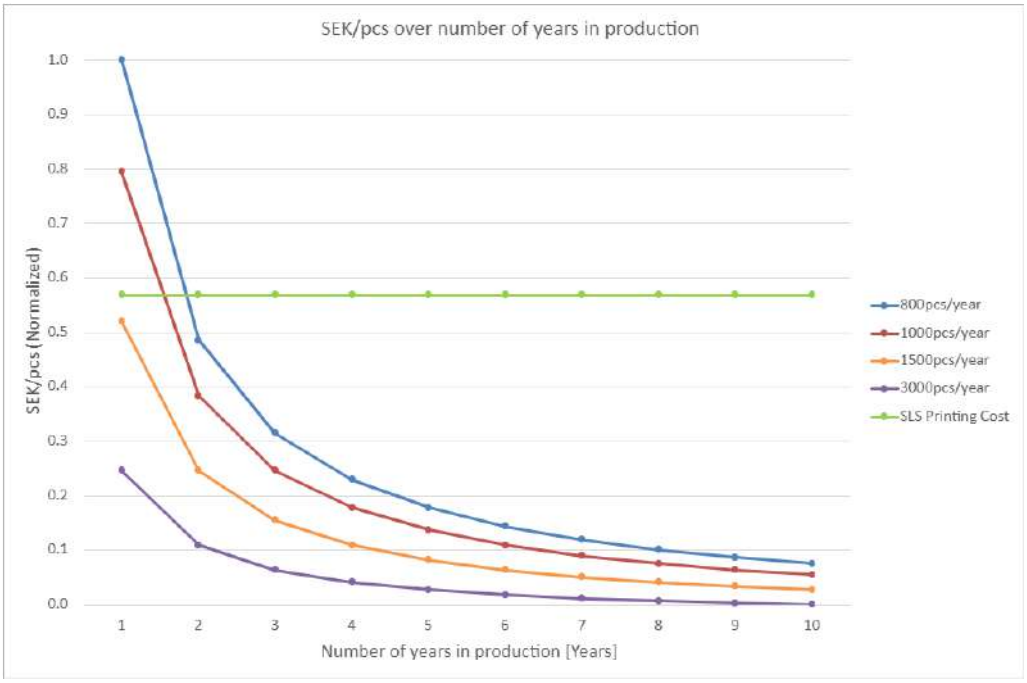

Figure 4.14: Comparison between manufacturing cost for IM and SLS printing. Values normalized to preserve proprietary data, trends remain representative

4.5.2 Ingress protection

To ensure the joysticks reliability in a cabin environment, protection against dust and vibration-induced ingress is essential. Fine dust may enter the cabin, and excessive vibrations can speed up the ingress by encouraging dust to penetrate seals and enclosures, potentially damaging sensitive electronics. Therefore, a solid particle protection rating of IP5K is required. This rating ensures resistance to most dust particles, with any ingress being minimal and not disruptive to functionality.

Regarding liquid ingress, the joystick benefits from its protected placement within the cab, which shields it from direct exposure to water or harsh splashes. However, component exposure varies based on their placement. Visible components such as switches, buttons, casings, and covers may be subject to incidental splashes from items handled by the operator. As a result, these elements must meet a liquid ingress rating of IP4. In contrast, non-visible components that are enclosed or otherwise shielded from direct contact can meet a lower requirement of IP2, as they are unlikely to be exposed to any liquid.

These specifications follow the VCE general environmental requirements for components installed inside the cabin. The required protection levels are IP5K4 for

exposed components and IP5K2 for internally shielded components, see protected zones in Figure 4.15. These levels were achieved through careful component selection and design integration. A limited amount of moisture or humidity is allowed to enter the joystick casing, as all buttons are either sealed to meet the required specifications by design or the terminals are coated with protective materials. This ensures continued functionality and prevents electrical failure under normal operating conditions.

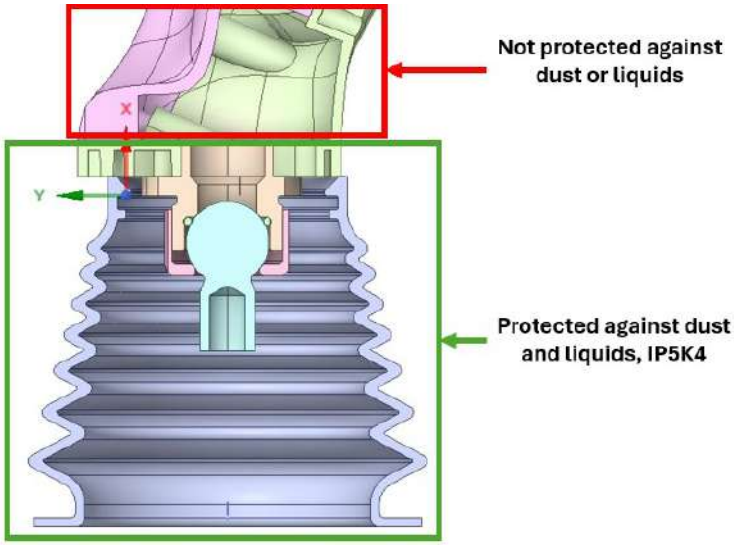

Figure 4.15: Ingress protection zones - Red zone is not protected and electronics need to be sealed. Green zones are protected to IP5K4

4.5.3 Alignment ridge

During assembly, aligning the edges of the two joystick halves proved challenging. To address this, an alignment lip was integrated along the interface boundary to secure the halves and ensure proper alignment, see Figure 4.16. In addition to aiding assembly, the lip contributes to the structural integrity of the joystick by distributing loads between the halves and minimizing misalignment under applied forces. An additional benefit of the lip is its ability to reduce water ingression.

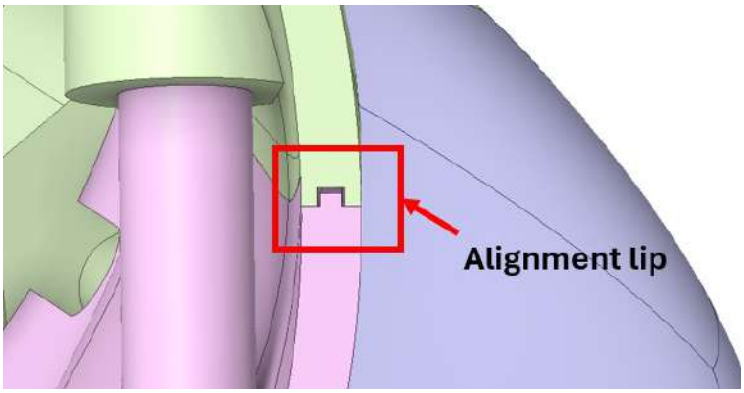

Figure 4.16: Alignment ridge

4.5.4 Structural analysis

In this chapter, selected results from the structural analysis of the IM shell are presented, the deformation and stress of remaining load cases are presented as Figures in A.6. Details regarding the application of the load case are specified in section 3.8.4. While the primary focus of the analysis was on deformation and stress, the contact conditions between components and the screw pretension were also evaluated.

4.5.4.1 Results

The highest deformation was observed in load case LC1, see Figure 4.17. In this case, a 300 N load was applied in the negative Y-direction across the front surface, resulting in a maximum deformation of just over 5.3 mm at the top region of the joystick. This scenario represents the operator using the joystick for additional support while rising from a seated position.

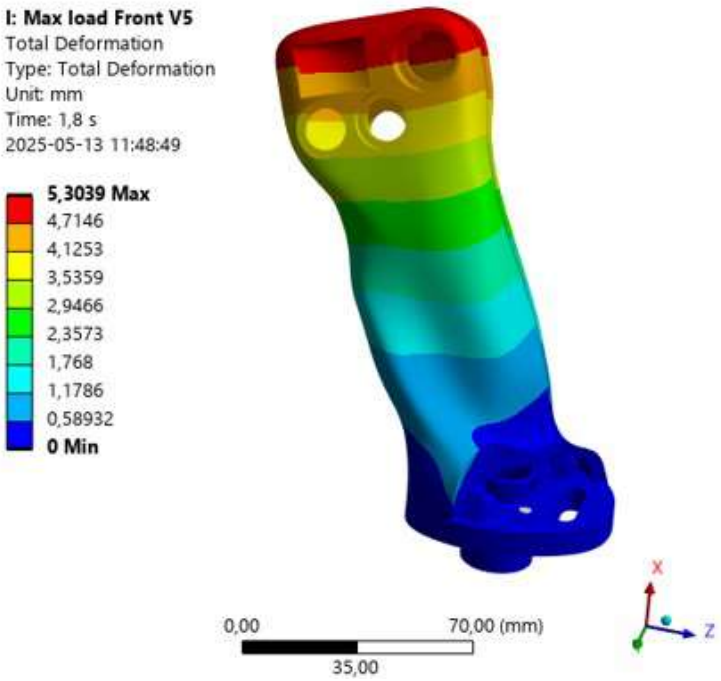

Figure 4.17: Deformation - LC1

The stress is concentrated near the base of the joystick, where the two shell halves are bolted together and the ball joint is mounted. Contact pressure in this region generates localized high stresses, see Figure 4.18. The maximum von Mises stress, excluding localized sub-element peak values, reaches stress levels within 80 MPa of the material's yield stress.

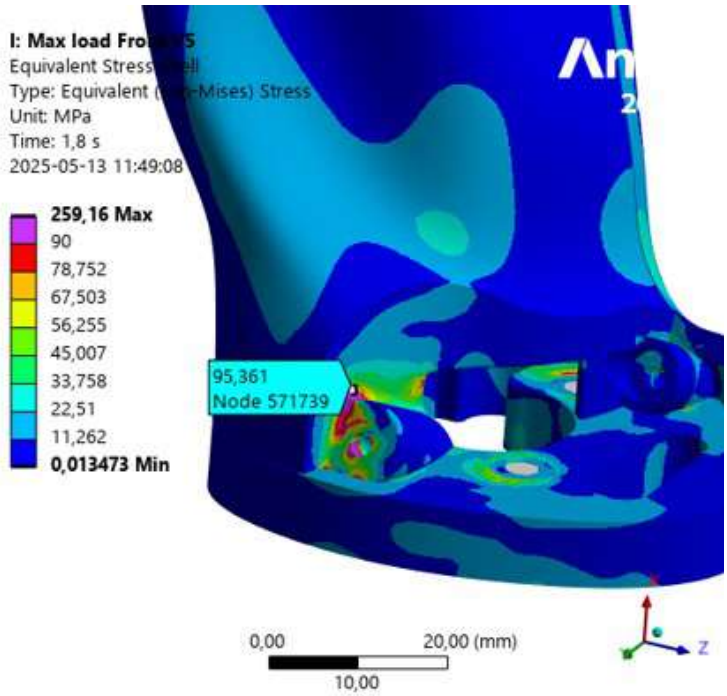

Figure 4.18: Von Mises stress, Joystick shell - LC1

4.5.4.2 Shear stress at lower attachment

The lower attachment point is subjected to high shear stress due to the bonded contact assumption, see Figure 4.19. At the surface, tangential forces develop as the applied load deforms the structure and the opposing surfaces tend to slide relative to each other. The resulting shear stress is concentrated within the first two element layers from the surface. This effect could be mitigated by explicitly modeling the screw, which would allow the load to be transferred through the base of the joystick rather than being absorbed solely by the surface nodes. Two possible modeling approaches include representing the screw as a solid cylinder or as a beam element, see Figure 4.20 and Figure 4.21.

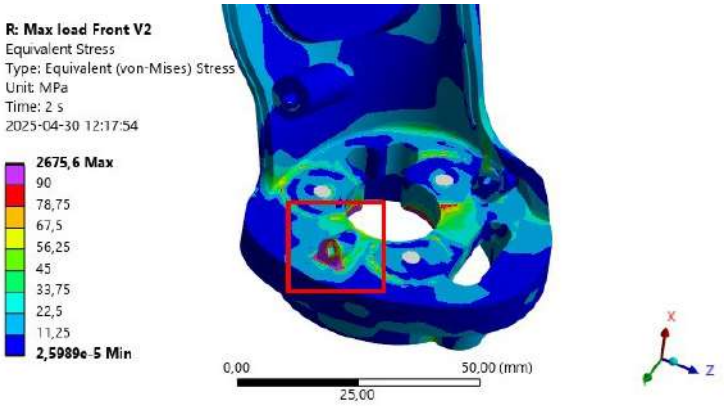

Figure 4.19: Shearstress from bonded contact assumption - LC1

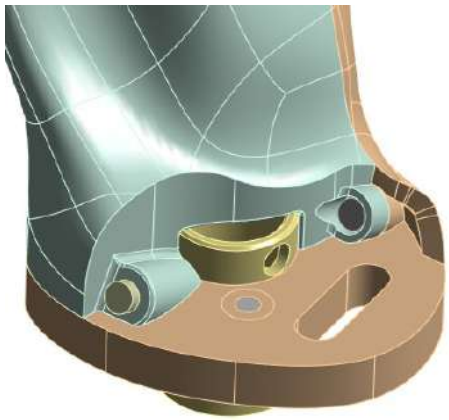

Figure 4.20: Bolt as a cylinder

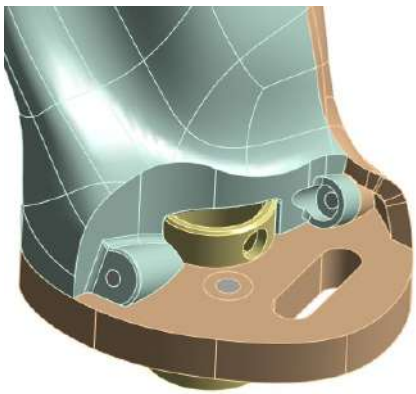

Figure 4.21: Bolt as a Beam element

The bolt modeled as a cylinder and a Beam element are alternatives to the bonded contact, see Figure 4.20 and 4.21. As the modeled bolt transfers the load into the material rather than right at the contact surface, the stress is lowered, and yielding is no longer a problem. The bolt modeled as a cylinder resulted in lower stress, but it has a local high-stress area that is neglected because of its singularity, see Figure 4.22. The simulation of the bolt, when modeled as a beam element, did not converge. Therefore, the bolt was modeled as a cylinder in the following simulations.

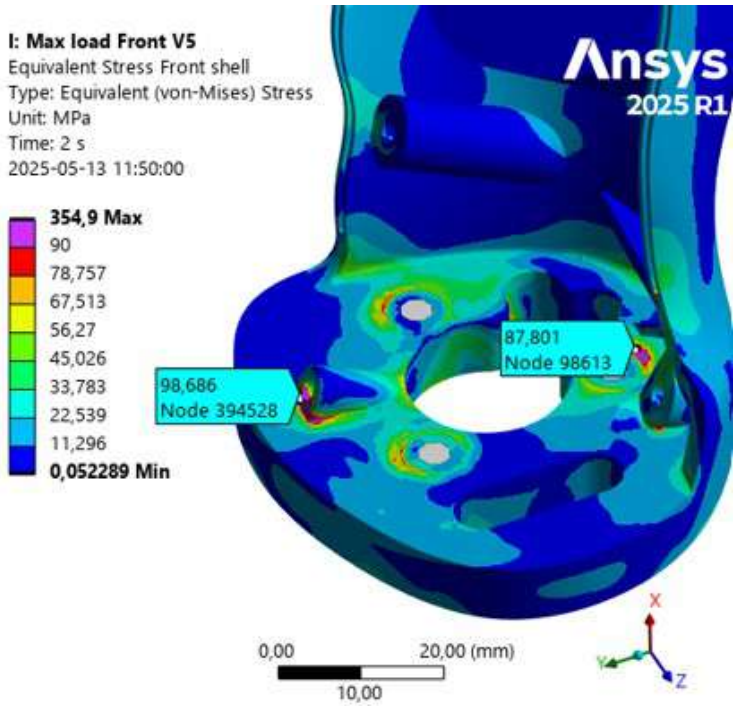

Figure 4.22: Shearstress from Bolt contact assumption - LC1

4.5.4.3 Clamping force

Maintaining a positive clamping force in the three screws securing the ball joint mechanism to the joystick ensures that separation under load is minimized or avoided

entirely. Across all evaluated load cases, the lowest resulting pretension was observed in LC3, where one screws preload dropped from the initial 1kN to 223N. This confirms that no separation occurs and suggests that the initial pretension could be reduced if needed. The highest screw load was recorded in LC4, reaching 2934N. With a calculated safety factor of 1.9.

Contact behavior was evaluated by analyzing the gap between components at their contact surfaces. Load cases LC2 and LC3 exhibited the largest gaps in the lower region, see Figure 4.23 and Figure 4.24. In LC3, the maximum gap reached 0.4mm, potentially creating a small opening into the joystick housing. However, this is considered acceptable given the severity of the load case and is not expected to affect the overall appearance or functionality of the joystick. Around the lip region, LC1 had sections with gaps and was deemed acceptable based on the relatively small gap, see Figure 4.25.

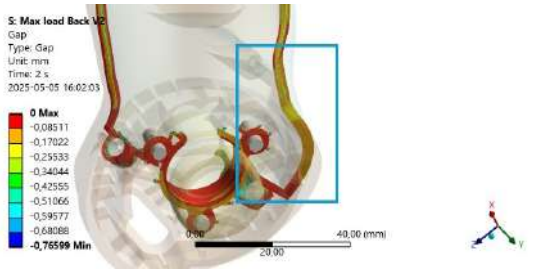

Figure 4.23: Gap in bottom region of joystick at load case LC2

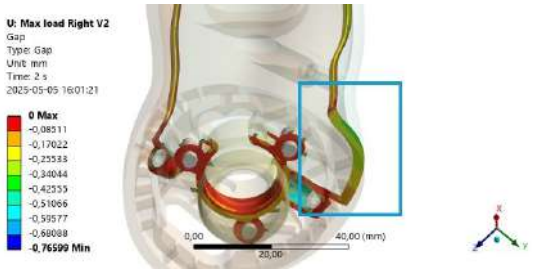

Figure 4.24: Gap in bottom region of joystick at load case LC3

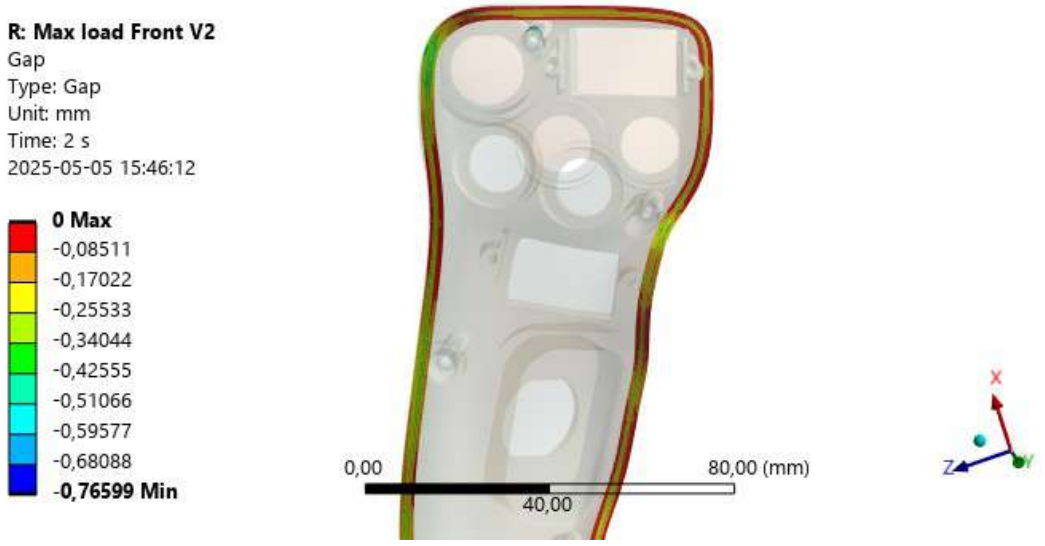

Figure 4.25: Gap in lip region at loadcase LC1

4.5.5 Dimensioning of ball joint adjustment mechanism

Based on the concept evaluation in Section 4.4.3, Concept A4 was identified as the most suitable for further development. The ball joint must withstand a force of $F = 200$ N applied in both the X and Y directions at a distance of $D = 130$ mm from the joint center. Under maximum loading conditions, the ball joint must remain fixed without slipping. The load application setup is illustrated in Figure 4.26.

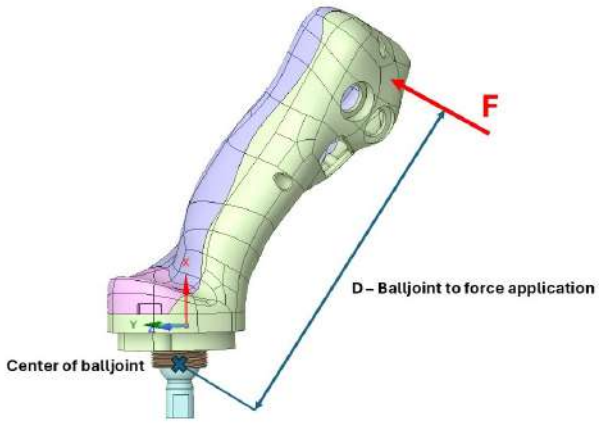

Figure 4.26: Distance from center of ball joint to force application

The angle α and β are symmetric about the horizontal axis and measure 34.2°, see Figure 4.27. Since a larger ball can generate the same resistive torque $M_{balljoint}$ as a smaller one but requires less clamping force, the ball joint was designed to maximize the use of available space. A ball with a diameter of 18mm and a M24x1 thread was selected. Using the given parameters in Equation 3.1-3.6, the resulting joystick torque was calculated as $M_{joystick} = D \cdot F = 0.14 \cdot 200 = 26$ Nm. To achieve this torque, the corresponding clamping force of $F_F = 25.84$ kN is required. An M24x1 fastener with an assumed thread friction of $\mu = 0.14$, a tightening torque of 53 Nm is needed to generate the necessary clamping force at the joint.

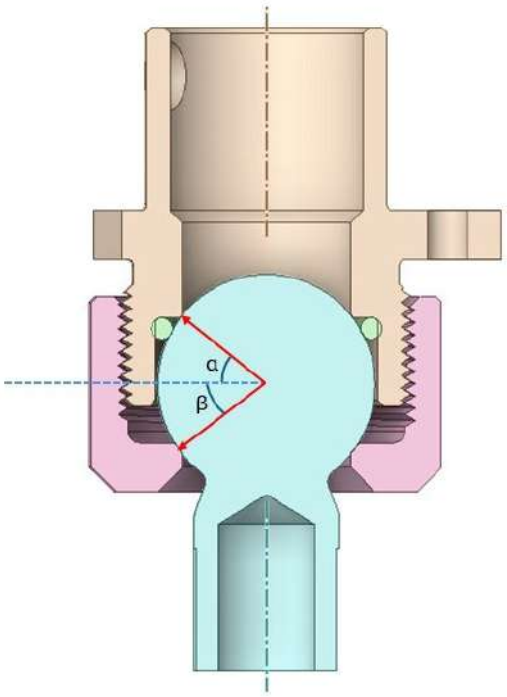

Figure 4.27: Angle to contact point

The load case which resulted in the highest stress in the top part of the ball joint mechanism was LC1. Excluding the sub-element high stress area of 355.4 MPa around the screw hole, the realistic highest stress is 235.02 MPA, see Figure 4.28. At the stress area, the joystick shell deformed and came in contact with the ball joint mechanism. A local contact point with a high force over a small area resulted in a relative high stress. The mild steel 1018 has a yield strength of 400 MPa and the safety factor is thereby in the range of 1.7. Since no cycle fatigue will occur at the specified max load, the safety margin is deemed high enough for the application.

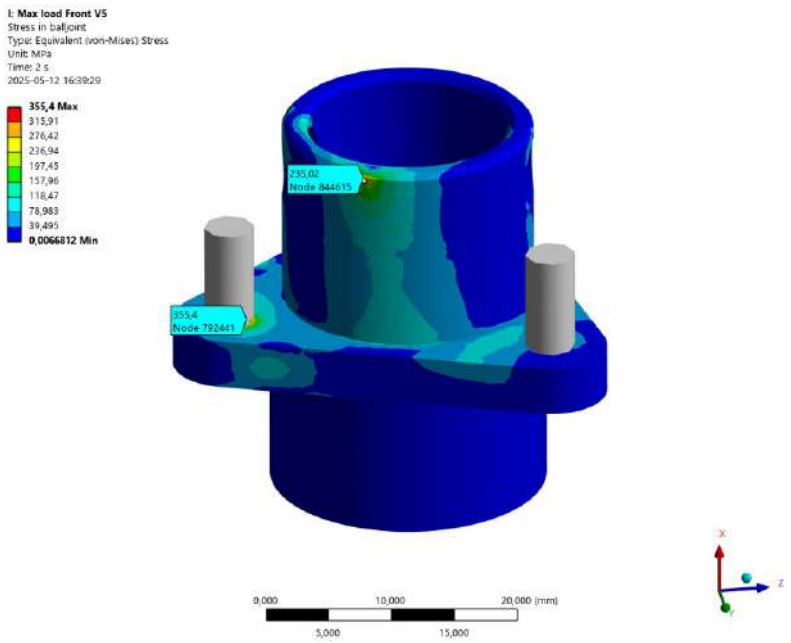

Figure 4.28: LC1: Worst loadcase for ball joint

An FEM validation was conducted to assess the stress in the ball joint when the nut is torqued to 53 Nm. The reaction force resulting from the remote displacement was analyzed, with the stress distribution shown in Figure 4.29 corresponding to a reaction force of 25.84 kN. The maximum stress, excluding localized peaks at the contact interfaces, is 380 MPa.

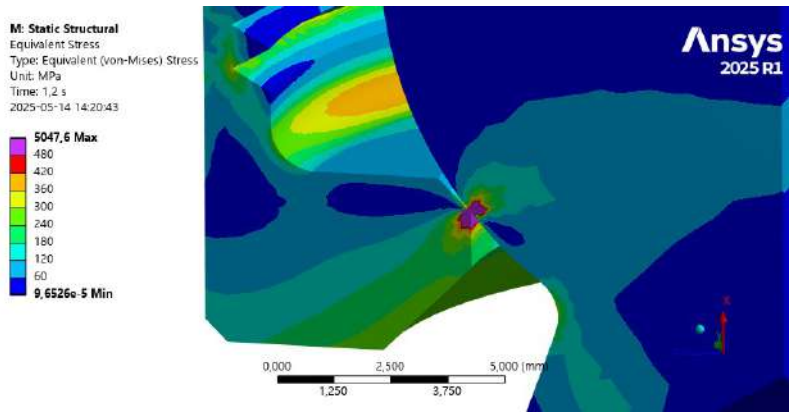

Figure 4.29: Stress distribution in ball joint at tightening torque

4.6 Final concept

Here, the final design of the joystick is presented in detail. The section describes its main features, components, and the reasoning behind the design choices made during development.

4.6.1 Overview of CAD model

The fully assembled joystick, together with a suggested base mount design, is illustrated in Figure 4.30. The base mount was not within the scope of this thesis, however, a proposed concept has been designed to get a feel for the overall size. The exact method of mounting the joystick base in the cab, whether from the armrest or from a floor-mounted control panel, has not yet been determined, as VCE will define this interface. The overall size of the joystick is shown in Figure 4.31, with an exploded wireframe view presented in Figure 4.32.

Figure 4.30: Overview of the fully assembled joystick together with a suggested base mount design

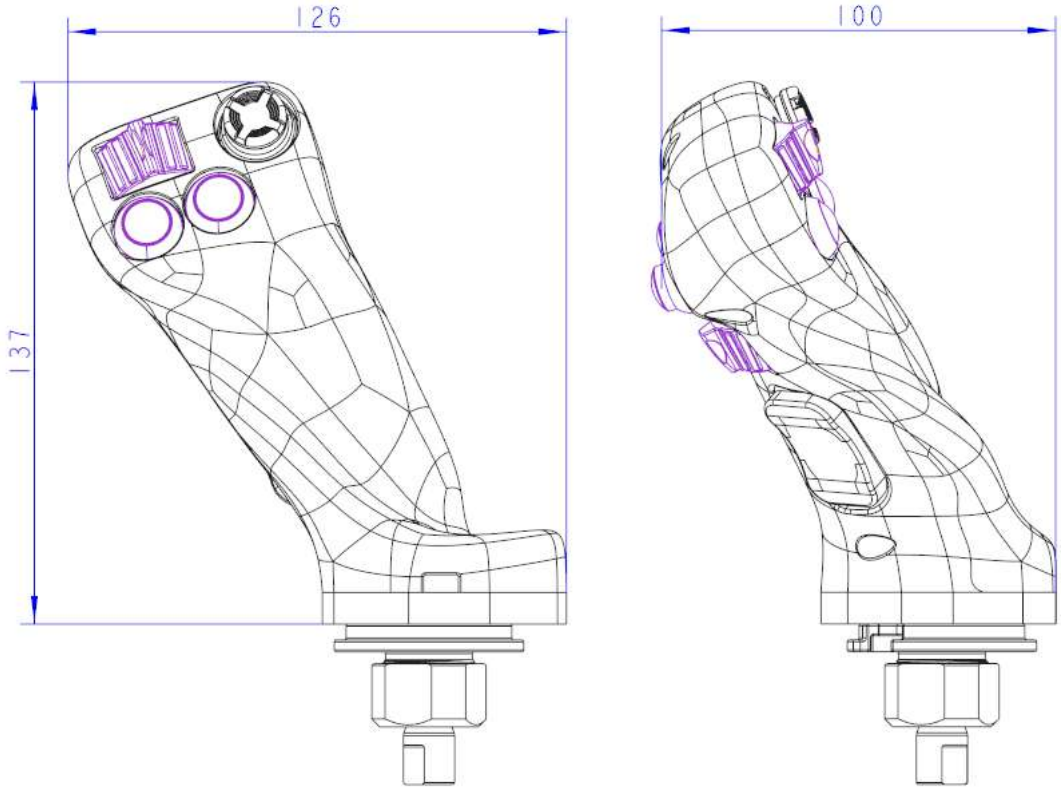

Figure 4.31: Rough size of the joystick handle

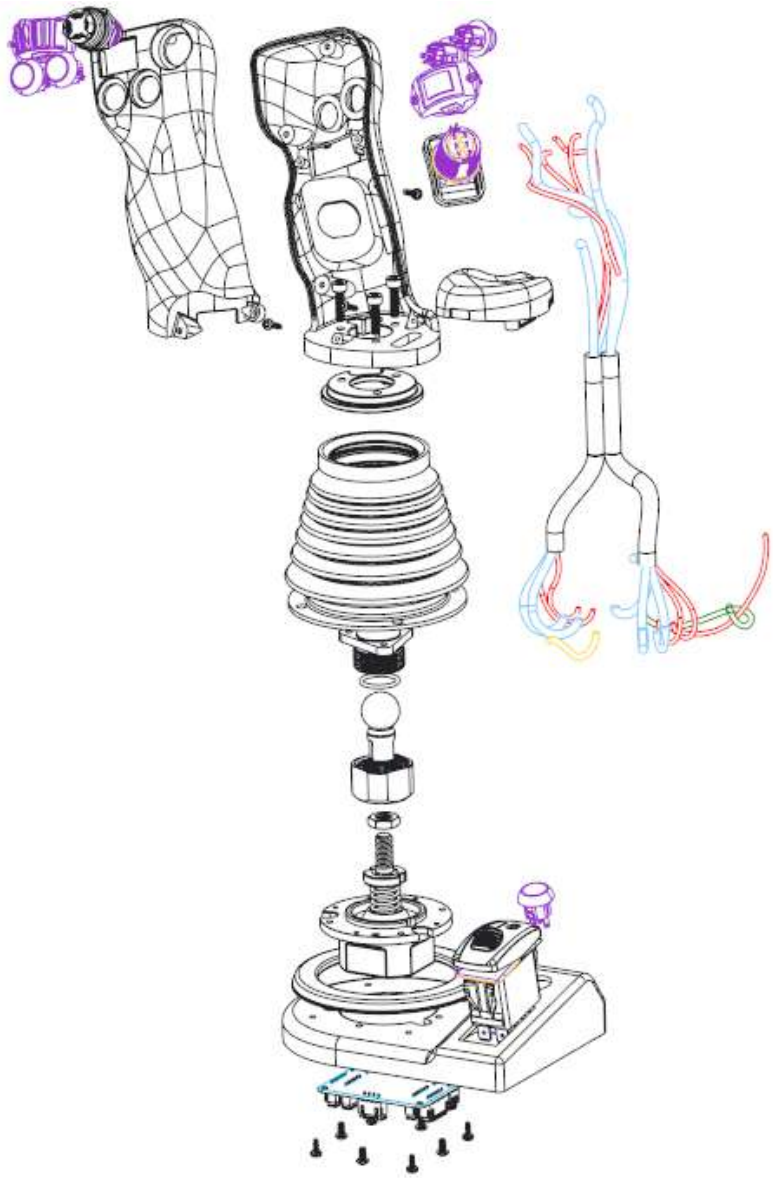

Figure 4.32: Exploded view of joystick assembly in wireframe appearance

4.6.2 Ball joint adjustment mechanism

Figure 4.33 illustrates the ball joint adjustment mechanism and all the components of the assembly. The main hydraulic function is sourced from a company and the only modification that would be necessary is to add an M8 external thread to the shaft. Further modifications to the main function were removing two slots to make room for guiding the harness down to the CAN PCB. Talking to the manufacturer, these modifications would be feasible in the context of possible series production. The ball shaft has a matching thread and is locked to the main function shaft using a low-profile M8 jam nut.

The mounting shaft features three threaded holes, allowing it to be secured using three M4 bolts from inside the handle. This design removes the need for threaded

inserts in the plastic joystick housing. Integrating the threads directly into the mounting shaft not only simplifies assembly but also reduces part count and overall manufacturing cost. While the final material has not yet been selected, a steel with mechanical properties similar to 1018, combined with a zinc coating for corrosion protection, would be suitable.

The role of the o-ring is to provide friction to the ball shaft when adjusting the joystick's angle. Without the o-ring, there would be a small window of adjustment where the mechanism is either locked or free moving, making it hard to perform small adjustments. When adjusting the mechanism, the nut would be slightly tightened, meaning that the o-ring is in contact with one side of the ball shaft and the other side is in contact with the metal. This provides enough friction to keep the joystick from falling over, but still allows for small adjustment. Once the desired joystick angle is acquired, the nut is fully tightened, compressing the o-ring and resulting in metal-metal contact on both sides of the ball shaft. This fully locks the ball shaft in position.

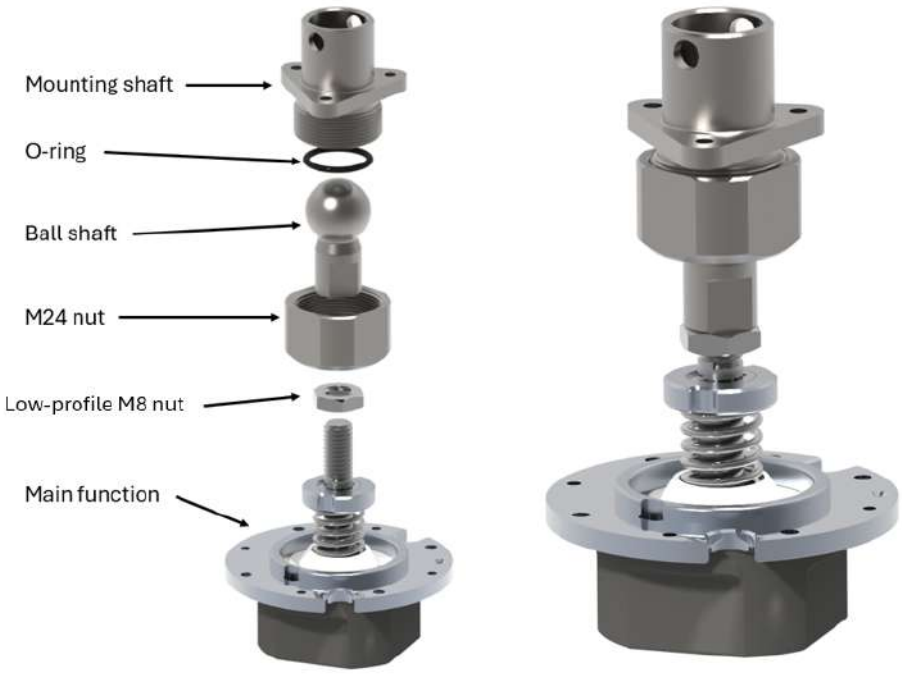

Figure 4.33: Render of Ball joint adjustment mechanism, exploded (Left) and assembled (Right) view state

When tightening the M24 nut an adjustable spanner must be used, and to make sure there is a way to resist the rotating motion when tightening, a hole in the mounting shaft can be used to insert a screwdriver. The hole is 5.5mm in diameter so any screwdriver or similar tool that fit can be used to hold the joystick stationary while tightening. The hole is accessed by removing the hand wrist support pad, see Figure 4.34.

Figure 4.34: Access hole for holding joystick stationary while tightening adjustment mechanism.

4.6.3 Rubber Boot

The silicone rubber boot is a flexible protection that allows unrestricted movement while protecting against water intrusion. The specific material type is not decided and would be up for discussion with the manufacturer.

To allow easy access to adjust the neutral position of the joystick handle using the ball joint mechanism, the top of the boot is forced over a boot flange lip, see Figure 4.35-4.36. This prevents the rubber boot from loosening when moving the joystick around, providing with easy accessibility for adjustment and requires no tools for installation.

The boot mount is fastened using four self forming screws from the inside of the base mount, see Figure 4.36. The motivation was to hide any visible screws from the outside for aesthetic reasons, but also to prevent any water from entering around the screw, if they were mounted from the outside. The rubber boot has four holes which the boot mount aligns with.

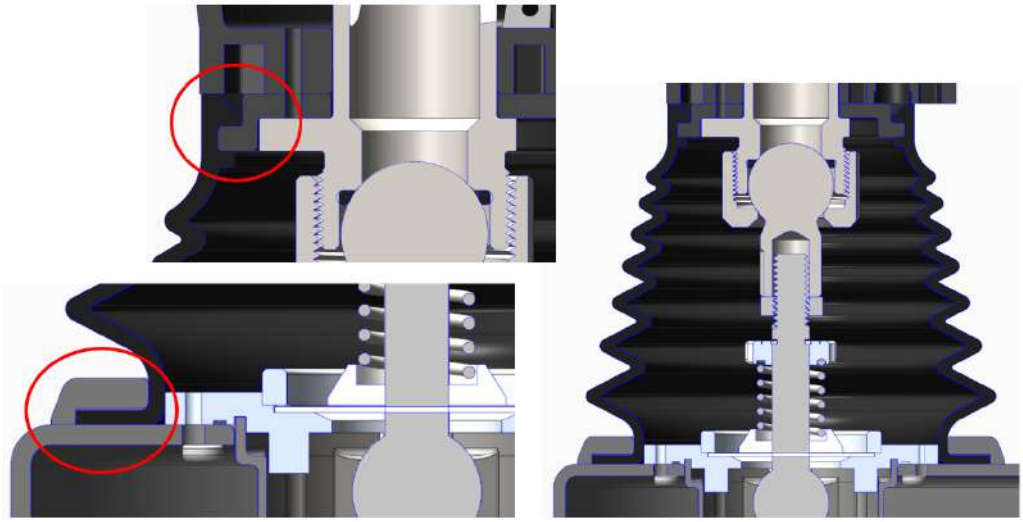

Figure 4.35: Cross-section showing mounting and sealing method for the rubber boot.

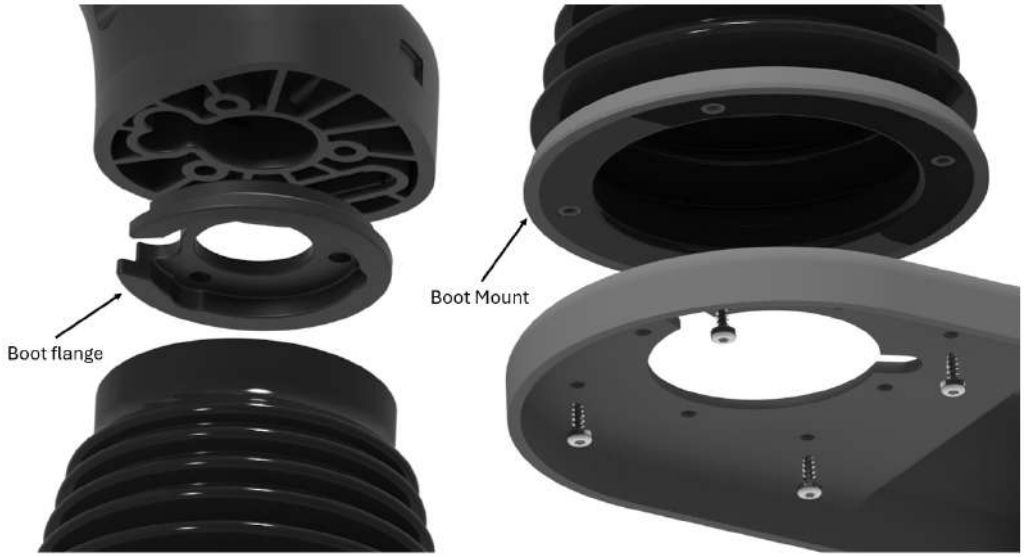

Figure 4.36: CAD render showing the boot flange and boot mounting.

4.6.4 Electronics Hardware Design

Due to the limited knowledge about electrical hardware design and since this was not the main focus of the thesis, it was convenient to connect each button with wires through the handle and down to the Controller Area Network (CAN) PCB as illustrated in Figure 4.37. Around the area from exiting the joystick handle and entering the base, there is a protective rubber sleeve (illustrated in black) which will prevent any chafing on the wires when movement occurs.

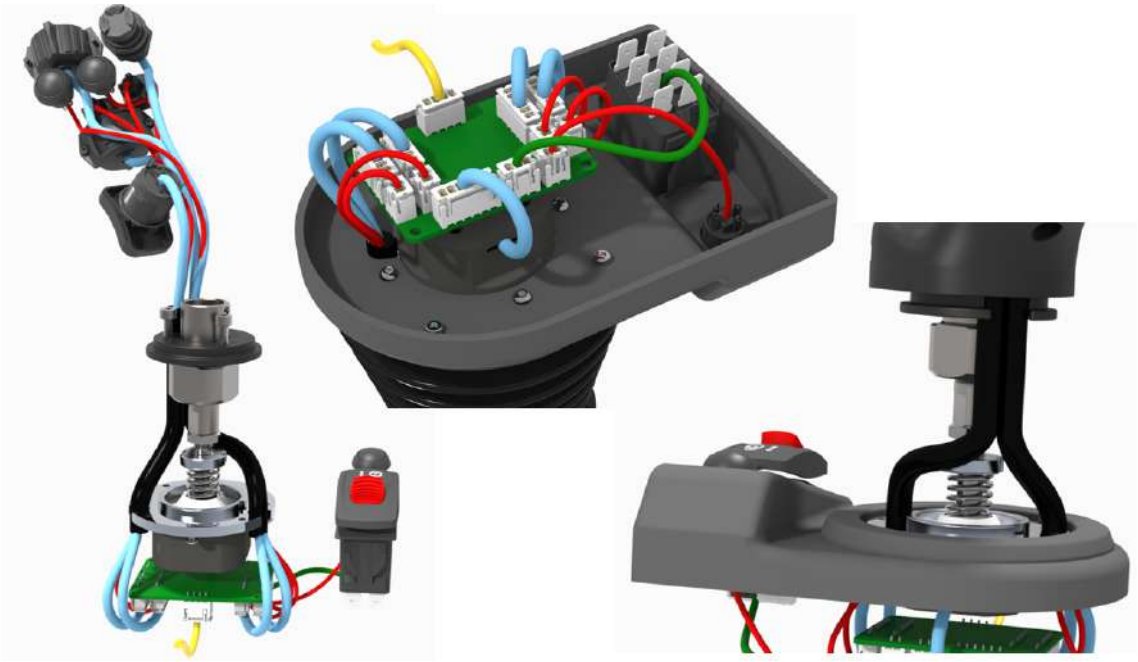

Figure 4.37: Overview of the wiring harness

The PCB takes the analog and digital signals from the buttons and converts them to CAN which are connected to the Electronic Control Unit (ECU). The PCB is intended to be mounted beneath the main function on the base mount using standoffs. The detailed PCB design is outside the scope for this thesis however, it is necessary to have a representative model since this will affect the assembly order and overall design concept.

The goal for the PCB was to be as small as possible to give more design freedom in the base mount. From internal conversations, it was estimated that an area of 30×30 mm (excluding connectors) would be enough to create the necessary connections. A simple schematic of the PCB with the number of pin outs for each connector and overall size can be seen in Figure 4.38. The space claim model of the PCB is illustrated in Figure 4.39, together with JST XH connectors.

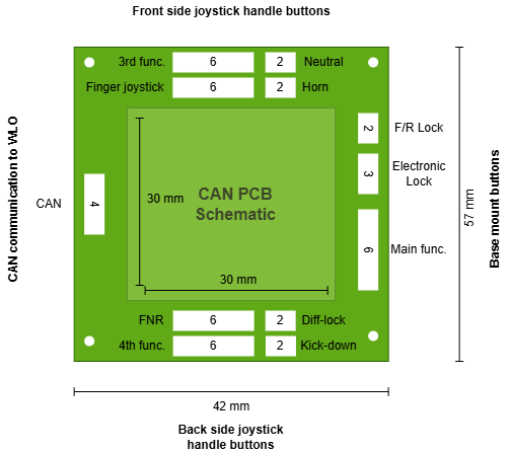

Figure 4.38: CAN PCB schematic with number pin outs

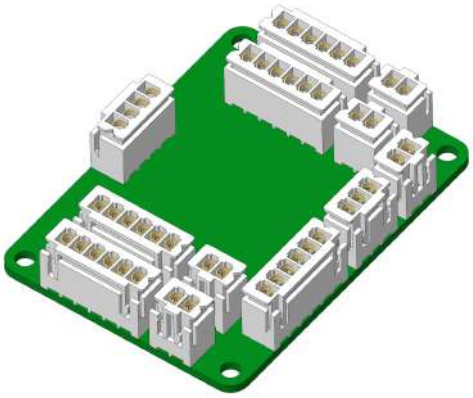

Figure 4.39: CAD model of the CAN PCB with JST XH connectors

4.6.5 Prototype validation

In order to validate the final CAD design, a prototype was manufactured. The ball joint mechanism was outsourced to be machined in Mild Steel 1018 in a CNC lathe and mill, see Figure 4.40. The joystick handle was 3D Printed in Nylon using SLS and the rest of the plastic parts were 3D Printed in PLA or PETG using FDM technology as seen in Figure 4.42. Buttons were provided from the respective manufacturers including the main function. The silicon rubber boot was molded using 3D Printed molds and hobby silicon, see Figure 4.41. For further details on the rubber boot manufacturing process, see A.5.

Figure 4.40: Ball joint prototype.

Figure 4.41: Silicone boot prototype

Figure 4.42: Joystick prototype made from Nylon using SLS.

Throughout the product development process, multiple joystick handle prototypes were manufactured, each featuring different shapes and button layouts. This was an iterative process in which each version received feedback that informed improvements for the next design. In total, ten prototypes were created, with the tenth serving as the final version shown in the figures. The primary focus during prototyping was on validating the button layout, ergonomics, and assembly process which was successful. More advanced testing such as for IP protection, weather resistance, or strength testing would require a prototype made from the final production materials.

4.7 DFMA

Both DFM and DFA principles were applied throughout the product development process. For the IM plastic joystick handles, DFM focused primarily on optimizing the split line to avoid undercuts and to ensure appropriate draft angles for efficient mold release. DFA was also integrated into the process and proved valuable in identifying components and assembly steps that would contribute to increased manual assembly costs. The analysis was visualized using a graph that highlighted the components with the highest impact on assembly cost.

4.7.1 DFA

First step is to decide on the assembly process for the joystick and all the parts for each assembly, see Figure 4.43. Yellow boxes explain the assembly step, white box represents a part, green boxes a sub-assembly, and blue boxes are the fully assembled joystick handle. Note that this assembly flowchart does not include the mounting of the joystick to the main function or any assembly steps included in the base mount.

For each part and sub-assembly a component handling and fitting analysis is performed, for which handling and fitting indexes H and F are calculated. The indexes are later used to calculate the *Cma*, which is the cost for manual assembly in SEK. Total manual assembly cost and assembly time was calculated to 105 SEK, 12.6 min. The cost estimates were deemed reasonable when compared to internal manufacturing data from the prior VSL. Labor rate was estimated to 500 SEK/h [44].

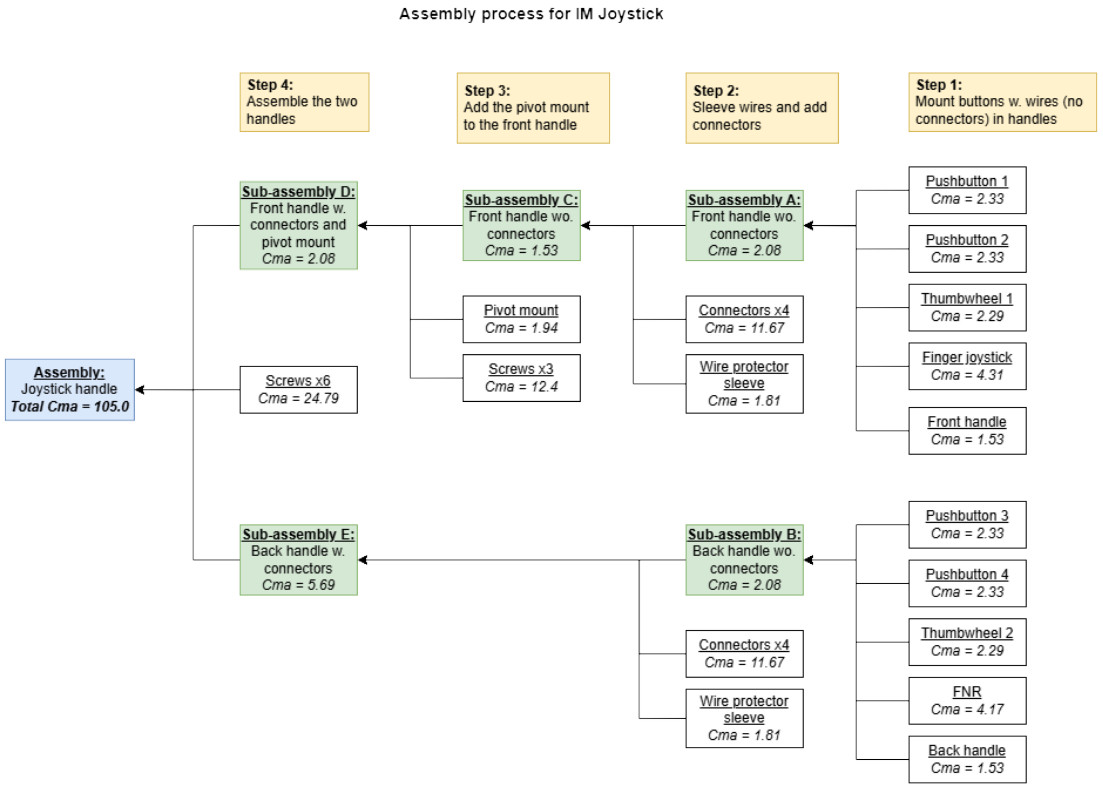

Figure 4.43: Assembly flowchart for joystick handle, $C_{\mathrm{ma}}[SEK]$

Cost for manual assembly is noted for each assembly step for all parts and sub-assemblies, but to make an easier comparison on what contributes to cost the most, they were plotted as seen in Figure 4.44. The horizontal axis represent all the parts and sub-assemblies in the process and vertical axis is the % contribution cost for each of those parts and assemblies on the total assembly cost.

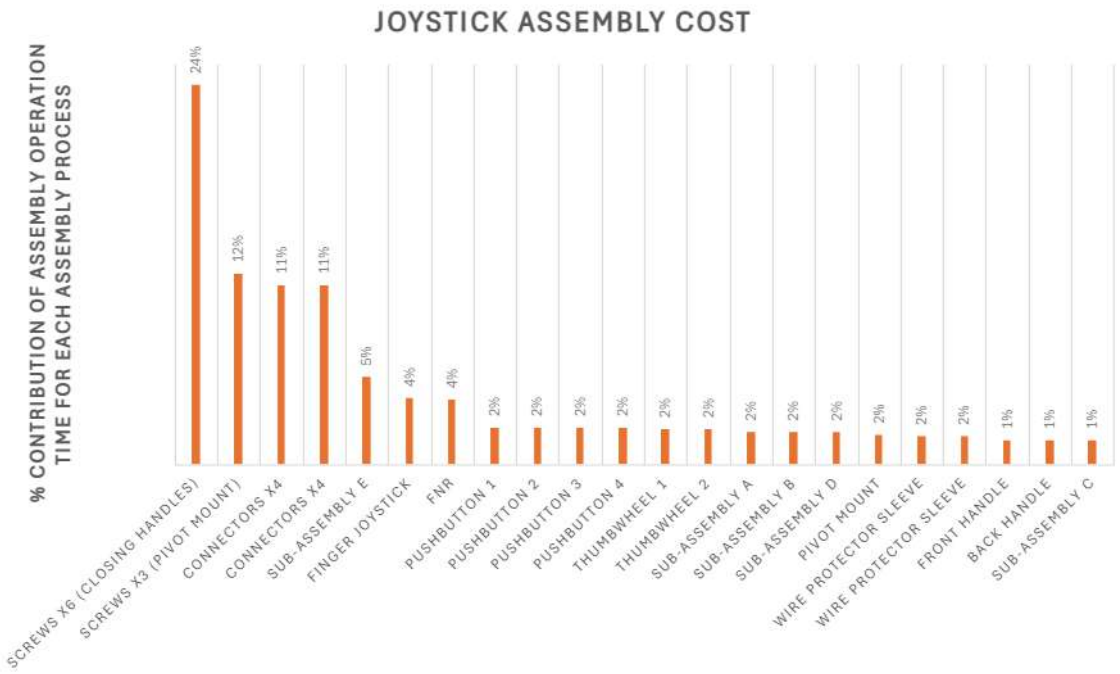

Figure 4.44: Percental assembly cost contribution for each assembly process

It can be concluded that assembling screws and fitting connectors to wires are the main contributors to assembly cost. Wires are assumed to be pre-crimped with crimp terminals but without the connector installed, due to the installation of the protective sleeve. The model considers several potential steps that could increase assembly time, for example, the risk of pinching wires in a certain assembly step. However, the model should only be used to estimate the manual assembly cost and the true value will depend on the manufacturer and other variables.

4.7.2 DFM

DFM was implemented in the design phase where manufacturing constraints affected the design of the joystick. The split line between the front and back half was decided by where the draft angle went from positive to negative. A negative draft angle generates undercuts and the part cannot be removed from the tooling. The pull-out direction was decided on early since the placement of buttons affected the pull-out direction. The front half was designed not to need any sliders as the buttons are placed parallel to the pullout plane, see Figure 4.45. The rear part of the shell has a pullout direction normal to the bosses, but for the buttons, three sliders are needed as they are angled to the pullout plane, see Figure 4.46.

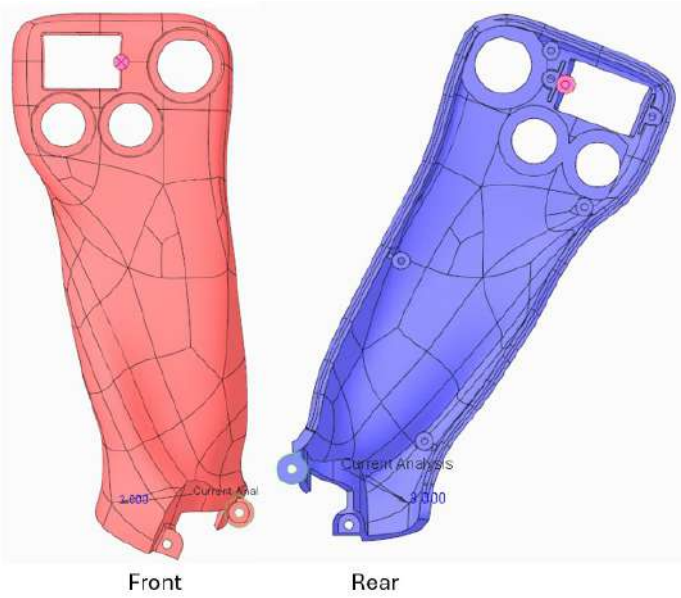

Figure 4.45: Draft analysis of the front part of the shell viewed from the front and rear

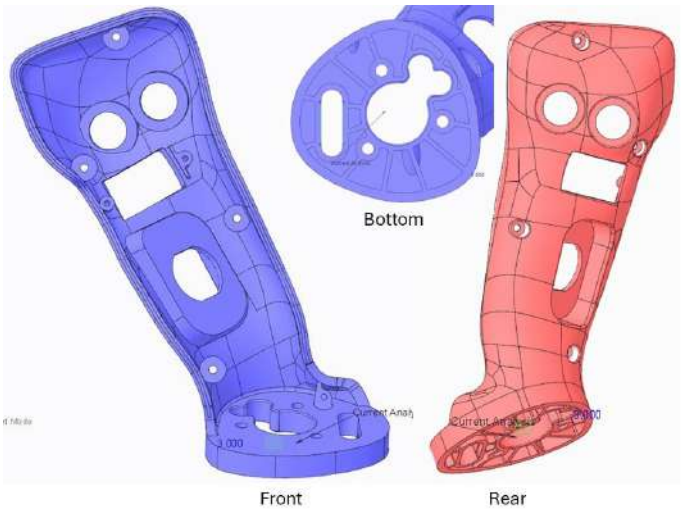

Figure 4.46: Draft analysis of the back part of the shell viewed from the front and rear

4.8 DOE

Definitive screening design identified significant factors for each response. There were instances due to inaccuracies in the simulations, responses displayed a lack of fit. Altogether, the remaining responses all share the five input factors, meaning a decision was made to focus on the Sink Mark to reduce the size of the optimization. The result from the screening design was that Sink Marks are significantly affected by the factors: Melt Temperature, Filling Time, and Gate Diameter, this will there-

fore be the reduced design used in the optimization stage.

A full factorial design experiment (3×3×3 runs) was conducted to optimize the significant factors affecting Sink Mark. Contour plots and response analysis showed significant effects, notably a previously undetected interaction between Filling Time and Melt Temperature ($p = 0.01723$), likely missed in the screening phase due to interaction correlations. Optimization determined that the ideal settings to minimize Sink Mark (to 0.0252 mm) are: Gate Diameter = 1 mm, Filling Time = 4 s, and Melt Temperature = 240°C. The model predicts the Sink Mark as a function of Gate Diameter, Filling Time and Melt Temperature.

Model validation checks prediction accuracy and prevents overfitting by using an 80/20 train-validation data split. The model performs well on both sets, with high RSquare, low RASE, and small, randomly scattered residuals, indicating good generalization and no overfitting.

4.8.1 Definitive Screening Design

The screening design consisted of 18 experimental runs. Simulation responses from these runs are presented in Table 4.7.

Table 4.7: Responses from the simulations for the Screening Design

	FACTORS					RESPONSE										
Run	Gate Location	Gate Diameter	Filling Time	Melt Temperature	Mold Temperature	Sink Mark [mm]	Pressure [MPa]	Temperature [C]	Max Shear Rate [1/s]	Max Shear Stress [MPa]	Frozen Layer Ratio [%]	Max Cooling Time [s]	Volumetric Shrinkage	Sprue Pressure [MPa]	Clamping Force [ton]	Flow Rate [mm3/s]
1	B	2	4	280	75	0.053	21	277.85	1403.767	54.112	76.262	58.636	3.178	27.34	8.647	6347.96
2	A	2	2	240	60	0.044	67.17	241.38	1941.675	47.356	70.619	37.663	2.722	72.115	13.237	12695.5
3	A	3	3	280	75	0.068	33.518	279.172	709.713	65.123	64.728	58.639	3.145	36.194	7.235	8475.67
4	B	1	3	240	60	0.036	52.083	240.672	841.479	55.524	83.573	37.713	2.713	63.722	13.29	8459.9
5	B	3	2	260	75	0.055	27.719	260.079	1020.991	42.895	64.246	57.581	3.293	32.788	7.35	12713.3
6	A	1	4	260	60	0.04	55.174	260.507	700	60.705	95.575	38.213	2.987	63.776	12.496	6345.61
7	B	3	2	240	67.5	0.048	41.108	240.51	1338.825	75.988	69.089	43.429	2.989	49.61	11.219	12713.3
8	A	1	4	280	67.5	0.047	39.297	280.367	700	73.351	90.172	44.92	3.189	45.811	9.072	6345.61
9	B	3	4	240	60	0.035	48.713	239.935	610.15	60.495	94.148	37.788	2.744	66.3	16.347	8556.7
10	A	1	2	280	75	0.056	31.008	280.396	800	68.849	64.076	58.002	3.241	36.715	8.974	12691.2
11	A	3	2	280	60	0.068	30.814	279.612	1251	86.64	69.191	41.03	2.854	34.02	6.466	12713.8
12	B	1	4	240	75	0.026	86.816	240.709	1088	42.876	81.583	52.459	3.424	94.315	18.44	6345.61
13	A	3	4	240	75	0.035	73.172	239.536	824	88.216	76.22	54.911	3.087	76.901	15.487	5356.9
14	B	1	2	280	60	0.063	19.289	280.338	921	43.906	68.575	40.974	3.031	27.183	5.019	12689.9
15	B	3	4	280	60	0.054	16.046	278.603	1167	56.006	91.02	41.055	2.706	26.055	6.132	8556.7
16	A	1	2	240	75	0.037	67.481	240.683	1051	43.257	65.279	52.459	3.244	76.288	13.824	12691.2
17	A	2	3	260	67.5	0.051	47.29	259.973	1131.535	65.387	69.051	45.876	3.003	51.375	9.92	8463.64
18	B	2	3	260	67.5	0.042	27.396	259.258	951	94.527	77.781	45.868	2.745	36.893	8.019	8463.1

Using JMP software, significant main effects and second-order interactions were studied for each response using a t-test, and the resulting p-values were examined. A significance level of 5% ($\alpha = 0.05$) was used, which is a standard threshold in statistics. This means there is a 5 % chance of wrongly identifying an effect that is not really there. Factors with p-values below 0.05 were considered statistically significant and were not eliminated during the screening process, as they are unlikely to be due to random chance. The confidence interval is therefore by definition $1 - \alpha = 95$ %.

An example on how the result was presented in the software for one of the responses is displayed in Figure 4.47. Here an example on the Cooling Time response with p-values for significant factors and two-way interactions are circled in red.

Factors responsible for main effects on Cooling Time:

- Mold Temperature
- Melt Temperature
- Gate Diameter
- Gate Location

Factors responsible for second-order effects on Cooling Time:

- Mold Temperature*Mold Temperature
- Gate Diameter*Mold Temperature
- Gate Diameter*Gate Diameter

Furthermore, analyzing the prediction profiler, non-linearities are caused by Gate Diameter and Mold Temperature.

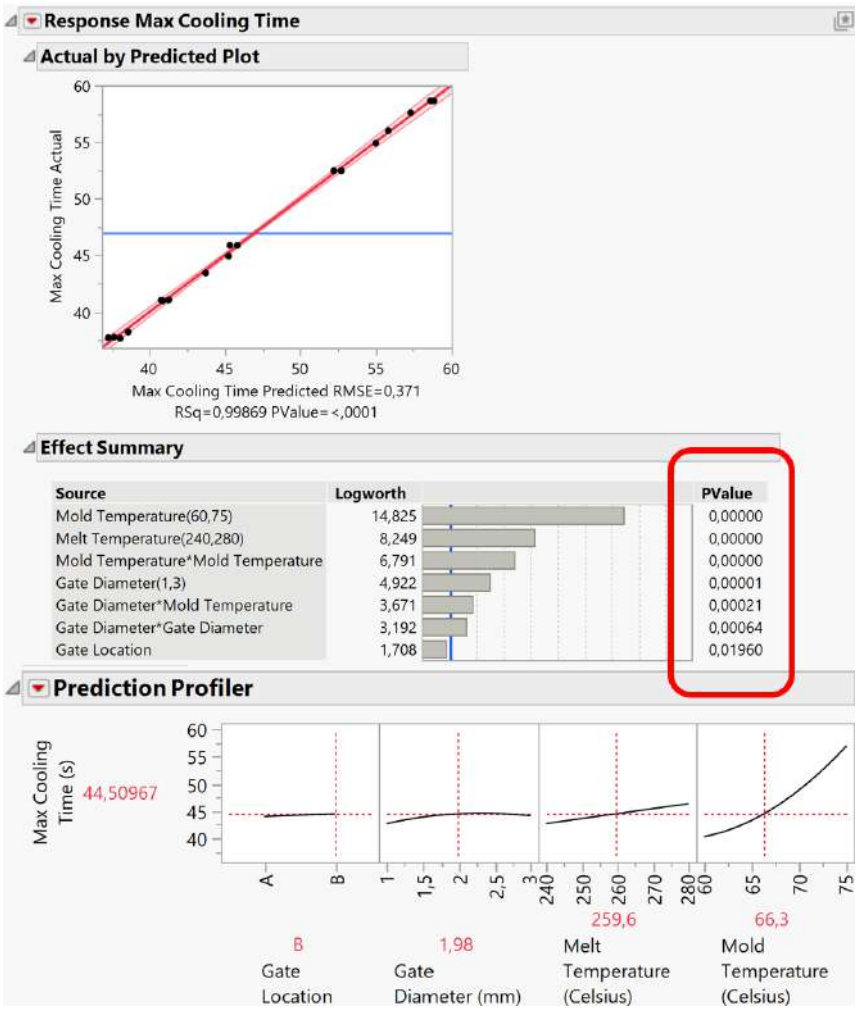

Figure 4.47: Screening result for Cooling Time with p values in red

The significant factors for all the responses are tabulated in Figure 4.8. Green means significant, p value close to 0 and red means close to p value = 0.05, not significant. It can be noted that some of the responses showed a lack of fit due to the data being too unpredictable. This was most likely due to how the simulation result was interpreted. Since the response expects a single value but the FEA simulations provide a finite number of values for the entire model over the range of the filling process, it was required to decide on how the simulations results should be extracted. All the results were extracted at the end of the filling process and the highest value for each response was recorded to make as fair a comparison as possible.

Table 4.8: All significant factors for the response variables with p-values

P-value < 0.05 = Significant

Sink Mark [mm]		Pressure [MPa]		Temperature [C]		Max Shear Rate [1/s]		Max Shear Stress [MPa]		Frozen Layer Ratio [%]		Max Cooling Time [s]		Volumetric Shrinkage		Sprue Pressure [MPa]		Clamping Force [Ton]		Flow Rate [mm3/s]	
Factor	P-value	Factor	P-value	Factor	P-value	Factor	P-value	Factor	P-value	Factor	P-value	Factor	P-value	Factor	P-value	Factor	P-value	Factor	P-value	Factor	P-value
Melt Temp	0	Melt Temp	0	Lack of fit		Lack of fit		Gate Dia	0.04849	Fill Time	0	Mold Temp	0	Lack of fit	0	Melt Temp	0	Melt Temp	0	Lack of fit	0
Fill Time	0.00001	Gate Loc	0.00143							Mold Temp	0.00007	Melt Temp	0		0	Gate Loc	0.00245	Fill Time	0.00052		
Gate Dia	0.00021	Fill Time	0.0298									Gate Dia	0.00001			Fill Time	0.009	Gate Loc	0.03584		
												Gate Loc	0.0196			Gate Dia	0.01116				
												Mold Temp*Mold Temp	0								
												Gate Dia*Mold Temp	0.00021								
												Gate Dia*Gate Dia	0.00064								

Another potential issue that may have influenced the results and contributed to unpredictability was the mesh size. In CREO Mold Analysis, there is no way to visualize the mesh or make any advanced changes like local refinements. The simulation mesh element size can be defined in 3 levels: Coarse, Medium and Accuracy. A mesh comparison was made to see how the mesh element size affects the response, see Figure 4.48. Shear Rate and Sink Mark were compared using Coarse and Accuracy mesh element size using factors defined in Run 1. These responses were picked since Shear rate showed a lack of fit and Sink Mark did not.

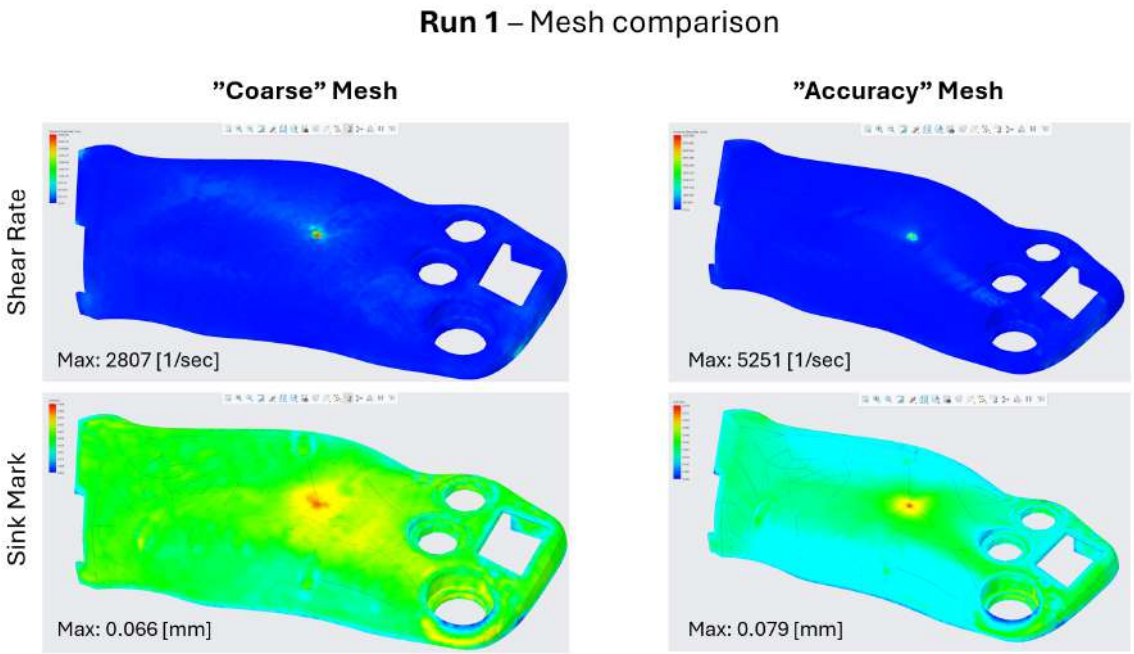

Figure 4.48: Mesh comparison for Run 1, showing Shear Rate and Sink Mark

In Figure 4.48, it was clear that for the Shear Rate simulation, there was a concentration at the gate entry and max Shear Rate differs significantly between the two simulations. The simulation has a hard time capturing the result, which leads to inaccurate values, which in the end creates the lack of fit issue. For the Sink Mark simulations, both results are realistic and a slight increase in max value was expected. This shows why the DoE had an easier time finding responsible significant factors.

Therefore, all the responses showing a lack of fit was not of interest for this thesis. However, this would not help eliminate any factors in the screening stage. The significant factors for the renaming responses, together complete all five factors which was started with. It was therefore decided that to keep the DoE optimization to a manageable level, the focus was on analyzing the significant effects on Sink Marks. The focus remains, therefore on the surface finish and understanding how to minimize Sink Marks and improve the aesthetics of the IM parts. Figure 4.49 illustrates how the system looks after the screening process and which factors and responses will be investigated for the optimization.

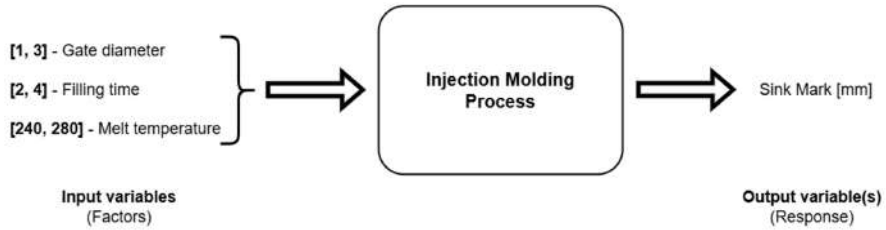

Figure 4.49: Remaining factors and responses after the Screening Design

4.8.2 Optimization

For the remaining three factors, a full factorial design ($3 \times 3 \times 3$ runs) was performed and results for Sink Mark are tabulated in Table 4.9. Insignificant factors, which were eliminated in the screening, were set to the center value: Mold Temperature = 67.5 Celsius & Gate Location = A.

Table 4.9: Full Factorial table design with simulation results

	FACTORS			RESPONSE
Run	Gate dia	Fill time	Melt temp	Sink Mark
1	1	2	240	0,037
2	1	2	260	0,049
3	1	2	280	0,066
4	1	3	240	0,031
5	1	3	260	0,042
6	1	3	280	0,062
7	1	4	240	0,027
8	1	4	260	0,039
9	1	4	280	0,059
10	2	2	240	0,044
11	2	2	260	0,056
12	2	2	280	0,066
13	2	3	240	0,039
14	2	3	260	0,051
15	2	3	280	0,060
16	2	4	240	0,034
17	2	4	260	0,045
18	2	4	280	0,065
19	3	2	240	0,045
20	3	2	260	0,057
21	3	2	280	0,069
22	3	3	240	0,038
23	3	3	260	0,051
24	3	3	280	0,074
25	3	4	240	0,034
26	3	4	260	0,053
27	3	4	280	0,071

Figure 4.50 illustrates the response using contour plots for the three combinations of Gate Diameter, Filling Time and Melt Temperature. Where red is an increase

and blue is a decrease in Sink Mark.

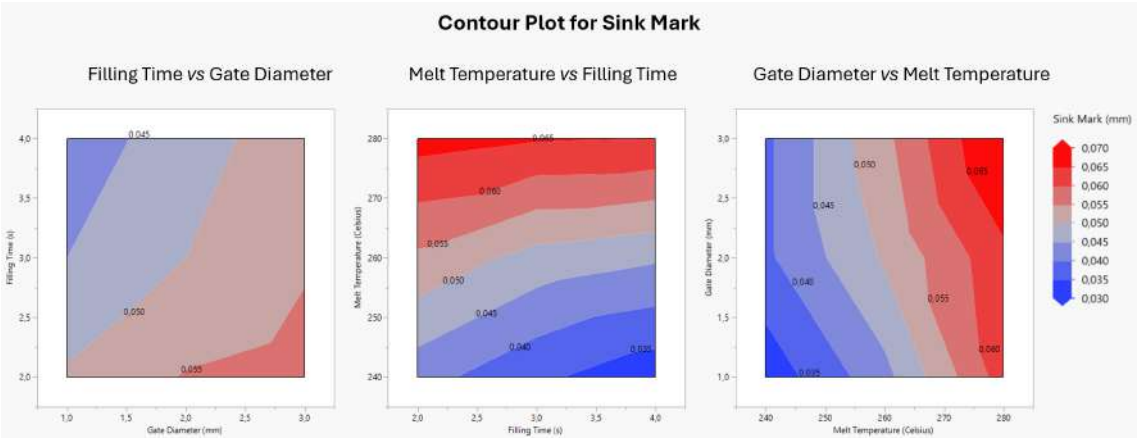

Figure 4.50: Contour plot for Sink Mark

Figure 4.51 shows the response for the experiment, displaying p-value and prediction profiler. The prediction profiler was set to maximize the desirability, in other words, minimize the Sink Mark. As expected the p-value for the significant factors were all $< 0{,}05$. It was noted that Filling Time*Melt Temperature showed an indication of significance (p-value 0.01723), which was not present in the Screening design. It was believed that this is due to the correlation between several two-factor to two-factor interactions in the Screening Design. Resulting in failing to identify Filling Time*Melt Temperature as a significant interaction.

Looking back at the correlation color map for the Screening Design, the absolute correlation for Gate Location*Gate Diameter & Filling Time*Melt Temperature = 0,466 and for Gate Location*Melt Temp & Filling Time*Melt Temperature = 0,311. Where 1 = correlation and 0 = no correlation. This could be part of the explanation to why the Screening design failed to identify Filling Time*Melt Temperature as significant. The finding does not affect the optimization result since the main effects were successfully identified however, it showed the importance of a correct design.

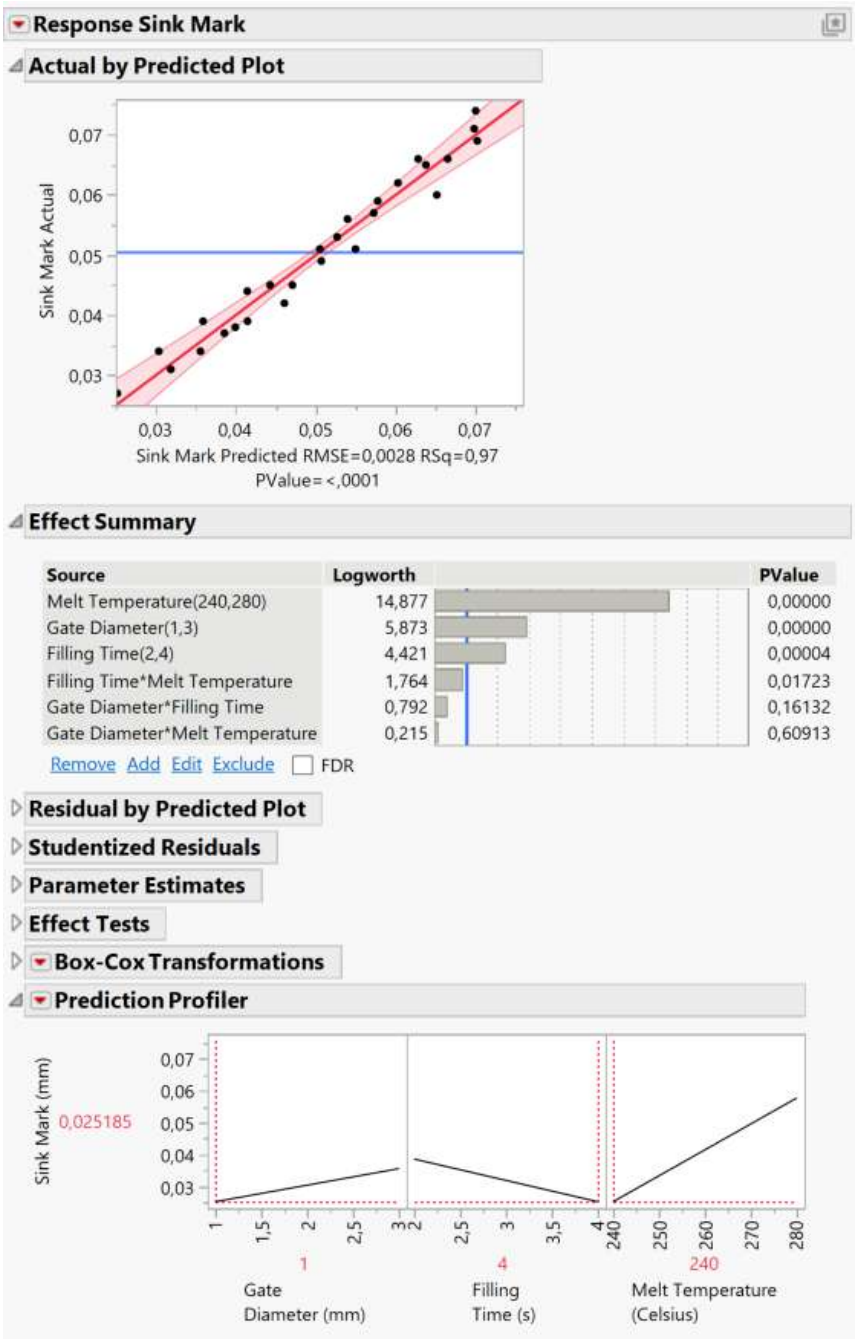

Figure 4.51: Response for the optimization experiment showing p-values and prediction profiler for Sink Mark

The conclusion from the optimization was that to minimize the Sink Mark, factors should follow the values defined in Table 4.10, which would yield a Sink Mark depth of 0.0252 mm. The predicted model (surrogate model) can be seen in Equation 4.1. As observed in the Prediction Profiler, the model is linear.

Table 4.10: Optimal factors for minimized Sink Mark

Factor	**Value**	**Unit**
Gate Diameter	1	mm
Filling Time	4	s
Melt Temperature	240	Celsius
Response		
Sink Mark	0.0252	mm

$$
\begin{aligned}
\text{Sink Mark} = {} & 0.0505185185 \\
& + 0.0044444444 \cdot (\text{Gate Diameter} - 2) \\
& - 0.0034444444 \cdot (\text{Filling Time} - 3) \\
& + 0.0146111111 \cdot \left(\frac{\text{Melt Temperature} - 260}{20} \right) \\
& + 0.0011666667 \cdot (\text{Filling Time} - 3) \cdot (\text{Gate Diameter} - 2) \\
& + 0.0004166667 \cdot \left(\frac{\text{Melt Temperature} - 260}{20} \right) \cdot (\text{Gate Diameter} - 2) \\
& + 0.0020833333 \cdot \left(\frac{\text{Melt Temperature} - 260}{20} \right) \cdot (\text{Filling Time} - 3)
\end{aligned}
\tag{4.1}
$$

4.8.3 Model Validation

The goal of the validation was to confirm that the model predicts the response accurately and does not overfit the data. Overfitting would mean that the model works well just for the specific given data points however, if different data were provided, the error would be great. A common solution to identify an overfitted model is to divide the data points into a training and validation set. This means that you use 80 % of the data points for training the model and use the remaining 20 % for cross validating the model. This will detect if the model is over fitted since the validation set was never part of the model prediction. Table 4.11 shows the same table design as used in the optimization however, with the 80/20 % training/validation split. The split is randomly selected.

Table 4.11: Table design showing the cross validation split between training and validation data points

	FACTORS			RESPONSE	
Run	Gate dia	Fill time	Melt temp	Sink Mark	Validation/Training
1	1	2	240	0,037	Training
2	1	2	260	0,049	Training
3	1	2	280	0,066	Validation
4	1	3	240	0,031	Training
5	1	3	260	0,042	Training
6	1	3	280	0,062	Validation
7	1	4	240	0,027	Validation
8	1	4	260	0,039	Training
9	1	4	280	0,059	Training
10	2	2	240	0,044	Training
11	2	2	260	0,056	Training
12	2	2	280	0,066	Validation
13	2	3	240	0,039	Validation
14	2	3	260	0,051	Training
15	2	3	280	0,060	Training
16	2	4	240	0,034	Training
17	2	4	260	0,045	Training
18	2	4	280	0,065	Training
19	3	2	240	0,045	Training
20	3	2	260	0,057	Training
21	3	2	280	0,069	Training
22	3	3	240	0,038	Training
23	3	3	260	0,051	Training
24	3	3	280	0,074	Training
25	3	4	240	0,034	Validation
26	3	4	260	0,053	Training
27	3	4	280	0,071	Training

Results from the crossvalidation run are displayed in Figure 4.52. As expected the training set has a better fit than the validation set, noted by the close to 1 RSquare (R^2) and low RASE, which is a result of the lower frequency of data points. Looking at the validation statistics, RSquare and RASE show no lack of fit and validate that the model is working.

Only looking at RSquared dose not necessarily mean the model is good, it could be overfitting. Same goes for a low RSquared, does not always mean the model is bad, could be noisy data. The residual plot is therefore observed, which tells the difference between observed and predicted value. Largest residual is around 0.004 mm which is a small comparison to the optimized value of 0.0252 mm. All the data points are randomly scattered and show no sign of a pattern, which further proves the model is doing a good job of capturing the response.

Crossvalidation

Source	RSquare	RASE	Freq
Training Set	0,9654	0,00225	21
Validation Set	0,9260	0,00438	6

Summary of Fit

RSquare	0,965358
RSquare Adj	0,950512
Root Mean Square Error	0,002753
Mean of Response	0,050952
Observations (or Sum Wgts)	21

Residual by Predicted Plot

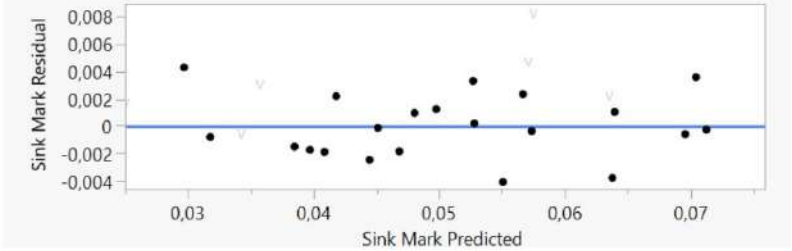

Figure 4.52: Statistical results from the cross validation

5
Discussion

This chapter reflects on the execution and outcomes of the project, whether the objectives were achieved as planned, and analyzes the reasons behind deviations. It evaluates different aspects of the results and provides insights into potential improvements and lessons learned for future work.

5.1 Discussion on DFA cost estimation

The equation used to estimate assembly cost and time was not particularly accurate without applying a significant correction factor, known as the Time Correction Factor (TC factor). Since the actual assembly time for the current VSL was available, the TC factor was calibrated based on the difference between the measured and calculated times. However, this approach is not ideal, as each assembly step may require a different correction factor. As a result, the total estimated assembly time for the new joystick could deviate from the actual time, given that the steps involved differ and may not share the same time adjustments. Nonetheless, because the assembly processes were relatively similar, the TC factor was considered adequate for an initial estimate.

Talking to engineers at CPAC, using this type of equation is not typically used in a real application. Instead, the focus is on dividing up the assembly process into stations, with the goal of keeping all the assembly times equal on each station to keep the workflow constant. You can have parallel and single-line workflows. The assembly time for each station is estimated individually, and the corresponding assembly cost is calculated based on hourly labor rates.

5.2 Discussion on DOE

The DOE provided interesting results on significant factors affecting many different types of responses in the IM process. Using a Significant Screening Design was a good choice as it provided a better chance of identifying significant factors, compared to standard screening designs, with only a small increase in the number of runs. The full factorial design was used since all two factor interactions could be identified. To provide the optimization with a reasonable number of input factors,

the problem was reduced to only studying the Sink Mark.

The input factor that was not evaluated was the geometry. Sink Marks are formed due to a sudden change in thickness, resulting in longer cooling time, hence making the thicker section contract, leaving a local shrinkage called Sink Mark. According to [46], "Depending on surface texture, sink marks are visible if they are 13 to 40 μm in depth or greater." Furthermore, through FEM simulations and physical validations it can be proven that the rib thickness should be less than 0.6 times the wall thickness to keep the sink mark below the visible level 30 μm [46]. This therefore suggests that the optimization goal should rather be to keep sink marks below the visible level, instead of having a goal to only minimize.

Interestingly in [46] the conclusion is that the most important process parameter (besides wall thickness) for controlling sink mark depth is packing pressure. Furthermore, it was found that the melt and mold coolant temperature only has minor effects. Runner and gate geometry can have a significant effect on sink mark since this can introduce large pressure losses. [46]

The melt temperature was found not to have a significant influence on the sink mark depth contradicts the results from the DOE screening performed in the thesis. [46] believes that there are two competing effects that cancel each other out. An increase in melt temperature lowers viscosity, reducing the pressure losses, meaning a more efficient packaging reducing sink mark. On the other hand an increase in melt temperature will create more shrinkage during cooling.

Regarding packing pressure, in Creo Mold Simulation this is not possible to control as an input variable, but could rather only be set as a max limit. Packing pressure will therefore never be significant since it is not an factor in the DOE. Using another mold simulation software would therefore be required in case packing pressure should be added as a factor.

5.3 Discussion on ergonomics

Further development should focus on ergonomics and incorporate feedback from a broader reference group. In this project, the reference group was limited due to time constraints and available resources. As a result, this small group had significant influence over the joystick's design and button placement, which introduces the risk that the final product may only appeal to a narrow user segment. Involving a more diverse group of users would likely result in a design better suited to a wider range of operators.

It was found that designing a joystick to suit everyone is nearly impossible, making it necessary to find a middle ground where most users are reasonably satisfied. The introduction of the adjustable hand rest support helps bridge this gap, accommodating a wider range of operators and improving overall satisfaction.

5.4 Discussion on IM vs. AM

Several factors played a role in choosing IM over AM, with cost being the main one. The AM version was simply too expensive in comparison. For the joystick to be competitive, both in terms of innovation and market appeal, it needs to either offer clear added value or be priced lower than similar products on the market, but preferably both. The production volumes were too high to keep the unit price low enough, and there was not enough complexity to add for the design freedom of the manufacturing method to compensate for the price.

There were concerns about using an AM component within the operator's reach, as AM is typically used for internal or covered parts that are not visible. This helps protect them from wear and environmental factors. In this case, issues like discoloration and changes in appearance over time were raised, especially after years of use. Coating the AM parts was suggested to protect them from wear, grease, and UV exposure. However, this would require extensive testing, as AM hasn't previously been used for mass-producing handles, and its long-term durability in this context remains uncertain.

Manufacturers and designers tended to be cautious about using AM in mass production, since it isn't a common practice. As a result, the idea wasn't rejected outright, but it also didn't generate much enthusiasm for further exploration. AM is well-suited for prototyping, and unless the cost gap compared to IM is reduced, it will most likely remain primarily a prototyping method.

5.5 Discussion on structural validation and load case

Structural validation was used to assess how well the joystick performs under load. The joystick met the specified load case in terms of both deflection and von Mises stress. While the safety factor was sufficient to ensure structural integrity, it could be slightly improved.

Frictional contacts between components significantly increased computational time. This could have been reduced by assuming bonded contacts in certain areas; however, doing so would have compromised the comparability of results. Therefore, the additional computational cost was deemed acceptable.

The load case could have been evaluated using a broader range of operators in a more natural seated posture, with the force measurement scale placed in a more representative location. In practice, the applied load is likely lower than 300 N, especially given the limited ability of users to exert significant pulling force on the

joystick. The selected load case represents a worst-case scenario, and the wall thickness in the model could potentially be reduced to save material.

The pretension of the bolt securing the ball joint mechanism was roughly estimated using typical torque values from CPAC's previous applications. However, no detailed analysis was carried out for this specific fastening method, relying instead on general assumptions of what might be reasonable. As a result, there is uncertainty regarding the appropriate torque values. If higher torque is required than anticipated, it could lead to durability issues, such as material creep, which may reduce bolt pretension over time and compromise the integrity of the joint.

5.6 Discussion on testing of prototype

The test rig was important in evaluating multiple prototypes with the reference group. It allowed for consistent replication of tests by enabling a repeatable seating position and arm placement. However, the rig is not a full replica of a WLO cab, so an exact match to the real environment was not achievable. As a result, there is a margin of uncertainty between the subjective evaluation of the joystick in the rig versus its performance in an actual cab. No tests have yet been conducted in a real WLO environment.

Furthermore, since electrical integration was not a focus in this project, the joystick has not been tested with functional electronics. This may lead to a different feel when used in real-world applications. Implementing a test bench that includes electronic functionality would support a more comprehensive evaluation of the joystick's geometry and overall performance.This should be carried out with a larger, more diverse group of operators to ensure feedback is gathered in a consistent and standardized method.

6
Conclusion

This project covers a broad range of topics, including the definition of a joystick specifically designed for WLO applications, ergonomic analysis, exploration of manufacturing techniques for the joystick handle, design optimization through DOE, structural validation using FEM software, development of a test rig for field evaluation, collection of user feedback through interviews, and a complete BOM ready for manufacturing.

Goal fulfillment

The functions required on the joystick for WLO were evaluated through a case-based approach, where different user scenarios were analyzed. A matrix evaluation was then used to determine which type of button would best suit each function.

DOE was the optimization tool used in the project. The initial objective of DOE was to obtain concrete feedback for optimizing the design of the plastic handles, but the focus shifted to a more theoretical investigation, resulting in less direct impact on practical design improvements.

FEA was successfully applied to verify that the joystick could withstand the anticipated load cases. Additionally, DFMA principles were implemented to ensure the joystick was suitable for injection molding and that manual assembly costs were accounted for in the overall production cost.

Future development

As the next step in the development process, field testing under real-world operating conditions would provide valuable insights to support the continued refinement of the joystick. Ideally, this testing should involve a diverse group of operators using the joystick in their daily workflows across various applications. To enable field testing, a complete electrical design must be developed, including PCB design and wire harness routing. Further refinement of the design, focusing on aesthetics and alignment with design guidelines, should be pursued in close collaboration with VCE.

References

[1] *De e najs*, Publisher: Mr.Hjortron, 2025. [Online]. Available: https://www.youtube.com/watch?app=desktop&v=V9nEPvca4vk (accessed on: 2025-05-22).

[2] *Construction equipment used*, Publisher: Volvo Construction Equipment, 2025. [Online]. Available: https://www.volvoceused.com/volvoceemea/construction-equipment/wheel-loaders/volvo-l-150-h/1df2111d-9d35-49ef-9683-7c72a2983d4d.html (accessed on: 2025-05-23).

[3] *Volvo picture*, 2025-01-08. [Online]. Available: https://www.volvoce.com/sverige/sv-se/.

[4] V. CE, https://www.volvoce.com/sverige/sv-se/attachments/compact-wheel-loader-attachments/, 2025.

[5] H. Dodiuk and S. H. Goodman, *Chapter 1 - Introduction* (Plastics Design Library), Fourth, H. Dodiuk, Ed. William Andrew Publishing, 2022, pp. 1–11, ISBN: 9780128216323. DOI: 10.1016/B978-0-12-821632-3.00009-9. [Online]. Available: https://www.sciencedirect.com/science/article/pii/B9780128216323000099.

[6] F. Mold, "11 types of plastic parts connection methods," [Online]. Available: https://firstmold.com/tips/parts-connection/ (accessed on: 2025-02-27).

[7] Ootsuka02, *Cantilever snap-fit*, https://commons.wikimedia.org/wiki/File:Cantilever$_S$nap−$fit.PNG$, [Illustration]. Retrieved on: May 23, 2025, 2025.

[8] Dukane, "What is ultrasonic welding?," [Online]. Available: https://www.dukane.com/resources/our-processes/ultrasonic-plastic-welding (accessed on: 2025-02-28).

[9] Plastopia, "Vdi 3400: The ultimate guide to texture standards," [Online]. Available: https://www.plastopialtd.com/vdi-3400/ (accessed on: 2025-02-24).

[10] P. network, "Injection molding: The definitive engineering guide," [Online]. Available: https://cdn.thomasnet.com/kc/5289/doc/Injection_Molding_the_Definitive_Engineering_Guide.pdf (accessed on: 2025-02-11).

[11] K. de Naoum and R. Piccoli, "All about the basics of plastic injection molding," [Online]. Available: https://www.xometry.com/resources/injection-molding/basics-of-plastic-injection-molding/#:~:text=An%20overview%20of%20the%20basics%20of%20plastic%20injection,difference%20between%20plastic%20injection%20molding%20and%203D%20printing. (accessed on: 2025-02-11).

[12] B. Rockey, *Injection moulding*, https://zetarmold.com/injection-mold-slider/, [Diagram]. Created for the Injection Molding Wikipedia article. Accessed on: Apr. 29, 2025, 2025.
[13] T. Nilsson, private communication, Mar. 2025.
[14] M. Tang, *What is an injection mold slider*, https://commons.wikimedia.org/wiki/File:Injection_moulding.png, May 25 2025.
[15] K. Kanishka and B. Acherjee, "Revolutionizing manufacturing: A comprehensive overview of additive manufacturing processes, materials, developments, and challenges," 2023. [Online]. Available: https://www.sciencedirect.com/science/article/pii/S1526612523009726?ref=pdf_download&fr=RR-2&rr=91036007ed38169d (accessed on: 2025-02-11).
[16] J. R. C. Dizon, A. H. Espera, Q. Chen, and R. Advincula, "Mechanical characterization of 3d-printed polymers," 2018. [Online]. Available: https://www.sciencedirect.com/science/article/pii/S2214860417302749?ref=pdf_download&fr=RR-2&rr=91031e26293f990f (accessed on: 2025-02-11).
[17] Formlabs, "Guide to resin 3d printers: Sla vs. dlp vs. msla vs. lcd," [Online]. Available: https://formlabs.com/eu/blog/resin-3d-printer-comparison-sla-vs-dlp/ (accessed on: 2025-05-2).
[18] E. P. Design, "Sheet lamination," [Online]. Available: https://engineeringproductdesign.com/knowledge-base/sheet-lamination/ (accessed on: 2025-05-2).
[19] S. Kumar, *Biomechanics in Ergonomics*. Taylor & Francis Group, 2007, p. 723.
[20] J. Methot, S. J. Chinchalkar, and R. S. Richards, "Contribution of the ulnar digits to grip strength," *The Canadian journal of plastic surgery*, vol. 18, no. 1, 2010. DOI: https://doi.org/10.1197/j.jht.2004.04.006.
[21] J. C. MacDermid, A. Lee, R. S. Richards, and J. H. Roth, "Individual finger strength:: Are the ulnar digits "powerful"?" *Journal of Hand Therapy*, vol. 17, no. 3, pp. 364–367, 2004. DOI: https://doi.org/10.1197/j.jht.2004.04.006.
[22] C. Adams and C. Berlin, *Production Ergonomics*. Ubinquity Press Ltd., 2017, p. 296.
[23] N. Adolfsson, K. Öberg, and A. Torén, "Förebyggande av belastningsskador vid arbete med armstödsburna reglage i mobila arbetsmaskiner," 2004. DOI: https://www.diva-portal.org/smash/get/diva2:959533/FULLTEXT01.pdf.
[24] T. Yakaou, K. Yamamoto, M. Koyama, and K. Hyodo, "Sensory evaluation of grip using cylindrical objects," vol. 40, no. 4, pp. 730–735, 1997. [Online]. Available: https://www.jstage.jst.go.jp/article/jsmec1997/40/4/40_4_730/_pdf (accessed on: 2025-02-2).
[25] C. Fransson and J. Winkel, "Hand strength: The influence of grip span and grip type," pp. 881–892, 1991. [Online]. Available: https://doi.org/10.1080/00140139108964832 (accessed on: 2025-02-2).
[26] L. Hanson, L. Sperling, G. Gard, S. Ipsen, and C. O. Vergara, "Swedish anthropometrics for product and workplace design," pp. 797–806, 2009. [Online]. Available: https://www.sciencedirect.com/science/article/pii/S0003687008001324?via%3Dihub (accessed on: 2025-02-2).

[27] M. Oliver, "Joystick dynamics and the effects of stiffness and speed on upper limb kinematics," May 2001. DOI: https://central.bac-lac.gc.ca/.item?id=NQ72455&op=pdf&app=Library&is_thesis=1&oclc_number=55595567.

[28] R. Rabbani, "The effect of temperature and humidity on electronic component reliability," 2023. [Online]. Available: https://www.lisungroup.com/news/technology-news/the-effect-of-temperature-and-humidity-on-electronic-component-reliability.html (accessed on: 2025-02-11).

[29] M. Nyström, private communication, Feb. 2025.

[30] D. Montgomery and C. St, *Design and Analysis of Experiments, 9th Edition*. Jul. 2022, ISBN: 9781119113478 (PBK) ; 9781119299455 (EVALC).

[31] SAS Institute Inc. "Jmp documentation." (2025), [Online]. Available: https://www.jmp.com/en/support/jmp-documentation (accessed on: 2025-05-17).

[32] N. Ottosen and H. Petersson, *Introduction to the Finite Element Method*, English. Prentice-Hall, 1992, ISBN: 0-13-473877-2.

[33] *What is finite element analysis (fea)?* Publisher: Ansys, 2025. [Online]. Available: https://www.ansys.com/simulation-topics/what-is-finite-element-analysis.

[34] I. Holland, "Fundamentals of the finite element method," *Computers Structures*, vol. 4, no. 1, pp. 3–15, 1974, ISSN: 0045-7949. DOI: https://doi.org/10.1016/0045-7949(74)90074-1. [Online]. Available: https://www.sciencedirect.com/science/article/pii/0045794974900741.

[35] I. Erhunmwun and U. Ikponmwosa, "Review on finite element method," *Journal of Applied Sciences and Environmental Management*, vol. 21, p. 999, Nov. 2017. DOI: 10.4314/jasem.v21i5.30.

[36] *Ansys contact types and explanations*, Publisher: Mechead, 2025. [Online]. Available: https://www.mechead.com/contact-types-and-behaviours-in-ansys/ (accessed on: 2021-03-7).

[37] K. G. Swift and J. D. Booker, *Process Selection: From Design to Manufacturing*. Elsevier Science Technology, 2003.

[38] *Design for manufacturing (dfm)*, Publisher: SIX SIGMA, 2025. [Online]. Available: https://www.6sigma.us/six-sigma-in-focus/design-for-manufacturing-dfm/ (accessed on: 2024-010-18).

[39] K. T. Ulrich, *Product design and development*. Tata McGraw-Hill Education, 2003.

[40] *Design of experiments - doe*, Publisher: DATAtab Team, 2025. [Online]. Available: https://datatab.net (accessed on: 2025-03-21).

[41] P. Franzén, private communication, Mar. 2025.

[42] *Apem xd joystick*, Publisher: APEM, 2025. [Online]. Available: https://www.apem.com/idec-apem/en_US/Joysticks/Handgrip-Hall-Effect/XD/c/XD?page=1 (accessed on: 2025-03-18).

[43] *Otto controls*, Publisher: OTTO, 2025. [Online]. Available: https://www.otto-controls.com/ (accessed on: 2025-03-18).

[44] L. Kremer, internal document, Feb. 2025.

[45] IKOT, *Chalmers ikot reports group 601-605*, internal document, May 2024.

[46] D. Battey and M. Gupta, "A parametric study of sink marks in injection-molded plastic parts using the finite element method," *International Polymer Processing*, vol. 12, pp. 288–299, Sep. 1997. DOI: 10.3139/217.970288.

A

Appendix

A.1 Interview 1

- Where do you work?
  - Uddevalla, in the section of dumping and crushed aggregate.
- How long have you worked with WLO?
  - Since 2004
- What types of WLO have you been in contact with?
  - Liebherr
  - CAT 980/988
  - Volvo F-H 90/180/220/350
- Pros and cons with the WLO?
  - Liebherr - worse than Volvo in terms of driver comfort but large cab
  - Hydrostat - slow acceleration, noise and high revving
  - Volvo - Seat cannot be retracted far enough
- Functions in WLO?
  - 2 lever and joystick for steering
  - Boom, Plow, Crusher bucket, Salt, Sand, High-tip and Crane arm
- User cases?
  - Kick-down - depending on usage of WLO but needed
  - Horn - Not so often, if someone is in the way, a com-radio button would be more usable
  - Functions that are good to have close - scale, full/half light, co-pilot control
- Ergonomics
  - Fatigue - bad positioning of CDC
- 3rd/4th function
  - low usage
  - 4th function is used rarely
  - 3rd and 4th function isn't used simultaneously
  - Idea - one thumb lever and a button switching from 3rd to 4th

A.2 Interview 2

- Where do you work?

  - Material handling, Forks, Grading bucket, loading/unloading, grader, snow removal, ditching bucket, road maintenance, construction servive and sweeper roller
- How long have you worked with WLO?
  - 25 years
- What types of WLO have you been in contact with?
  - Volvo 4200/L60/L35/L70
- User cases?
  - Kick-down - No if pedal in the floor
  - Electronic lock - seldom, better positioning on the a-pillar
- Ergonomics
  - Pretty happy with the comfort
- 3rd/4th function
  - 4th func. only for sweepers
  - 3rd func. is often used
  - Idea - one thumb lever and a button switching from 3rd to 4th, positive

A.3 Interview 3

- Operator Experience
  - 52 years of experience operating construction vehicles, including large and compact WLOs and excavators.
- General
  - How comfortable is the joystick, overall impression? (Short answer)
    * Not a fan of single-lever systems in large WLOs and prefers multi-lever setups. Does not believe single-lever designs should be used in WLOs.
    * Overall impression was positive; the hand fit well. However, the ergonomics of the SVAB L8 joystick were rated higher. Wrist support was positive and supportive. The concept of interchangeable wrist supports was considered impractical for multi-user machines and felt more like a gimmick.
    * The resting position for the thumb felt slightly off. A more extended palm rest was suggested for better contact.
- Geometry
  - How do you experience the grasp size of the joystick?
    * Grasp diameter was good, and the geometry fit the operator's hand as intended.
  - How do you experience the grasp length of the joystick?
    * Joystick handle length was good, and the thumb could comfortably reach all front-facing buttons.
- Positioning
  - How do you experience the placement of the 3rd and 4th function?
    * Both functions were easy to operate simultaneously and could be used during joystick X and Y movement. Small correction capability via the thumbwheel was important.

    - Mentioned a potential risk of the thumb getting stuck between the thumbwheel and handle—recommended minimizing that gap.
  - What thumb wheel would you use as the 3rd function?
    - Front-side thumbwheel for the 3rd function; back-side thumbwheel for the 4th function.
  - How do you experience the button placement for kick-down, diff-lock, horn and neutral? (Programmable)
    - Placement of all push buttons was good and easily accessible. Rear push buttons were particularly appreciated for their effective positioning. The feel and type of push buttons were positively noted.
    - The idea of a base configuration for all programmable buttons was appreciated, allowing customization via the co-pilot. Symbols on the buttons themselves were not deemed necessary, as long as they are clearly shown in the co-pilot interface.
  - How do you experience the FR placement?
    - There is a risk of pinching near the FR switch. The operator was unfamiliar with momentary 2-position FR switches compared to 3-position latching FNR, but noted it would be easy to get used to.
    - Suggested the FR be about 5 mm longer and positioned slightly lower on the handle, closer to the base.
- Texture
  - What surface texture would you appreciate to have on the joystick handle?
    - Preferred a smooth, hard surface over textured ones, citing concerns about wear and ease of cleaning.
    - Also noted that the armrest surface should be breathable and allow smooth arm movement without sticking—though this is not directly related to the joystick.
- Feel of Function
  - How is the movement feel of the joystick? (Springforce)
    - Movement felt similar to other machines. No strong feedback on spring force, but noted potential for natural oscillations when driving on uneven terrain.
  - How is the movement feel of the joystick? (Stroke length)
    - Important that there is no dead-space in the center of the joystick's movement range.
  - How do you consider the length to the rotation axis?
    - Movement felt natural overall with no negative feedback.

A.4 Requirement specification

Chalmers			Requirement specification				
			Created: 2025-01-21 *Modifies:*	*Demand/Wish*	*Weight for W*		
	Criteria		*Target*			*Verification method*	*Requirement setter*
	General description						
		Configurations	Armrest mounted electrical multi-function levers used to control hydraulic functions in Volvo CE's wheel loaders. The SL should be available in 3 different configurations based on number of functions that can be maneuvered with the Handle/Grip.				Project
1	**Loads**						
	1.1	External force	The mechanism, mounting screws and joystick axle shall withstand forces both at end stops and sideways when someone leans against the top of the lever handle. Maximum allowed force applied at top of handle: **300N**	D		Physical testing and CAE	Project
	1.3	External force balljoint mechanism	Without the balljoint sliding, the maximum allowed force applied at top of handle: **200N**	D		Physical testing and CAE	Project
2	**Environment**						
	2.1	General environment exposure	The SL components shall be able to withstand the exposure to different environmental conditions; dirt, road salt, grease, fluids, oils, gases, solar radiation.	D		Physical testing	Project
	2.5	IP-rating, electrical components	IP5K4 for visible parts IP5K2 for non-visible parts	D		Physical testing	Project
3	**Lifespan**						
	3.2	Lifespan, buttons and switches	1 million cycles	D		Physical testing	Project
4	**Mechanical requirements**						
	4.1	Size and position	The overall size of the SL, should not exceed the following dimensions: - Length (in machine backward-forward direction): 110mm - Width: 130mm - Height: 140mm	D		Measure in CAD	Project
5	**Weight**						
	5.1	The weight of the complete SL	<2kg	D		Measure in CAD	Project
6	**Ergonomics**						
	6.1	General ergonomics	The design of the SL and all evaluations of the SL should be based on the operators natural hand position when seated in a Volvo WLO seat with armrest for electrical levers. The design should allow the operator use a full hand-operation	D			Project
	6.2	Prevention of accidental activation	A mechanism should be provided that allows the operator to activate and deactivate the lever including thumb lever switches for 3rd and 4th function. The edges of the lever and the thumb lever switches shall be smooth and designed for prevention of the operator to get caught with a slew or a strap on clothing. Switches placed on lever handle should be positioned in a way that limits accidental activation to a minimum.	D			Project
	6.3	Lever forces and movement characteristics	The SL lever should have a clearly distinguished neutral position and characteristic of lever forces that clearly separates the left-right movement and backward-forward movement.	D			Project

	6.4	Hand and wrist support	There should be a hand/wrist support integrated in the SL lever that gives support for fingertip maneuvering and full hand grip maneuvering of the SL lever.	W	3		Project
	6.5	Physical ergonomics	Suit 5th percentile female to 95th percentile male	D			Project
	6.6		Provide a comfortable grip with wrist and hand angles as close to neutral plane	D			Project
	6.7		Allow maneuvering of 3rd and 4th function simultanously without changing grip	W	3		Project
	6.8		Provide haptic feedback	W	2		Project
	6.9		Heated grip	W	1		Project
7	**Recycling**						
	7.1	Design for Recycling	All materials shall be suited for recycling. Special attention is to be paid to parts accessibility, ease of extraction at the end of life, dismantling, and existence of recycling process.	D			Project

A.5 Rubber Boot Manufacturing

Here the manufacturing for the prototype rubber boot will be illustrated and explained. The material used was moldable silicon rubber (R PRO 20) with shore hardness of 20A. It is a two-component mix with a working time of 40 minutes. Molds were 3D Printed in PLA and no post-processing was done and no release agent was applied before the molding took place. It would be possible to apply filler and sand smooth the layer lines however, this was skipped to save time and the final result more than exactable. Figure A.1 shows the 3D Printed mold partially assembled before molding took place. The mold outside shell was split in two parts, while the core was four parts collapsible.

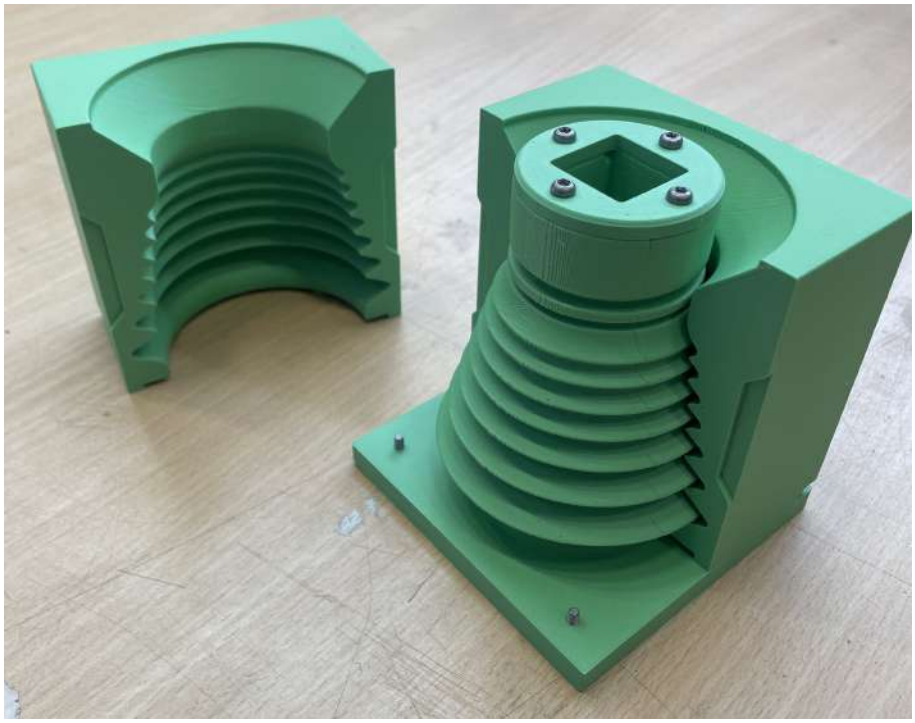

Figure A.1: 3D Printed mold before closed

Once the mold was closed, the silicon was mixed and poured into the mold. A funnel was created in the mold geometry to make the filling easier and the execs part was later cut of. Figure A.1 shows the mold when it was filled. Due to the rather thin wall thickens of the boot (2 mm) and complex geometry, a drill was used to vibrate the mold. This helped however, there were still certain spots with air bubbles. Degassing in a vacuum chamber helped however, there were still certain areas with trapped air. Figure A.3 shows the rubber boot once it was de-molded.

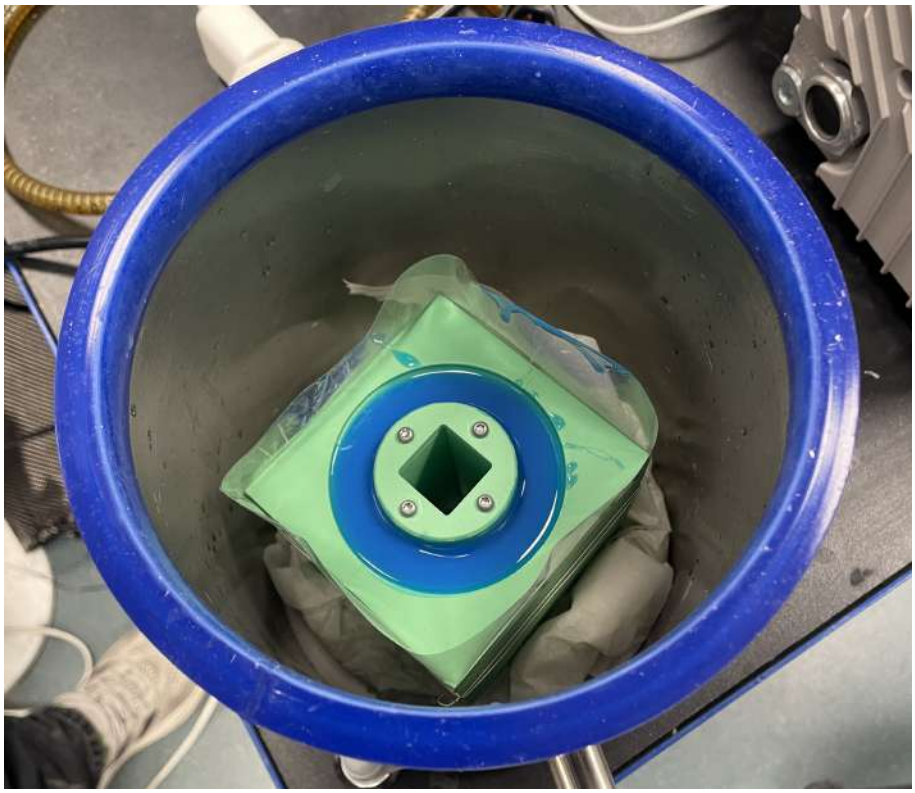

Figure A.2: Filling the mold and degassing in a vacuum chamber

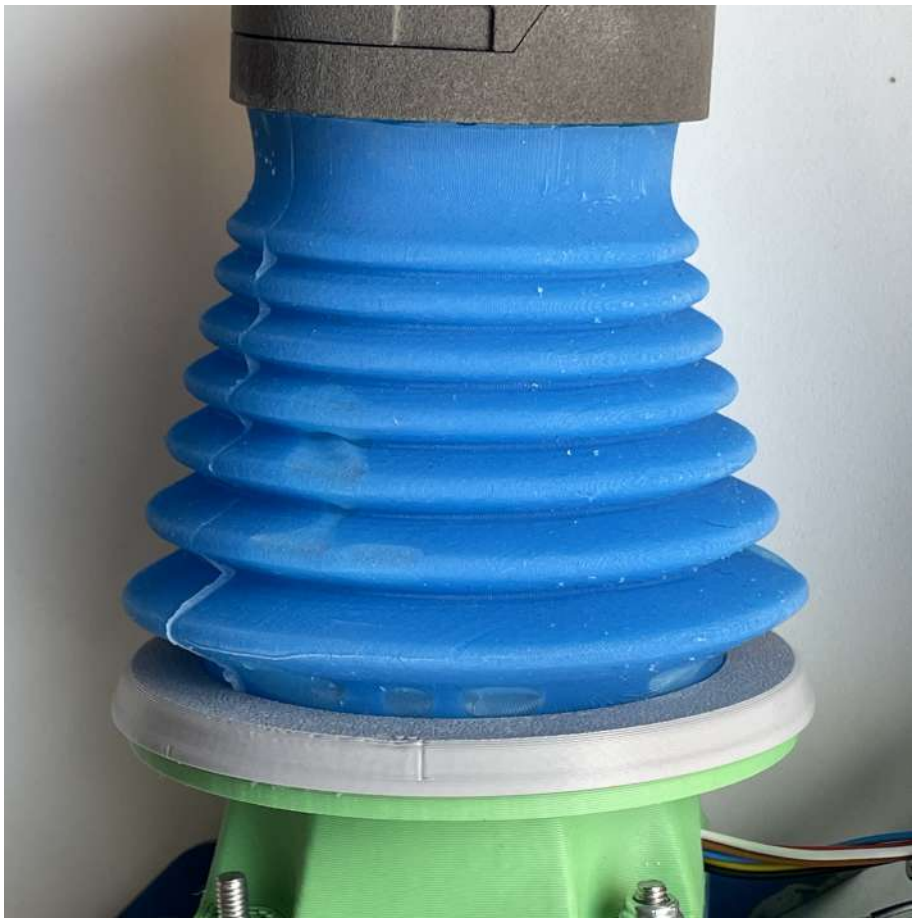

Figure A.3: Silicon boot after de-molding

A.6 FEM

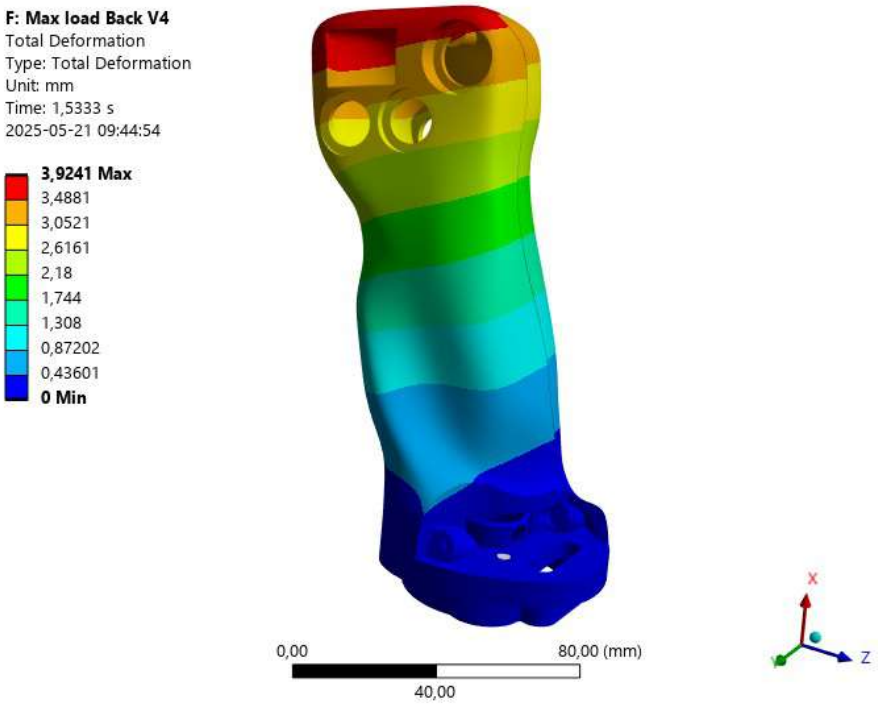

Figure A.4: Deformation - LC2

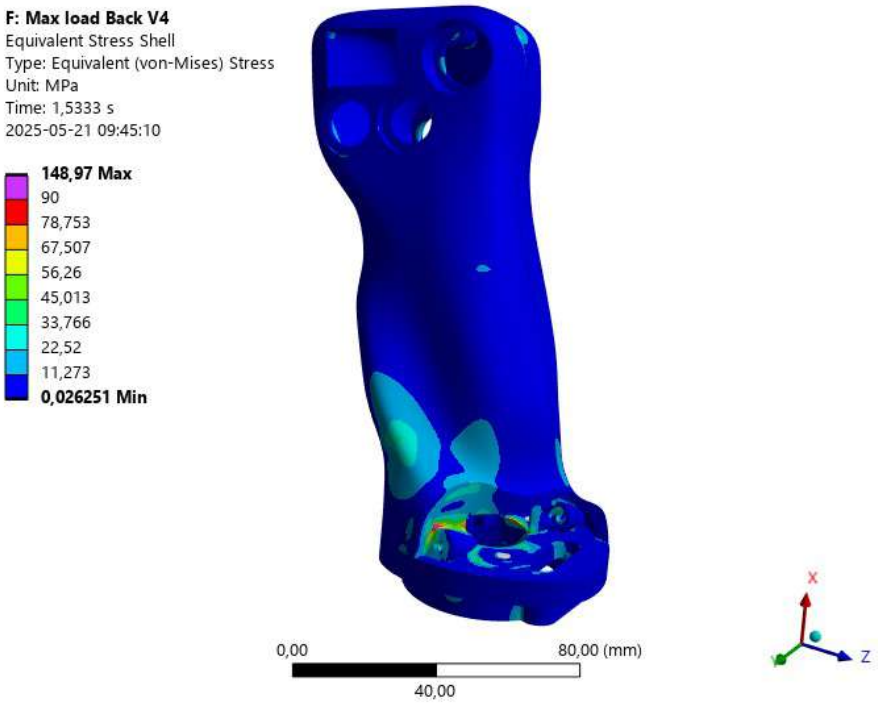

Figure A.5: von Mises stress - LC2

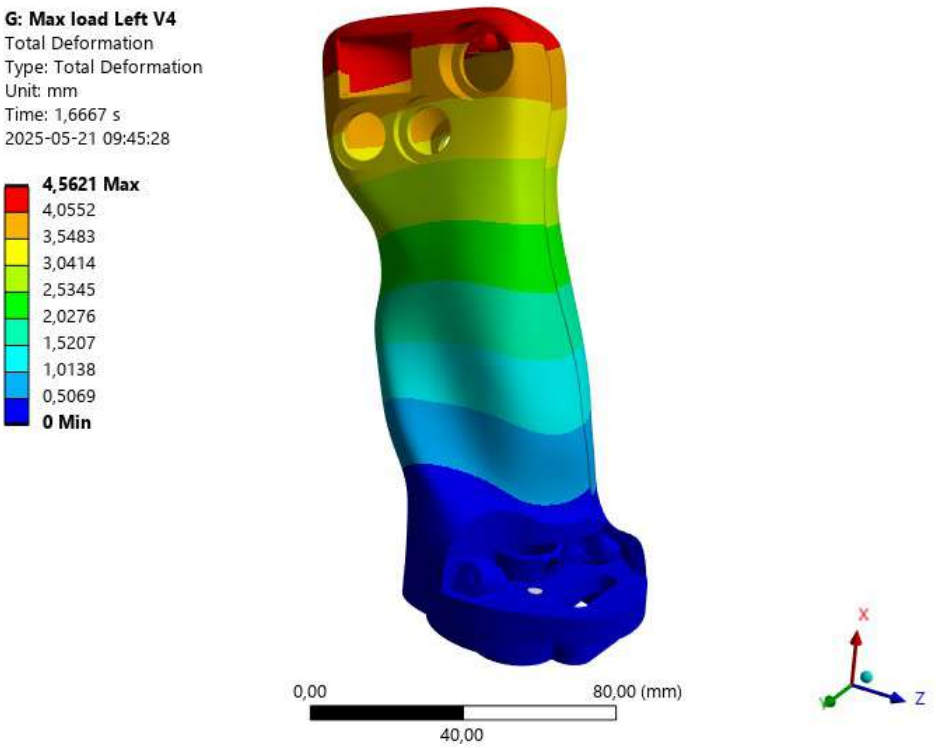

Figure A.6: Deformation - LC3

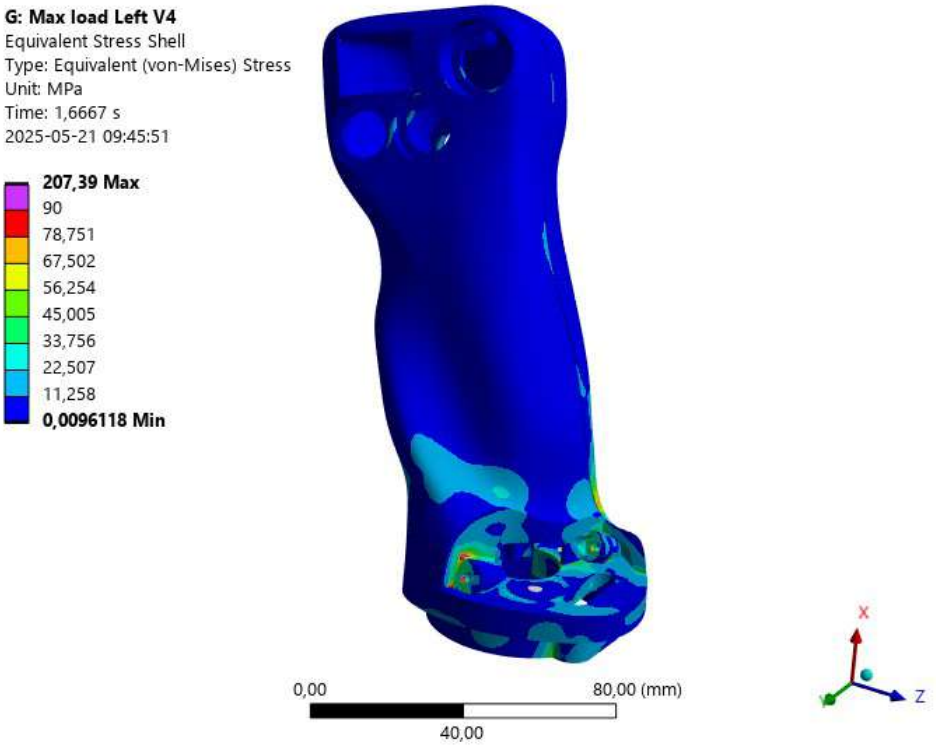

Figure A.7: von Mises stress - LC3

X

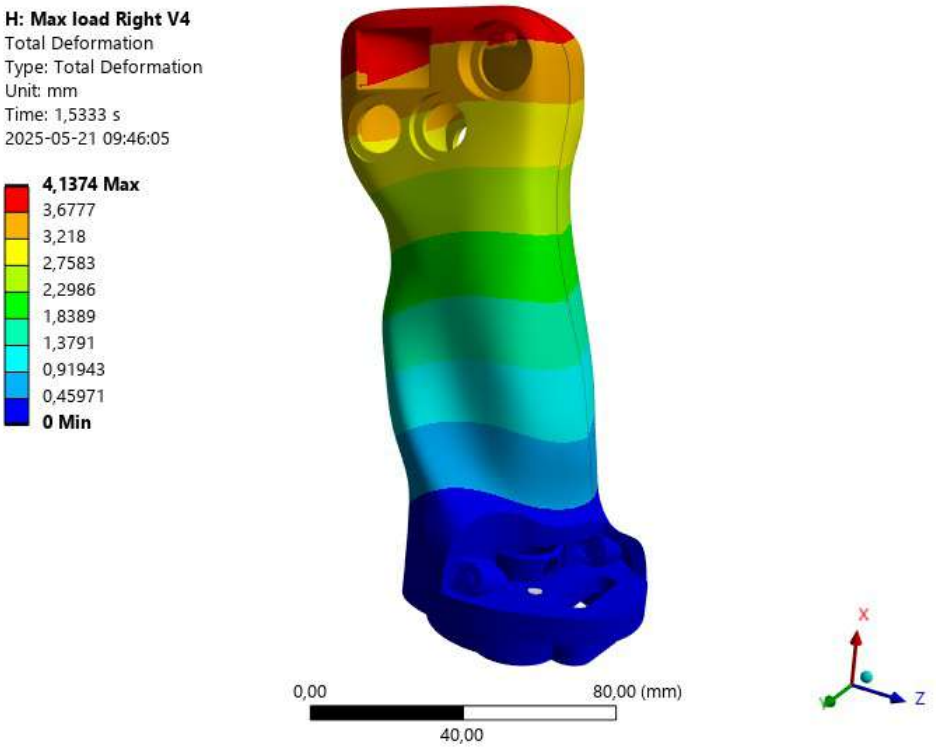

Figure A.8: Deformation - LC4

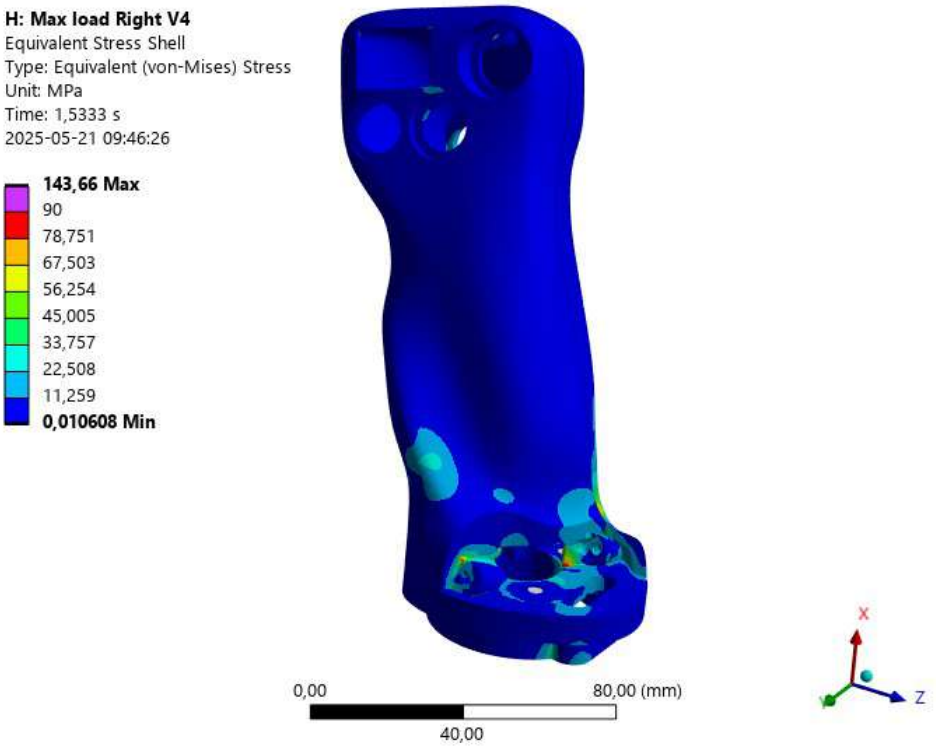

Figure A.9: von Mises stress - LC4

Department of Industrial and Materials Science IMSX30
CHALMERS UNIVERSITY OF TECHNOLOGY
Gothenburg, Sweden 2025
www.chalmers.se

CHALMERS